Distribution Agreement

In presenting this thesis or dissertation as a partial fulfillment of the requirements for an advanced degree from Emory University, I hereby grant to Emory University and its agents the non-exclusive license to archive, make accessible, and display my thesis or dissertation in whole or in part in all forms of media, now or hereafter known, including display on the world wide web. I understand that I may select some access restrictions as part of the online submission of this thesis or dissertation. I retain all ownership rights to the copyright of the thesis or dissertation. I also retain the right to use in future works (such as articles or books) all or part of this thesis or dissertation.

Signature:

_____ _____

Cecilia Prudente Date

Approval Sheet

Neuroanatomical Substrates for Head Movements in Humans

By

Cecília N. Prudente

Doctor of Philosophy
Graduate Division of Biological and Biomedical Sciences
Neuroscience

_____
H.A. Jinnah, M.D., Ph.D.
Advisor

_____
Ellen J. Hess, Ph.D.
Committee Member

_____
Xiaoping P. Hu, Ph.D.
Committee Member

_____
Mark S. LeDoux, M.D., Ph.D.
Committee Member

_____
Krish Sathian, M.D., Ph.D.
Committee Member

_____
Yoland Smith, Ph.D.
Committee Member

Accepted:

_____
Lisa A. Tedesco, Ph.D.
Dean of the James T. Laney School of Graduate Studies

_____
Date

Neuroanatomical Substrates for Head Movements in Humans

By

Cecília N. Prudente
P.T., Universidade Federal de Minas Gerais (Brazil), 2005
M.S., Universidade Federal de Minas Gerais (Brazil), 2007

Advisor: H.A. Jinnah, MD, Ph.D.

An abstract of
a dissertation submitted to the Faculty of the
James T. Laney School of Graduate Studies of Emory University
in partial fulfillment of the requirements for the degree of
Doctor of Philosophy
in Graduate Division of Biological and Biomedical Science, Neuroscience

2015

Abstract

Neuroanatomical Substrates for Head Movements in Humans

By Cecília N. Prudente

The neuroanatomical substrates for head movements in humans are not well delineated. It is not clear whether neck muscles are controlled by the ipsilateral or contralateral hemisphere, and the location of the neck motor region in the motor homunculus is still debated. The lack of fundamental information regarding head control is relevant to cervical dystonia (CD), a disorder characterized by involuntary contractions of neck muscles and abnormal head movements. Current understanding of the neuroanatomical basis of CD is very limited. Multiple brain regions have been implicated, but findings across different studies are inconsistent. This thesis addresses the neuroanatomical basis of head movements in normal individuals and in CD using functional magnetic resonance imaging (fMRI) and neuropathology methods. The studies had two main goals: to delineate the neural substrates for normal head movements and to identify abnormalities associated with CD.

The initial studies investigated patterns of brain activity during isometric head rotation with fMRI in healthy volunteers. Significant activation was observed bilaterally in the precentral gyrus, both medial and lateral to the hand area. Next, brain activity was studied in individuals with CD using the same conditions. Isometric head rotation in the CD group produced less activation in the medial precentral gyrus in the same region identified as involved in head rotation in normal individuals. Analysis of CD data normalized according to the direction of abnormal movements indicated that moving the head in the same direction as the abnormal movements involved more activity in the cerebellum and pons, whereas moving the head in the opposite direction involved more activity in the primary somatosensory cortex. These findings provide evidence of potential cortical and subcortical areas that may be affected in CD. The final studies involved postmortem brain samples of CD cases and age-matched controls to identify neuroanatomical changes associated with CD. A broad survey of brain regions revealed no abnormalities, but there was patchy loss of Purkinje cells in the cerebellum. Quantitative analyses confirmed a significantly lower Purkinje cell density in CD in comparison to controls, suggesting abnormal cerebellar physiology in this disorder.

Collectively, these findings begin to fill a critical gap in the understanding of normal and abnormal head movements in humans. Furthermore, the results may help guide future medical or surgical interventions for CD targeting relevant brain regions, as well as future cellular and animal studies.

Neuroanatomical Substrates for Head Movements in Humans

By

Cecília N. Prudente
P.T., Universidade Federal de Minas Gerais (Brazil), 2005
M.S., Universidade Federal de Minas Gerais (Brazil), 2007

Advisor: H.A. Jinnah, MD, Ph.D.

A dissertation submitted to the Faculty of the
James T. Laney School of Graduate Studies of Emory University
in partial fulfillment of the requirements for the degree of
Doctor of Philosophy
in Graduate Division of Biological and Biomedical Science, Neuroscience

2015

Acknowledgements

I would like to express my special appreciation and gratitude to my advisor Dr. “Buz” Jinnah. You have been a remarkable mentor for me. Thank you for encouraging my research and for allowing me to grow as a scientist. I am very proud of what we have achieved together, thank you for the opportunity. Your advice and support on both research and my career have been invaluable.

I am enormously grateful to all the volunteers that participated in the imaging studies, as well as the brain donors and their family members. My thesis would not have been possible without their generosity and willingness to contribute to these experiments, my education and, most importantly, to science.

I would like to thank my thesis committee, Dr. Ellen Hess, Dr. Xiaoping Hu, Dr. Mark LeDoux, Dr. Krish Sathian, and Dr. Yoland Smith, for the bright suggestions and for the encouragements along the way. I cannot thank enough for everything I learned from all of you.

I would like to show my great appreciation to Dr. Krish Sathian for the exceptional guidance in neuroimaging and for providing me with a great atmosphere to do research in his lab. Thanks for the brilliant insights and for taking so much interest in my project. I would also like to thank Dr. Ellen Hess for the frequent insights and for constantly motivating me to strive towards my goal.

I would like to show my appreciation to all the additional collaborators and their lab members for the great contributions to my thesis and my training: Dr. Mark LeDoux, Dr. Yoland Smith, Dr. Xiaoping Hu, and Dr. Cathrin Buetefisch. I also thank Dr. Teresa Kimberley for the assistance with data analysis and for the generous help with the Brain Voyager software.

To all the Jinnah/Hess lab members, past and current, thanks for the insightful suggestions, entertaining discussions, and for the constant scientific and emotional support. A special thanks to Ami, Cicely, Chang, Christine, Diane, Doug, Martin, Matt, Rob, Rong, Sam and Xueliang.

It also has been my privilege to work closely with Randall Stilla, I have enjoyed the opportunity to watch and learn from your knowledge and experience. Thanks for making the world of neuroimaging seem less scary. In addition, I would like to thank Simon Lacey, Shivangi Singh and Gregory Kowalski for the assistance with data analysis.

I also would like to thank everyone involved in helping with subject recruitment. This includes Doug Bernhard, Laura Rose, Ami Rosen, Diane Sutcliffe, Dr. Buz Jinnah, Dr. Marian Evatt, Dr. Alan Freeman, Dr. Stewart Factor, The Dystonia Coalition, the National Spasmodic Torticollis Foundation, and the Dystonia Global Registry.

I am very grateful for the funding sources available for supporting my thesis. The experiments would not have been possible without the financial support from the Research Supplement to Promote Diversity in Health-Related Research (U54 NS06571-03S1), the Emory University Research Committee (URC) UL1 RR025008, and the Pilot Projects Program from the Emory Biomedical Imaging Technology Center.

I would like to express my appreciation to the Neuroscience program, especially to Dr. Shawn Hochman, Dr. Ron Calabrese, Dr. Yoland Smith, Dr. Leonard Howell, Dr. Malu Tansey, Sonia Hayden and Gary Longstreet. Thanks for believing in me and in my career. I would also like to thank my peers in the Neuroscience program for sharing part of this journey with me and making things easier along the way.

To the Graduate Division of Biological and Biomedical Sciences, the Laney Graduate School and Emory University, I also express my appreciation for giving me the opportunity to develop as a scientist.

Words cannot express how grateful I am to all of my friends and relatives who supported and believed in me. To my dear friends Kathy, Cathy, and Brian, thanks for being my family in Atlanta and my friends for life. To Rodrigo, Camila, Sophia, Danielle, Paulo, Theo and Lux, thanks for taking care of me and making Brazil seem a bit closer. I also appreciate the love and support from Enara, Roseane, Manoela, Luisa, Mariana, os Nasciutti, os Prudente, Guga, and Pretinho.

Finally, I would like to thank my parents, Derli and Maria Célia, and my siblings, Arthur, Lucas and Marina, for being my best friends and most cheerful supporters. Even from far away you have encouraged me and celebrated with me every step of this long process. Without your love and support I would not have completed this work.

Table of Contents

Tables and Figures

Chapter 2: Imaging the neuroanatomical substrates for normal head movements

Chapter 3: Imaging the neuroanatomical substrates for head movements in cervical dystonia

Chapter 4: Neuropathology of cervical dystonia

Chapter 5: Discussion and final conclusions

Abbreviations

ACC	nucleus accumbens
AD	Alzheimer’s disease
ANG	angular gyrus
BG	basal ganglia
BL	blepharospasm
BOLD	blood oxygenation level dependent
BoNT	botulinum toxin
BS	brainstem
CAUD	caudate
CBL	cerebellum
CD	cervical dystonia
CD_{NORM}	cervical dystonia group normalized to side of torticollis
CING	cingulate gyrus
CN III	cranial nerve III
CN IV	cranial nerve IV
CNF	cuneiform nucleus
COD	complication of disorder
CTX	cerebral cortex
CVD	cardiovascular disease
DTI	diffusion tensor imaging
ECU	extensor carpi ulnaris
EMG	electromyography
EPI	echo planar imaging
F	female

FA	flip angle
FD	facial dystonia
FHD	focal hand dystonia
fMRI	functional magnetic resonance imaging
GABA	gamma-aminobutyric acid
GDRS	Global Dystonia Rating Scale
GFAP	glial fibrillary acidic protein
GP	globus pallidus
H&E	hematoxylin/eosin
Hemi	hemisphere
het	heterozygous
HIP	hippocampus
hom	homozygous
HT	hand tremor
ID	identifier
INC	interstitial nucleus of Cajal
INS	insula
iPar	inferior parietal cortex
L	left
LOC	locus ceruleus
M	male
M1	primary motor cortex
MB	midbrain
MOG	middle occipital gyrus
MTG	middle temporal gyrus

NA	not available or not applicable
NBM	nucleus basalis of Meynert
NFT	neurofibrillary tangles
NR	not relevant
NS	not significant
NT	neck tremor
PAG	periaqueductal gray
PCG	precentral gyrus
PMd	dorsal premotor area
PMI	post-mortem interval
PMv	ventral premotor area
PPN	pedunculopontine nucleus
Pre-SMA	pre- supplementary motor area
PACE	Prospective Acquisition Correction
PET	positron emission tomography
PUT	putamen
R	right
RF	reticular formation
RN	red nucleus
ROI	region of interest
S1	primary somatosensory cortex
S2	secondary somatosensory cortex
SC	spinal cord
SCM	sternocleidomastoid
SD	standard deviation

SM	sensorimotor cortex
SMA	supplementary motor area
SN	substantia nigra
sPar	superior parietal cortex
sTL	superior temporal lobe
STN	subthalamic nucleus
STS	superior temporal sulcus
TE	time to echo
TG	tegmentum
THAL	thalamus
TMS	transcranial magnetic stimulation
TWSTRS	Toronto Western Spasmodic Torticollis Rating Scale
TR	time to repetition
uINI	ubiquitinated intranuclear inclusions
vs.	versus

Chapter 1: Introduction

Head movements in humans are highly complex. Head movements are generated by several neck muscles and joints acting synergistically in a variety of combinations. At the most basic level, neck muscles must be able to support the human head in an upright position against gravity, as well as allow the head to move in different directions. Notably, the head carries most of the sensory systems that enable humans to function effectively in a three-dimensional environment. Thus, without adequate head movement control, efficient spatial orientation and motor responses to visual and auditory stimuli could not occur.

While the mechanics and dynamics of normal head movements have been studied to some extent, the neuroanatomical substrates controlling head movements in humans are not well delineated. Animal studies have suggested that the frontal eye fields, primary motor cortex (M1), basal ganglia, cerebellum and brainstem are involved in the control of head movements (Peterson and Richmond, 1988; Isa and Sasaki, 2002; Peterson, 2004). Local activation or inactivation of many of these regions in various animal species lead to activation of neck muscles and movements of the head, but how they relate to various head movements in humans is not clear (Evinger, 2005).

Some fundamental questions about the neural basis of head control in humans remain uncertain. It is not clear whether neck muscles are controlled by the ipsilateral, contralateral or bilateral cortical hemispheres (Bender et al., 1964; Balagura and Katz, 1980; Benecke et al., 1988; Gandevia and Applegate, 1988; Berardelli et al., 1991; Odergren and Rimpilainen, 1996; Thompson et al., 1997; Anagnostou et al., 2011). In addition, several studies have debated the location of the representation of neck muscles in the precentral gyrus. Evidence points to either a medial or a lateral neck motor region in relationship to the hand representation (Rasmussen and Penfield, 1948;

Penfield and Rasmussen, 1950; Obrador, 1953; Thompson et al., 1997; Kang et al., 2011; Pirio Richardson, 2014).

Studies of the neural basis of head movements face important methodological limitations, since most techniques available, such electrophysiology and neuroimaging, require the head to be still. The only neuroimaging study of normal individuals examined visually guided head movements in a small number of subjects, and the imaging sequences were actually collected between movements (Petit and Beauchamp, 2003). Thus, the relevance of these data for isolated head movements is uncertain.

The lack of fundamental information regarding the neural control of head movements is relevant to cervical dystonia (CD), a disorder characterized by involuntary contractions of neck muscles and abnormal head movements (Dauer et al., 1998; Albanese et al., 2013). In CD, the head can be deviated in any direction, with the most common abnormality involving turning right or left in the horizontal plane (torticollis) (Jankovic et al., 2015). Current understanding of the neuroanatomical basis of the disorder is limited. There is little or no evidence for overt structural anatomical abnormalities, since traditional clinical imaging methods such as computed tomography and structural magnetic resonance imaging (MRI) do not reveal any obvious abnormalities (Neychev et al., 2011; Standaert, 2011; Zoons et al., 2011). Furthermore, the few histopathology studies of CD have revealed no consistent abnormalities (Foerster, 1933; Grinker and Walker, 1933; Alpers and Drayer, 1937; Tarlov, 1970; Garcia-Albea et al., 1981; Zweig et al., 1986; Jankovic et al., 1987; Gibb et al., 1988; Zweig et al., 1988; Holton et al., 2008). Imaging investigations in acquired or sporadic CD have indicated microstructural defects in the somatosensory cortex, cerebellum and cervical spinal cord (Ghika et al., 1998; Naumann et al., 2000; LeDoux and Brady, 2003; Alarcon et al., 2004; Kumandas et al., 2006; Zadro et al., 2008; Pantano et al., 2011; Prell et al., 2013; Piccinin et al., 2014a; Ramdhani et al., 2014). On the other hand,

functional neuroimaging studies have pointed to abnormal function in multiple areas, including M1, premotor areas, somatosensory cortex, caudate nucleus, putamen, cerebellum, and thalamus (Galardi et al., 1996; Magyar-Lehmann et al., 1997; Naumann et al., 2000; de Vries et al., 2008; Obermann et al., 2008). Therefore, the findings by different imaging modalities suggest that subtle anatomical defects may occur in CD.

Considering the gap in knowledge about the control of head movements in normal individuals, we first addressed the neuroanatomical basis of normal movements using functional MRI (fMRI). Functional imaging methods require the head to remain still during scanning for optimal results. To overcome this requirement and allow investigation of head control, we used a novel approach: patterns of brain activity were examined during isometric head tasks. During an isometric task, muscle contractions are maintained for a few seconds in the absence of overt movement. Thus, by using isometric head rotation during fMRI scanning we were able to study the activation profile related to horizontal head rotation without the performance of actual head movements. Importantly, previous fMRI studies have investigated isometric hand movements in normal individuals, but not isometric head tasks (van Duinen et al., 2008; Keisker et al., 2010).

Next we addressed which of these regions might be responsible for abnormal head movements in CD, again using fMRI. The focus in both normal individuals and in CD was on rotational head movements, because these are the most commonly affected in CD. Prior studies in CD have investigated neural activation patterns during tasks with the upper extremities (Zoons et al., 2011), which do not provide information about brain activity associated with head control. Therefore, our studies represent the first fMRI investigation of a task directly related to the abnormal movements observed in CD.

Lastly, we investigated whether there are anatomical abnormalities in post-mortem tissue of CD individuals in comparison to age-matched controls. In these

studies, we examined several brain regions in six cases using immunostains for specific histopathological processes and quantitative comparisons between CD cases and controls. These studies were the largest and most comprehensive autopsy study ever conducted for CD.

Overall our work provides a more precise view of how the brain controls normal head movements and enabled the identification of potential cortical and subcortical regions affected in CD. By combining fMRI and histopathology methods, we employed well-established anatomically-oriented methods with complementary strengths. Identifying the areas involved in controlling neck muscles is relevant for the understanding of normal head movements, the pathophysiology of CD, the design of animal models for this disorder, and, eventually, the development of more effective treatments for CD.

Chapter 2: Imaging the neuroanatomical substrates for head movements in normal individuals*

2.1. Introduction

Head movements in humans are highly complex. At the most basic level, neck muscles have to support the head against gravity. Head movements also orient sensory structures of the head, especially those for vision, with both slow tracking movements and rapid redirections (Richmond et al., 1999). Furthermore, the head needs to be stable during eye-hand coordinated tasks and during movements or perturbations of the whole body. Finally, head movements are used by humans for nonverbal communications, like nodding and shaking the head, bowing, tilting the head backwards or sideways.

2.1.1. Directions of head movements

Humans are able to perform head movements in three main directions: flexion-extension (A), lateral tilt (B), and horizontal rotation (C) (**Figure 2.1**). Each of those movements occurs mainly in one plane of motion: flexion-extension occurs in the sagittal plane, lateral tilt happens in the coronal plane, and horizontal rotation occurs in the transversal plane.

* *Contents of this chapter were published as a peer reviewed manuscript in the Journal of Neuroscience. Reference: Prudente et al., J Neurosci*. 2015; 35(24): 9163-9172.

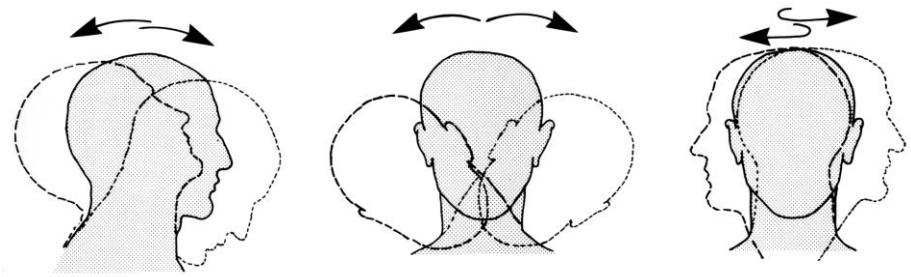

Figure 2.1: Directions of head movements. Flexion-extension (A), lateral tilt (B), and horizontal rotation (C). Modified from Peterson and Richmond (1988).

2.1.2. Muscles involved in head movements

Head movements are mediated by several superficial and deep muscles acting on seven cervical vertebrae and the cranium (Peterson and Richmond, 1988). During head movements, the forces of gravity require synergistic activation of different muscle patterns depending on the direction and speed of movement, the initial position of the head, the presence and magnitude of loading on the head, and the joints around which the movement is made.

Head movements are controlled by an intricate musculature that follows a similar organization in primates and most laboratory quadrupeds. The muscles primarily involved in head movements are arranged in three layers (**Figure 2.2**). The outermost layer of long muscles connects the skull to the shoulder girdle and it is formed by the sternocleidomastoid and trapezius. Under this outer layer a second set of muscles links the skull with the vertebral column and it is formed by the splenius capitis, longissimus capitis, semispinalis capitis, rectus capitis posterior major, rectus capitis posterior minor, rectus capitis anterior major, rectus capitis anterior minor, rectus capitis laterallis, obliquos capitis superior, and obliquos capitis inferior. A third and deeper set of muscles

closely interlinks the vertebrae of the cervical and thoracic region. This last layer is formed by the splenius cervicis, longissimus cervicis, and semispinalis cervicis.

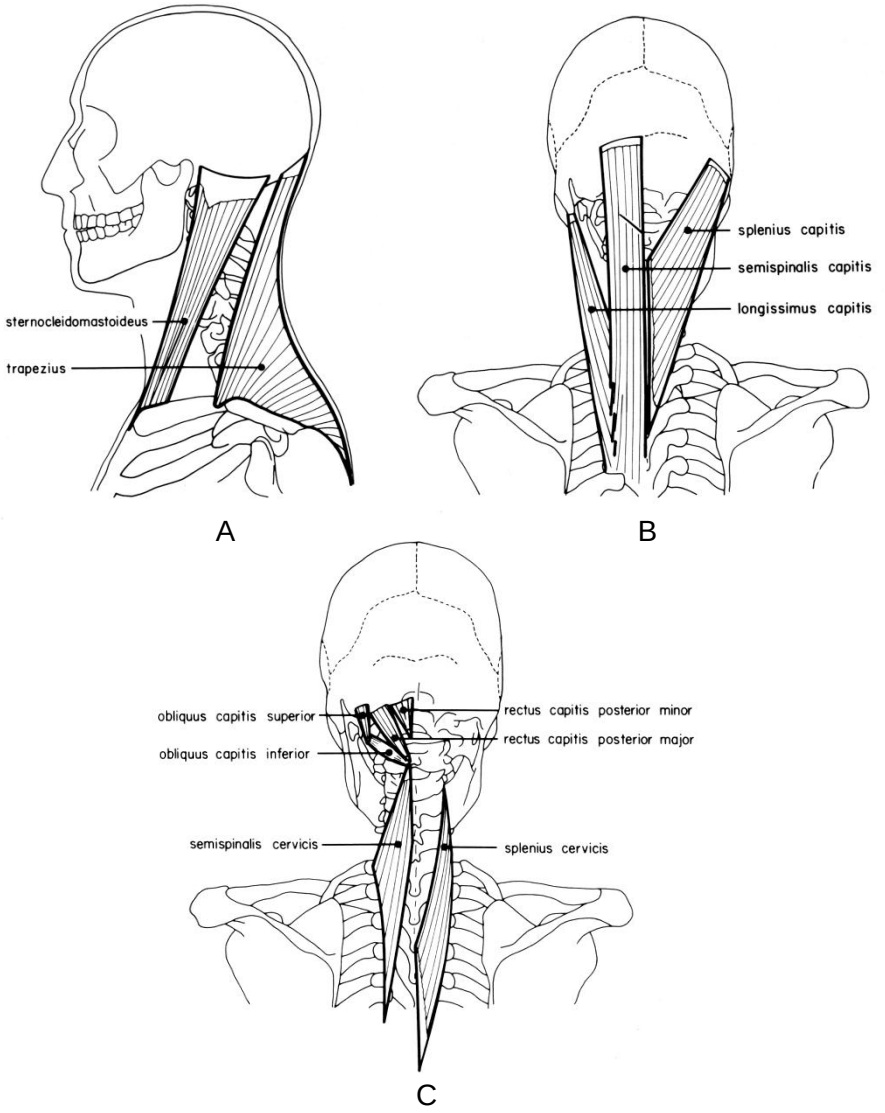

Figure 2.2: Neck muscles involved in head movements. Neck muscles are organized in 3 layers: superficial (A), intermediate (B) and deep (C). Modified from Peterson and Richmond (1988).

There are other neck muscles that are involved in head movements indirectly by stabilizing or moving the lower cervical and upper thoracic vertebrae. These muscles

include the interspinales, multifidus spinae, intertranvessari, longus cervicis, scalenus, rhomboideus major and minor and the levator scapulae.

2.1.3. Neuroanatomical substrates for head movements in humans

The different types of head movements performed by humans (posture, voluntary, tracking, saccades, reflexive) suggest that they may require distinct control mechanisms and different neural pathways, similar to what has been proposed for eye movements. Animal and human studies have suggested that specific regions in the cerebral cortex, basal ganglia, cerebellum and brainstem are involved in the control of head movements (Peterson, 2004). However, how these different regions contribute to head movements remains largely unexplored.

2.1.3.1. Primary motor cortex

Regarding the primary motor cortex (M1), two fundamental questions remain unanswered. First, it is still debated whether head movements are controlled ipsilaterally (Balagura and Katz, 1980; Anagnostou et al., 2011), contralaterally (Gandevia and Applegate, 1988) or bilaterally (Benecke et al., 1988; Berardelli et al., 1991; Thompson et al., 1997) (**Table 2.1**). Second, the exact location of the neck area in the somatotopic organization of M1 is not clear (**Figure 2.3**). Classic experiments that mapped M1 by direct electrical stimulation suggested that the neck area is represented laterally on the convexity of the cerebral hemisphere, between the finger and face areas (Rasmussen and Penfield, 1948; Penfield and Rasmussen, 1950). In contrast, other studies have suggested that the neck area is located more medially, between the representations of the trunk and arm (Obrador, 1953; Thompson et al., 1997; Kang et al., 2011; Pirio Richardson, 2014). This last location corresponds to the representation

of the head and neck in the somatosensory homunculus (Penfield and Rasmussen, 1950).

Table 2.1: Prior reports of the hemisphere controlling head movements in humans

Ipsilateral	Contralateral	Bilateral
Beevor (1909)*	Hanajima et al. (1998)**	Penfield and Rasmussen (1950)**
Balagura and Katz (1980)*	Kang et al. (2011)*	Benecke et al. (1988)**
Willoughby and Anderson (1984)*		Gandevia and Applegate (1988)**
Mastaglia et al. (1986)*		Berardelli et al. (1991)**
Manon-Espaillat and Ruff (1988)*		Odergren and Rimpilainen (1996)**
Anagnostou et al. (2011)*		Odergren et al. (1997)**
		Thompson et al. (1997)**
		DeToledo and Dow (1998)*

The hemisphere controlling movements was taken from the results reported by each study, because the interpretations sometimes did not match the actual results provided. *Studies of stroke or epilepsy cases. **Studies of electrical or magnetic stimulation of the precentral gyrus.

2.1.3.2. Other brain regions

Evidence for the role of other brain regions in head movements is even more limited. Motor areas such as the premotor cortex and supplementary motor area may be active during head movements, similarly to movements of the limbs. In addition, electrophysiological observations in humans and non-human primates suggest that the frontal and supplementary eye fields also are involved in head movements (Bizzi and Schiller, 1970; Petit and Beauchamp, 2003; Elsley et al., 2007; Proudlock and Gottlob, 2007; Goonetilleke et al., 2011). Yet, there is still uncertainty on whether the eye fields control eye-head coordinated movements or independent eye and head movements.

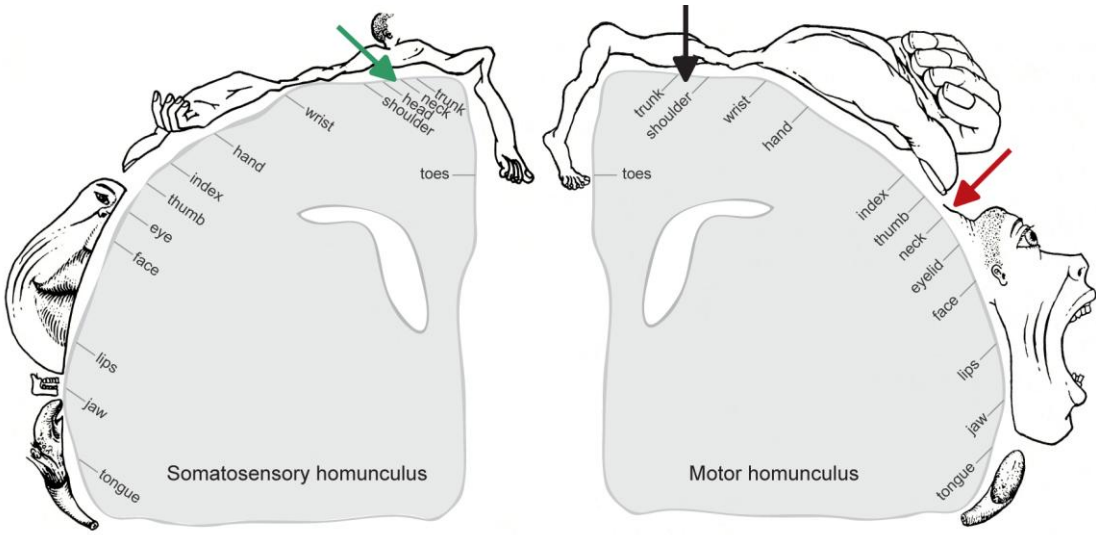

Figure 2.3: Representation of the neck region in the motor and sensory homunculi according to different studies. The neck motor area identified by Penfield and Rasmussen (1950) is indicated by the red arrow and has been replicated in many textbooks of neurobiology. The black arrow indicates the neck area suggested by other studies (Obrador, 1953; Thompson et al., 1997; Kang et al., 2011). The green arrow represents the neck area in the somatosensory homunculus. Modified from Penfield and Rasmussen (1950).

Anatomical tracing and electrophysiological investigations have implied somatotopic representations in the basal ganglia and cerebellum (Gerardin et al., 2003; Manni and Petrosini, 2004; Nambu, 2011; Mottolese et al., 2013), but data concerning the representation of the head or neck are limited. Studies in animals have revealed an essential role of the interstitial nucleus of Cajal and surrounding midbrain regions in the control of head movements (Hassler and Hess, 1954; Foltz et al., 1959; Malouin and Bedard, 1982; Klier et al., 2002; Farshadmanesh et al., 2007; Klier et al., 2007; Farshadmanesh et al., 2008). Furthermore, there are several subcortical areas that have direct projections to the cervical spinal cord and, consequently, may be involved in controlling neck muscles. These pathways include the vestibulospinal, reticulospinal, interstitiospinal, tectospinal and fastigiospinal tracts (Peterson, 2004). However, it is important to note that these subcortical tracts have been identified mainly with targeted

injections of classic neuronal tracers in rodents and cats, animals that differ from humans in terms of head posture and movements. As a result, the relevance of those subcortical tracts for the neural control of normal head movements in humans remains unclear.

2.1.4. Limitations of studying the neuroanatomical substrates for head movements

There are several reasons for the lack of conclusive information on the neural systems controlling head movements in humans. The classical mapping studies involving electrical stimulation of the exposed motor cortex could not be conducted with the head free to move. More recent neurosurgical mapping studies aimed at delineating surgical targets use a fixed frame to hold the head and, therefore, head movements are restrained. Similarly, animal studies rely on fixed head preparations. Studies attempting to use transcranial magnetic stimulation (TMS) have shown that consistent neck responses are difficult to elicit in all subjects (Hanajima et al., 1998; Pirio Richardson, 2014). Finally, neuroimaging methods cannot be conducted when the head is moving because head motion degrades data quality.

2.2. Objectives and significance

The purpose of the following experiments was to determine the neuroanatomical substrates for head motor control in humans using an isometric head task during functional magnetic resonance imaging (fMRI). In isometric tasks, muscles are activated without actual movements because the joint angle and muscle length do not change during contraction. Prior studies have shown that isometric hand contractions activate similar brain regions as actual hand movements (van Duinen et al., 2008; Keisker et al., 2010), suggesting that isometric head tasks can be used to explore the patterns of brain

activation related to head movements. Therefore, isometric head tasks may represent a method to bypass the technical limitations of assessing head movements during fMRI.

These experiments will provide some fundamental information regarding the neural systems controlling head movements in humans, which is a prerequisite for understanding disorders that affect the control of head movements, such as head tremor and cervical dystonia.

2.3. Materials and methods

2.3.1. Participants

All procedures were approved by the Emory University Institutional Review Board, and all participants gave informed consent. All subjects were neurologically normal and had the ability to perform a full range of head movements in all directions. Participants were excluded if they had significant orthopedic problems affecting the cervical spine, difficulty lying in the supine position, abnormal head movements at rest, significant neck pain, contraindications for MRI, or untreated psychiatric problems. Eighteen participants were scanned, but all data from one was excluded due to excessive motion (see below). Thus, data from 17 participants (12 women, 5 men) were included in the final analyses; their mean age was 56.8±14.5 years (range 30-74 years); 14 were right-handed and 3 were left-handed.

2.3.2. MR scanning

Scans were performed on a 3 Tesla Siemens TIM™ Trio scanner (Siemens Medical Solutions, Malvern, PA) using a quadrature transmit-receive head coil at the Emory Biomedical Imaging Technology Center. Total scanning time was approximately 25 minutes. Functional images with blood oxygenation level dependent (BOLD) contrast were acquired using a T2*-weighted single-shot gradient-recalled echoplanar imaging

(EPI) sequence with the following parameters: 30 axial slices of 4 mm thickness, repetition time (TR) 2040 ms, echo time (TE) 30 ms, flip angle (FA) 90°, in-plane resolution 3.4×3.4 mm^2, and in-plane matrix 64×64. Following the functional imaging runs, a 3D T1-weighted sequence (MPRAGE) of 176 sagittal slices of 1 mm thickness was obtained with TR 2300 ms, TE 3 ms, inversion time 1100 ms, FA 8°, in-plane resolution 1×1 mm^2, and in-plane matrix 256×256. Acoustic noise attenuation was provided by headphones (Etymotic Research, Elk Grove Village, IL) that also were used to convey instructions and audio cues for each task.

2.3.3. Experimental design

Scanning was conducted during isometric head or hand tasks. All tasks were practiced outside the scanner first. Head tasks consisted of isometric horizontal head rotation to the right or left. Subjects were instructed to perform an isometric sub-maximal contraction in the direction of head rotation to either side. Actual head movements during tasks were prevented by firm foam padding around the head and restraining straps within the head coil, placed tightly across the forehead and chin. In order to avoid eye movements, subjects were asked to look at all times at a white cross projected on a black screen, viewed via a mirror mounted inside the head coil.

Hand tasks were investigated as a positive control. Hand movements were chosen because they reliably give robust signals and because their cortical representations have been more extensively mapped than other body regions closer to the neck, such as the shoulder or lower face. Hand tasks consisted of isometric wrist extension with one or the other hand, the arm being positioned in a neutral position between pronation and supination. Note that right wrist extension was therefore associated with a rightward movement effort and left wrist extension with a leftward movement effort, matching the corresponding directions for head rotation. Participants

were asked to extend the wrist of either hand with a sub-maximal contraction against sandbags placed along the lateral aspect of both arms and hands. The sandbags prevented any changes in joint angles and ensured isometric contractions.

Functional data were collected during 2 runs. A block design was used with alternating blocks of active tasks and rest periods (**Figure 2.4**). Each run consisted of 16 active blocks (4 per condition), separated by rest periods of 12.24 s; a rest period also occurred at the start and end of each run. The task conditions were: isometric head rotation to the right, isometric head rotation to the left, isometric right wrist extension, and isometric left wrist extension. Task blocks were interleaved in a predetermined pseudo-random sequence. Each active block lasted 20.4 s and involved 4 repetitions of a single task separated by periods of 1 s.

The timing of stimulus presentations was provided by audio cues controlled by Presentation software (Neurobehavioral Systems, Albany, CA). Immediately preceding each block, a verbal cue was presented for 1 s to prepare the subject for the next condition. The following cues were used: “relax”, “press right cheek”, “press left cheek”, "press right wrist" or “press left wrist”. Empirically, these cues were found in pilot studies to lead to less head movements compared with instructions to “rotate” or “turn” the head. Timing for each movement during task blocks was cued by beeps played at a frequency of 0.2 Hz.

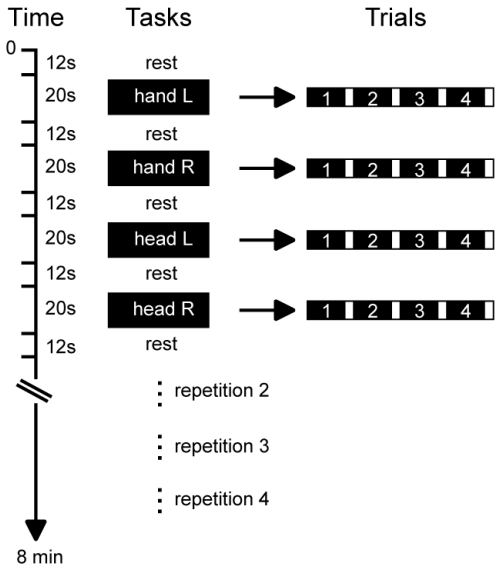

Figure 2.4: Experimental design. Tasks consisted of isometric head rotations to the right or left, and right or left wrist extensions. Each active block consisted of 4 trials of the same task. The sequence of active tasks blocks was pseudo-randomly repeated 4 times within each run. L, left; R, right.

2.3.4. Electromyography (EMG)

Because the presence or absence of actual movements could not verified by visualizing during scanning, compliance with isometric tasks during practice and scanning was confirmed by surface EMG of the sternocleidomastoid (SCM) and the extensor carpi ulnaris (ECU) muscles bilaterally (**Figure 2.5**). The SCM is an agonist in contralateral horizontal rotation of the head, while the ECU is an agonist for wrist extension. Recordings were collected using MRI-compatible electrodes and Brain Vision Recorder version 1.20 (Brain Products GmbH, Munich, Germany). EMG signals were recorded at a sampling rate of 5000 Hz. EMG procedures, electrode placement and safety guidelines followed published protocols (van Duinen et al., 2008; Criswell and Cram, 2010; Noth et al., 2012). The safety guidelines dictated use of the transmit-receive head coil (see above) rather than other available coils permitting higher-resolution, parallel imaging. EMG signals were MR corrected, filtered with a low-cutoff

frequency of 20 Hz and rectified using Brain Vision Analyser version 2.0 (Brain Products GmbH, Munich, Germany). Recordings were verified during scans and offline. After all data were collected, EMG signals were evaluated by an observer blinded to tasks to verify activatation of the correct muscles.

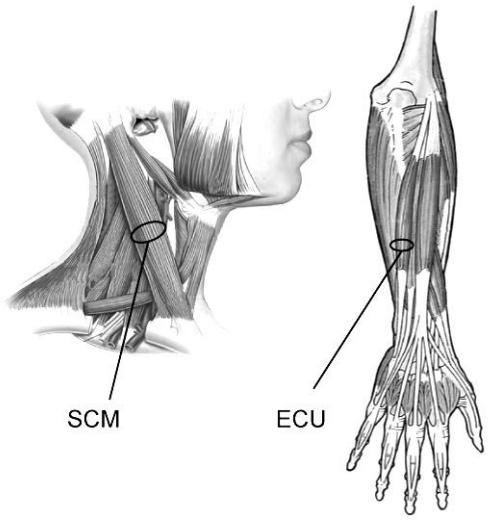

Figure 2.5: Sternocleidomastoid (SCM) and extensor carpi ulnaris (ECU) muscles. Modified from: http://rpm-therapy.com/2011/trigger-point-muscle-sternocleidomastoid/sternocleidomastoid2/ and www.rudyard.org.

2.3.5. Head motion correction

Several measures were taken to ensure that head motion was minimized. These included practice periods before scans, stabilization of the head with firm supports in the scanner, motion correction of imaging data, and analysis of actual head motion during scans. Motion correction of imaging data was completed in two stages to account for head motion during scanning.

The first motion correction step occurred during data acquisition using the scanner's inbuilt software Prospective Acquisition Correction (3D-PACE) (Thesen et al., 2000). 3D-PACE allows detection and correction of head motion during data acquisition and is able to compensate for translation (displacement) and rotation in the x, y and z planes within a single scanning run. With 3D-PACE, each brain volume is compared

with the previous one and head motion is calculated and displayed in real-time. For acquisition of the next dataset, slice position and orientation are adjusted according to the altered position of the head. Thus, the correction of motion is done prospectively on the actual imaging data acquired every TR.

The second motion correction step involved the alignment of brain volumes using sinc interpolation in BrainVoyager to account for head movements that occurred between different runs. When multiple runs of a task are collected during a scanning session, 3D-PACE corrects for movement within each run. However, subjects may potentially move between runs. To compensate for this potential between-run movement, an intra-session alignment of all brain volumes was conducted. For this alignment, a target brain volume was selected from the functional run collected closest in time to the structural scan because images collected during this run had the smallest variance in space with images from the structural scan. All other brain volumes within the scanning session were aligned to this target volume in BrainVoyager, using an algorithm that matches structure better than the algorithm used by 3D-PACE. This intra-session alignment of all brain volumes over a scanning session produces the most precise alignments.

2.3.6. Head motion analysis

In addition to the motion correction of imaging data, we also examined actual head motion during scanning. This analysis determined how much motion correction was required by 3D-PACE, since the software does not store a log file with the movement parameters required for correction. We examined the “raw” data (not corrected by 3D-PACE) in BrainVoyager, which generated motion log files with the 6 motion parameters representing the amplitude of head movement that actually occurred during scanning. These motion log files from BrainVoyager were exported to MATLAB

R2014a (version 8.3.0.532, The MathWorks Inc., USA) and analyzed with custom scripts. In MATLAB, rotation values were transformed from degrees to millimeters using each subject's brain dimensions for the transformation. Next, all data were evaluated for movement amplitude in each plane. Additional analyses included searching for trends in head movement direction and task-related head motion.

In keeping with prior recommendations for acceptable head motion during fMRI scanning, we used a threshold of 1.75 mm (approximately half the size of a functional voxel) as the maximum head motion allowed in any plane (Poldrack et al., 2011). Consequently, if head motion was greater than 1.75 mm, either during an active task period or during rest, we selected a continuous sequence of blocks including the instant with excessive head movement and beginning and ending with a rest period. This continuous sequence of blocks was then removed from the final data analysis. We attempted to balance block numbers for each task within a run to minimize potential contributions of unbalanced trials numbers on activation magnitude maps. Using these criteria, all data for one subject were excluded because substantial portions of the data showed excessive head movement. For 3 other subjects, data for 1-3 blocks of active and rest periods were excluded because of excessive head motion

2.3.7. Imaging data analysis

Image processing and analysis was performed using BrainVoyager QX 2.8.4 (Goebel et al., 2006). Individual functional data were preprocessed utilizing cubic spline interpolation for slice scan time correction, sinc interpolation for intra-session alignment of functional volumes (as described above), and high-pass temporal filtering to 2 cycles per run to remove slow drifts in the data. Anatomic 3D images were processed, co-registered with the functional data, and transformed into Talairach space (Talairach and Tournoux, 1988). For group analyses, the data were spatially smoothed with an

isotropic Gaussian kernel (full-width half-maximum 4 mm) (White et al., 2001) and normalized across runs and subjects with the percent signal change transformation. BOLD signal time-courses were obtained by averaging at individual data points across blocks of the same type and then averaging across participants.

We used a two-stage strategy to delineate brain regions involved in the control of head movements. Because our primary aim was to identify the hemisphere and regions of M1 associated with isometric head rotation to the right or left, the first stage was a region of interest (ROI) approach focused on the precentral gyrus, which includes M1. The second stage was an exploratory whole-brain analysis to investigate which regions other than the precentral gyrus were active during isometric head rotation. Statistical analyses consisted of individual analyses using the general linear model method to model the hemodynamic response during active blocks in comparison to baseline, followed by group-level analysis treating participant as a random variable. Group activations during isometric head rotation to either side were contrasted with the rest condition using Student's t-test on a voxel-by-voxel basis with a voxel-wise significance level of $p<0.05$, corrected for multiple comparisons with a 3D extension of the cluster-correction method (Cluster Threshold Estimator plugin in BrainVoyager) (Forman et al., 1995). Specifically for the ROI approach, the bilateral precentral gyrus was used as a mask in the general linear model analysis. This mask was defined using known anatomical landmarks to identify its boundaries (central sulcus, precentral sulcus, longitudinal fissure, cingulate sulcus and lateral sulcus).

Group results for the ROI and whole-brain analyses were displayed on an “averaged anatomical brain” created in BrainVoyager by first selecting a representative (target) Talairach-normalized brain from the 17-participant group. We then individually aligned the 16 remaining participants' Talairach-normalized brains to the target brain (co-registration to match gyral/sulcal pattern, followed by sinc transformation). The 16

transformed brains were then averaged. Finally, the 16-participant average brain was combined with the single target brain, creating a Talairach template which was used to display the activations for the 17-participant group. Activations were localized with respect to 3-dimensional anatomy with the help of MRI atlases (Duvernoy, 1999; Schmahmann et al., 1999; Cho, 2010). Considering that handedness may affect brain activation maps, fMRI data for the right-handed subgroup (n=14) were examined separately, but no major differences were observed in comparison to the whole group. For this reason, the results presented here represent the findings for all 17 participants.

2.4. Results

2.4.1. Task confirmation

Participants were able to complete all tasks adequately as judged by observations during training and EMG during scanning. For 2 subjects, appropriate task performance was verified only manually during training because EMG could not be conducted. For the remaining participants, the appropriate muscles for each task were activated correctly on average of 96.9 percent of all trials (**Table 2.2**).

Table 2.2: Task confirmation with electromyography

Muscle	Task	Active (%)
right ECU	wrist extension, right	99.0
left ECU	wrist extension, left	97.1
right SCM	head rotation, left	97.1
left SCM	head rotation, right	94.2

Muscle activity is shown as percent of trials in which there was obvious muscle activation in comparison to background. ECU, extensor carpi ulnaris; SCM, sternocleidomastoid.

2.4.2. Head motion during scans

To verify that isometric head rotation was not associated with significant head movements, head translation and rotation were examined in all 3 planes using the

uncorrected head motion data. For each participant, the analysis generated 1 measurement for each of the 6 movement parameters for every TR analyzed, yielding 53,244 data points for the whole group. After exclusion of 1-3 blocks with excessive motion for 3 participants (see Materials and Methods), the final analysis was completed with a total of 49,788 data points. **Figure 2.6** shows the distribution of head motion measurements and their amplitudes. The vast majority of head motion (99.9%) was below our threshold of 1.75 mm, which is considered within acceptable limits for most fMRI studies (Poldrack et al., 2011). We also verified the distribution and average of head motion amplitudes during rest, hand and head tasks for all 3 planes of translation and rotation. These measurements suggested that tasks and rest periods had comparable movement during scanning (**Figure 2.7** and **Table 2.3**).

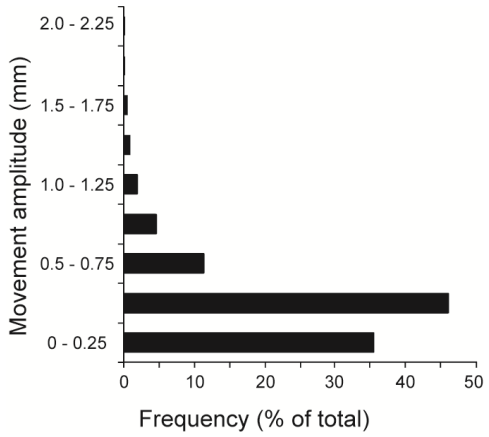

Figure 2.6: Distribution of total head motion measurements and their amplitudes for all subjects. The y axis represents the amplitude of each movement measured in mm. The x axis shows the distribution of head motion measurements as % of total values generated (n=17 subjects; total data points: 49,778). Measurements for translational and rotational movements were combined.

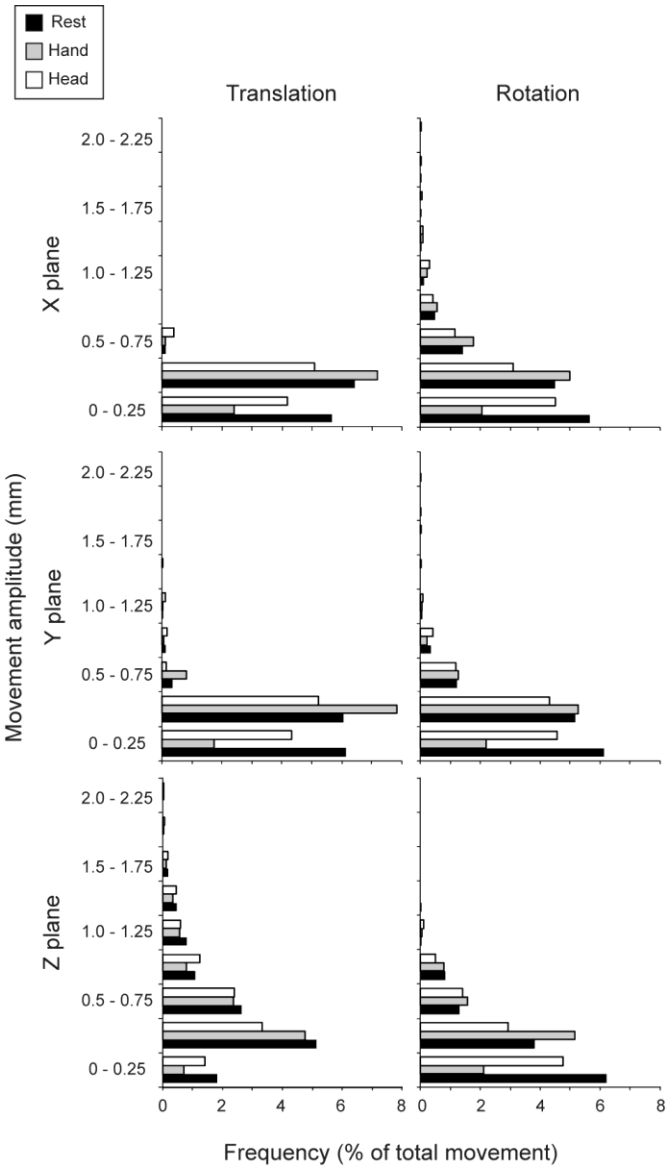

Figure 2.7: Head movements during rest, hand and head tasks. The y axis represents the amplitude of each movement measured in mm. The x axis shows the distribution of head motion measurements as a percentage of total values generated (n=17 subjects, total data points: rest: 9,654; hand tasks: 7,620; head tasks: 7,620). Translational and rotational movements are shown for all 3 planes separately (x, y and z).

Table 2.3: Head motion during scans

Translation (mm)				Rotation (mm)			
Task	Plane	Mean	SD	Task	Plane	Mean	SD
rest	x	0.08	0.07	rest	x	0.28	0.26
	y	0.11	0.12		y	0.16	0.17
	z	0.33	0.31		z	0.21	0.17
hand	x	0.08	0.06	hand	x	0.26	0.23
	y	0.11	0.11		y	0.15	0.14
	z	0.32	0.30		z	0.21	0.16

Translation (mm)				Rotation (mm)			
Task	Plane	Mean	SD	Task	Plane	Mean	SD
	x	0.10	0.08		x	0.31	0.31
head	y	0.13	0.14	head	y	0.19	0.17
	z	0.37	0.33		z	0.24	0.18

SD, standard deviation.

2.4.3. ROI analysis of hand tasks

Isometric hand tasks were evaluated to provide a positive control and activation landmark for subsequent head tasks. Activation maps, Talairach coordinates and BOLD signal curves for hand tasks in comparison to baseline are shown in **Figure 2.8** and **Table 2.4**. Consistent with prior studies, isometric wrist extension with the right or left hand showed significant activation of contralateral precentral gyrus in the area known as the "hand knob" (Yousry et al., 1997). For isometric right wrist extension, significant activation also was observed in a precentral area located more laterally and ventrally to the hand knob.

2.4.4. ROI analysis of head tasks

Activation maps and BOLD signal curves for head tasks in comparison to baseline are shown in **Figure 2.8**; Talairach coordinates are given in **Table 2.4**. Isometric head rotation to the right showed significant activation of 2 foci in the contralateral precentral gyrus: one was medial and anterior to the hand knob, whereas the other was located lateral and ventral to the hand knob. In contrast, isometric head rotation to the left showed significant activation of bilateral precentral gyrus with 2 foci in each hemisphere: one located medial and anterior to the hand knob, and the other lateral and ventral to the hand knob. For head rotation to either side, the location of the medial precentral foci in each hemisphere was symmetrical. However, the location of the lateral foci did not exactly match between hemispheres (**Figure 2.8**), which may

have may be due to anatomical variations between participants or true asymmetry between hemispheres.

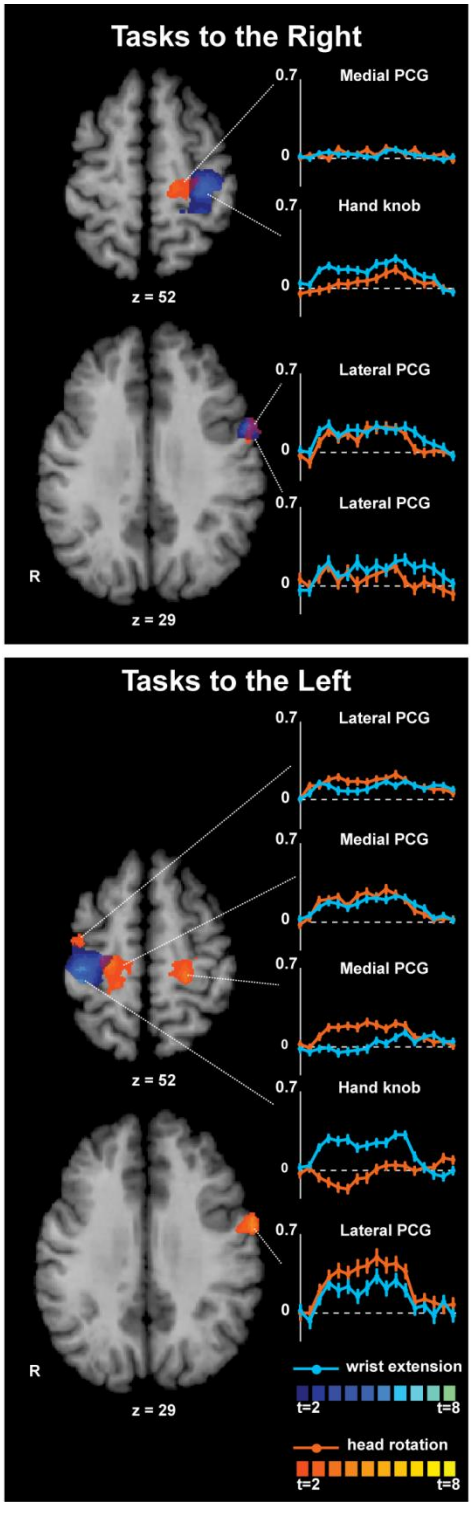

Figure 2.8: Region of interest analysis of the precentral gyrus for isometric wrist extension and head rotation tasks in comparison to rest. Activation maps for hand and head tasks to the same side were superimposed to allow comparisons of the anatomical distribution of activation patterns. Areas with significant activation are shown in blue for hand tasks and in orange for head tasks ($p<0.05$, corrected for multiple comparisons). Color t-scales for each condition are shown at the bottom. Blood oxygenation level dependent (BOLD) signal curves for each focus of activation show the average percent signal change over time (y axis: % BOLD response; x axis: time measured in scans, from -1 to 15 scans). The dashed line shown in each curve represents 0% or baseline level for the BOLD response. PCG, precentral gyrus.

Table 2.4: Talairach coordinates, maximum *t*-values (t_{max}), and *p*-values for the ROI analysis

Isometric task	PCG Region	Hemi	x	y	z	t_{max}	*p*
Wrist extension, right	hand knob	L	-27	-28	49	5.32	0.00
	lateral/ventral	L	-54	5	31	4.90	0.00
Wrist extension, left	hand knob	R	36	-25	49	6.17	0.00
Head rotation, right	medial	L	-15	-22	49	3.42	0.00
	lateral/ventral	L	-54	-1	31	3.69	0.00
Head rotation, left	medial	R	21	-22	52	3.83	0.00
	medial	L	-21	-28	52	3.94	0.00
	lateral/ventral	R	30	-13	46	3.57	0.00
	lateral/ventral	L	-57	2	34	5.76	0.00

Hemi, hemisphere; L, left; M1, PCG, precentral gyrus; R, right; ROI, region of interest.

It is noteworthy that the precise anatomical boundaries for M1 proper, the dorsal premotor area (PMd), and the ventral premotor area (PMv) in humans are only partly delineated (Picard and Strick, 2001; Rizzolatti et al., 2002; Mayka et al., 2006). Consequently, it is not clear whether the medial precentral area identified in head tasks represents M1 or lies within PMd. Similarly, it is not clear whether the lateral precentral focus in the left hemisphere activated during isometric head rotation to both sides and during right wrist extension should be considered as part of M1 or PMv. The lateral precentral focus in the right hemisphere most likely belongs to PMv because of its location on the precentral sulcus. Considering that M1, PMd and PMv have direct projections to the spinal cord, these three areas can potentially control neck muscles. Therefore, regardless of the precise cortical areas, our results suggest that the medial and lateral precentral areas are involved in isometric head rotation.

The BOLD signal time courses for each condition (**Figure 2.8**) showed that activation in the left lateral precentral focus was not specific to body region during rightward tasks. In contrast, there appeared to be greater selectivity (albeit relative) for the head in both left and right lateral precentral foci during leftward tasks. BOLD signal time courses for the left medial precentral focus showed low, non-selective activity

during rightward tasks but seemed more head-specific for leftward tasks; whereas the right medial precentral focus was non-selectively active for leftward tasks.

2.4.5. Whole-brain analysis of hand tasks

Maps and Talairach coordinates of activations for hand tasks in comparison to baseline are shown in **Figure 2.9** and **Table 2.5**. Isometric right wrist extension evoked contralateral activation in the hand knob, supplementary motor area (SMA), PMd, PMv, postcentral gyrus, parietal and frontal operculum, and putamen. There also was significant activation of the ipsilateral cerebellar hemisphere in lobules IV and V. Isometric left wrist extension activated the contralateral hand knob, bilateral SMA, contralateral postcentral gyrus and parietal operculum. There was significant activation of the ipsilateral cerebellar hemisphere, again mainly in lobules IV and V. These results are consistent with prior studies of both isometric and actual hand movements (Picard and Strick, 2001; Gerardin et al., 2003; van Duinen et al., 2008; Keisker et al., 2010; Mottolese et al., 2013)

2.4.6. Whole-brain analysis of head tasks

Maps and Talairach coordinates of activations for head tasks in comparison to baseline are shown in **Figure 2.9** and **Table 2.6**. Isometric head rotation to the right significantly activated the contralateral precentral gyrus, the bilateral SMA, anterior insula, frontal operculum, and posterior putamen. Ipsilateral activation was observed in the mid-insula, anterior putamen, globus pallidus, and ventrolateral thalamus. No significant activation was observed in the cerebellum. This may be due to threshold effects, since the uncorrected maps revealed activation of bilateral cerebellum. Isometric head rotation to the left evoked bilateral activation of M1, SMA, anterior and mid-insula, frontal and parietal operculum, putamen, globus pallidus, and postcentral

gyrus. In addition, there was significant activation of the ipsilateral caudate, ventrolateral thalamus and middle occipital gyrus, contralateral pre-SMA and middle cingulate gyrus. Cerebellar activation occurred in the ipsilateral hemisphere (lobules IV, V, VI, Crus I and dentate nucleus) and spread slightly into the adjacent vermis (vermal lobules V and VI).

The BOLD signal curves for each condition (**Figure 2.9**) suggested that putaminal activation was more prominent ipsilaterally than contralaterally during head rotation to either side. The BOLD curves also showed that the ipsilateral lobules VI and Crus I demonstrated specificity for isometric head rotation to the left in comparison to left wrist extension.

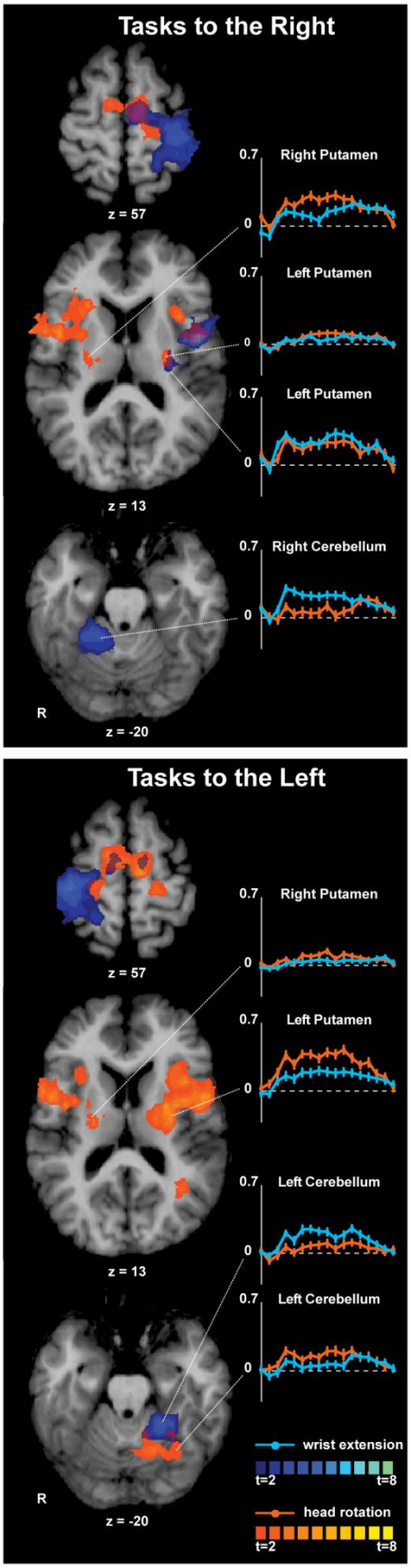

Figure 2.9: Whole-brain analysis for isometric wrist extension and head rotation tasks in comparison to rest. Activation maps for hand and head tasks to the same side were superimposed to allow comparisons of the anatomical distribution of activation patterns. Areas with significant activation are shown in blue for hand tasks and in orange for head tasks ($p<0.05$, corrected for multiple comparisons). Color t-scales for each condition are shown on the right. Blood oxygenation level dependent (BOLD) signal curves from selected sites show the average percent signal change of the BOLD response over time (y axis: % BOLD change; x axis: time measured in scans, from -1 to 15 scans). The dashed line shown in each curve represents 0% or baseline level for the BOLD response.

Table 2.5: Talairach coordinates, maximum *t*-values (t_{max}) and *p*-values for whole-brain analyses of hand tasks versus baseline

Isometric task	Region	Hemi	x	y	z	t_{max}	*p*
Wrist extension, right	SMA	L	-6	-13	52	7.02	0.00
	PMd	L	-21	-19	64	6.07	0.00
	PMv	L	-54	5	22	5.75	0.00
	postcentral gyrus	L	-33	-28	46	5.68	0.00
	parietal operculum	L	-60	-34	34	5.78	0.00
	frontal operculum	L	-45	-1	13	5.73	0.00
	putamen	L	-27	-10	4	4.25	0.00
	cerebellum, lobule IV	R	9	-43	-14	5.12	0.00
	cerebellum, lobule V	R	27	-40	-23	5.76	0.00
Wrist extension, left	SMA	L	-9	-10	55	3.18	0.01
	SMA	R	3	-10	46	4.36	0.00
	SMA, superior	R	6	-13	64	3.43	0.00
	postcentral gyrus	R	36	-31	49	5.99	0.00
	parietal operculum	R	51	-22	37	4.60	0.00
	cerebellum, lobule IV-V	L	-9	-46	-14	4.08	0.00
	cerebellum, lobule V	L	-18	-43	-17	4.46	0.00
	cerebellum, lobule V-VI	L	-27	-40	-23	4.53	0.00

Hemi, hemisphere; L, left; PMd, dorsal premotor area; PMv, ventral premotor area; R, right; SMA, supplementary motor area.

Table 2.6: Talairach coordinates, maximum *t*-values (t_{max}) and *p*-values for whole-brain analyses of head tasks versus baseline

Isometric task	Region	Hemi	x	y	z	t_{max}	*p*
Head rotation, right	SMA	L	-6	-13	52	4.09	0.00
	SMA	R	9	-7	55	3.12	0.01
	anterior insula	L	-33	11	13	4.16	0.00
	anterior insula	R	24	20	13	4.12	0.00
	mid-insula	R	36	-1	7	3.65	0.00
	frontal operculum	L	-39	8	7	4.32	0.00
	frontal operculum	R	42	-1	13	4.72	0.00
	putamen, anterior	R	27	-1	7	4.24	0.00
	putamen, posterior	L	-27	-16	13	3.41	0.00
	putamen, posterior	R	24	-10	7	4.94	0.00
	globus pallidus	L	18	-6	4	3.46	0.00
	ventrolateral thalamus	L	15	-10	4	3.44	0.00
	ventrolateral thalamus, inferior	L	18	-16	13	2.47	0.03
Head rotation, left	SMA	L	-9	-13	55	5.07	0.00
	SMA	R	9	-13	61	4.47	0.00
	Pre-SMA/ cingulate gyrus	R	8	-1	40	2.89	0.01
	cingulate sulcus	L	-18	11	34	2.97	0.01
	posterior cingulate sulcus	R	21	-34	31	2.80	0.01
	postcentral gyrus	R	60	-19	31	3.61	0.00
	parietal operculum	R	57	-31	31	3.98	0.00

Isometric task	Region	Hemi	x	y	z	t_{max}	*p*
Head rotation, left (cont.)	postcentral gyrus / parietal operculum	L	-61	-34	34	5.02	0.00
	postcentral gyrus / parietal operculum	L	-57	-28	25	4.79	0.00
	STS/MOG	L	-30	-55	19	3.79	0.00
	frontal operculum	L	-48	2	13	4.83	0.00
	frontal operculum	R	39	-4	13	4.64	0.00
	anterior insula	L	-36	11	7	6.31	0.00
	anterior insula	R	30	14	10	2.97	0.01
	mid-insula	L	-39	-1	4	6.49	0.00
	mid-insula	R	33	-1	10	3.55	0.00
	caudate head	L	-15	-1	31	4.20	0.00
	ventrolateral thalamus	L	-15	-13	4	4.28	0.00
	putamen, mid	L	-27	-13	10	4.94	0.00
	putamen, mid	R	24	-4	13	2.79	0.01
	putamen, posterior	L	-27	-10	4	6.26	0.00
	putamen, superior	R	24	-10	16	4.40	0.00
	globus pallidus	L	-18	-10	7	4.08	0.00
	globus pallidus	R	21	-14	13	3.57	0.00
	cerebellum, lobule VI	L	-15	-61	-17	4.58	0.00
	cerebellum, crus I	L	-36	-49	-39	3.92	0.00
	dentate nucleus	L	-18	-34	-32	3.32	0.00

Hemi, hemisphere; L, left; MOG, middle occipital gyrus; R, right; SMA, supplementary motor area; STS, superior temporal sulcus.

2.5. Discussion

Our studies demonstrate that isometric wrist extension activates similar brain regions as prior studies have shown for actual hand movements (Picard and Strick, 2001; Gerardin et al., 2003; van Duinen et al., 2008; Keisker et al., 2010; Mottolese et al., 2013). These results open the door to using fMRI to identify brain regions involved with head movements. Overall, isometric head rotation elicited bilateral activation in the precentral gyrus, SMA, insula, frontal operculum and putamen, as well as ipsilateral activation in the thalamus and cerebellum. Our findings clarify some of the conflicting results obtained with other methods regarding the hemisphere controlling head movements and the location of the regions controlling neck muscles in the motor homunculus, and also point to other brain areas involved in head movements in humans.

2.5.1. Is M1 control ipsilateral, contralateral or bilateral?

The hemisphere controlling head movements has been debated extensively, with previous studies providing evidence for ipsilateral, contralateral or bilateral control (**Table 2.1**). These differences may be due to the different methods used. For instance, nearly all studies suggesting ipsilateral control were based on the assessment of neck muscle weakness after stroke (Beevor, 1909; Balagura and Katz, 1980; Willoughby and Anderson, 1984; Mastaglia et al., 1986; Manon-Espaillat and Ruff, 1988; Anagnostou et al., 2011). In contrast, most studies suggesting bilateral or contralateral control used electrical or magnetic stimulation in healthy individuals (Penfield and Rasmussen, 1950; Benecke et al., 1988; Gandevia and Applegate, 1988; Berardelli et al., 1991; Thompson et al., 1997; Hanajima et al., 1998; Pirio Richardson, 2014). Moreover, many studies focused on the role of the contralateral SCM in horizontal head rotation, ignoring the ipsilateral splenius capitis and other suboccipital muscles. In fact, the splenius capitis may be more important than the SCM for horizontal rotation of the head (Vasavada et al., 1998).

We found bilateral precentral gyrus activation during isometric head rotation to the left, whereas rightward head rotation evoked only contralateral activity. This is likely due to threshold effects, since there also was ipsilateral activation for rightward head rotation that failed to survive correction for multiple comparisons (data not shown). These findings suggest that head movements are controlled bilaterally, although contralateral control may be more prominent, as proposed by others (Gandevia and Applegate, 1988; Berardelli et al., 1991; Thompson et al., 1997). Consistent with this idea, head rotation is mediated by synergistic muscles on opposite sides of the body; the ipsilateral splenius capitis combined with the contralateral SCM. Thus bilateral activation in M1 may reflect bilateral muscular control of head rotation. Alternatively, the bilateral

M1 activation could reflect the fact that 10-15% of corticospinal tract fibers projecting to motor neurons are uncrossed in humans (Lemon, 2008).

2.5.2. Is the neck region in the precentral gyrus medial or lateral?

Another basic question has been the location of the neck motor area within the precentral gyrus (**Figure 2.3**). Some studies suggested this area lies in a region medial to the representation of the upper limb (Obrador, 1953; Thompson et al., 1997; Kang et al., 2011; Pirio Richardson, 2014). TMS over this medial area induced motor evoked responses in the contralateral (Pirio Richardson, 2014) or bilateral (Thompson et al., 1997) SCM. A case report of a small stroke in this medial precentral region was associated with ipsilateral head tilt, suggesting weakness of contralateral neck muscles (Kang et al., 2011). Conversely, classic mapping studies placed the neck motor area in a region more lateral than the hand area (Rasmussen and Penfield, 1948; Penfield and Rasmussen, 1950). These same studies mapped somatosensory areas to parallel locations in the post-central gyrus, with the sole exception of the neck. Our results argue for a more medial representation of the neck motor area in the motor homunculus, a location that is more in line with prior studies mapping the neck sensory region.

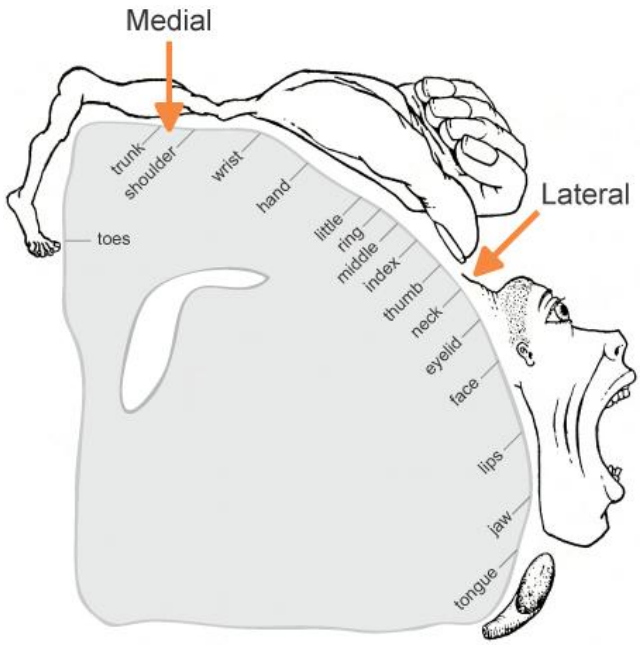

Figure 2.10: Possible location of the medial and the lateral foci identified in our fMRI studies of isometric head rotation. The orange arrows indicate the location of these two foci in relationship to the original homunculus by Penfield and colleagues. Modified from Penfield and Rasmussen (1950).

We identified 2 foci in the precentral gyrus of each hemisphere showing significant activation during isometric head rotation. In both hemispheres, one focus was located medial to the hand knob, whereas the other was more lateral and ventral. The possible location of the medial and the lateral foci identified in our fMRI studies is represented in **Figure 2.10**. However, these areas do not correspond precisely with the Penfield homunculus (Rasmussen and Penfield, 1948). There are some possible explanations for these differences. First, in the Penfield studies the head was somewhat restrained by towels, so some subtle or weak movements may have been missed. Second, Penfield's results for head movements were obtained from only 9 patients, and motor responses were not consistent. For comparison, the experiments involving limb movements included more than 200 patients (Penfield and Rasmussen, 1950). Finally, the neck area in the motor homunculus represented different head movements, such as

flexion, retraction or contraction of the trapezius. Contralateral rotation of the head was also observed, as a result of stimulation in the anterior margin of the precentral gyrus, in the region just anterior to the hand representation (**Figure 2.11**). The authors proposed that head rotation is a movement more related to orienting the eyes and ears, and it may not be elicited from M1 (Rasmussen and Penfield, 1948). Therefore, they decided to exclude its locus from the motor homunculus.

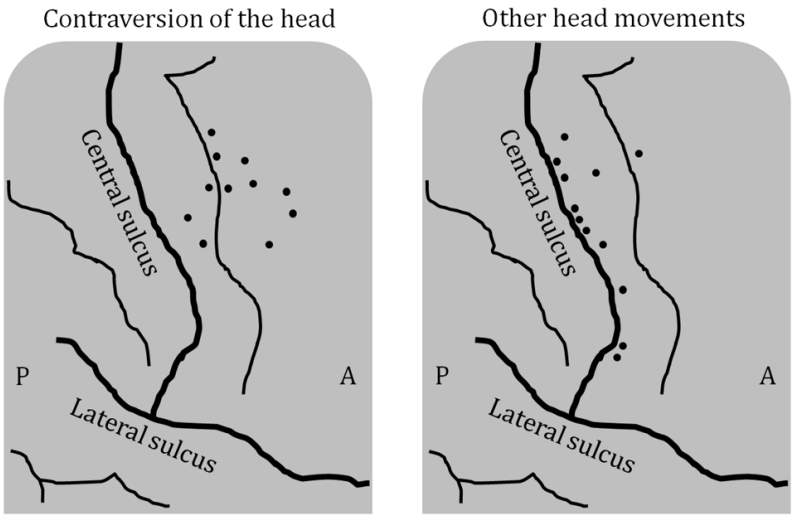

Figure 2.11: Stimulation site for contralateral head rotation (left) and other head movements (right) according to Rasmussen and Penfield (1948). The region involved in contralateral head rotation was not included in the original motor homunculus. Modified from Rasmussen and Penfield (1948). A, anterior; P, posterior.

Medial and lateral neck areas in each hemisphere also were identified in a TMS study of the cortical representation of the SCM (Thompson et al., 1997). The authors suggested that the medial head area represented the SCM, while the lateral area represented the platysma. Although we did not monitor the activity of the platysma, this muscle is not typically involved in head movements of any type and, therefore, this explanation seems unlikely. However, it remains possible that our medial and lateral precentral foci may control different sets of muscles. Activation of our lateral precentral

focus occurred during head rotation to both sides and during right wrist extension. This could be due to movements required to stabilize the body during isometric tasks. As we only recorded EMG in the SCM and ECU, we cannot exclude this possibility. Alternatively, the lateral focus may be involved in any isometric motor task or in performing movements after sensory cues. Activation of the inferior precentral gyrus was reported in a study of isometric finger movements at different force levels (van Duinen et al., 2008). Activity in this area extended to the frontal operculum and lateral insula, similarly to what was observed in the present study. The authors proposed that this area is not directly responsible for hand movements, but rather in monitoring feedback and guiding motor performance. Therefore, our findings suggest that the lateral precentral focus may be involved in any isometric task, while the medial precentral focus has a more prominent role in generating head movements.

2.5.3. Is the activation in the precentral gyrus M1, PMd or PMv?

As noted above in the Results section, it is not clear whether the medial and the lateral foci identified in the precentral gyrus in our studies belong to M1 proper, PMd or PMv.

The precentral gyrus is the cerebral cortical region located immediately anterior to the central sulcus. In humans, the precentral gyrus corresponds to Brodmann area 6, which is approximately 9 mm anterior to the hand representation in the central sulcus. Consequently, M1 proper does not occupy the precentral gyrus (Picard and Strick, 2001), except for its most medial portion. In nonhuman primates, the premotor cortex has been divided into dorsal (PMd) and ventral (PMv) areas on the basis of anatomical and physiological differences (Picard and Strick, 2001; Rizzolatti et al., 2002; Mayka et al., 2006). No distinction between dorsal and ventral premotor cortex has classically been made in humans (Rizzolatti et al., 2002). Therefore, it is not possible to establish a

definite correspondence between the functional subdivisions of the monkey motor areas and the same regions in humans. In addition, it is challenging to identify the boundaries of M1 proper, PMd and PMv based on structural MRI data.

Tracing studies in nonhuman primates have shown that those three regions have direct connections with the spinal cord (Picard and Strick, 2001) and, therefore, may be involved in controlling neck muscles. Also, PMd and PMv are densely interconnected with M1. Thus, regardless of the cytoarchitectonic and functional subdivisions, our findings argue for an important role of the medial and lateral precentral foci in controlling isometric head rotation in humans.

2.5.4. Role of other brain regions

Animal studies have shown that head movements can be elicited by experimental manipulations of many regions including the frontal eye fields, cerebellar fastigial nucleus, caudate nucleus, interstitial nucleus of Cajal, red nucleus, reticular formation and superior colliculus (Isa and Sasaki, 2002; Klier et al., 2002). Similar evidence comes from human studies showing that lesions in various subcortical regions can cause abnormal movements of the head (LeDoux and Brady, 2003).

The basal ganglia are thought to have a somatotopic organization (Scholz et al., 2000; Gerardin et al., 2003; Nambu, 2011), but data concerning the neck are limited. Our studies revealed bilateral activation of the putamen (with ipsilateral predominance) during isometric head rotation to either side, with activation for head tasks located more dorsal than that for hand tasks. Bilateral basal ganglia activation has been reported for movements with the hands and other body parts, even when M1 activation is unilateral (Scholz et al., 2000; Gerardin et al., 2003).

Historically, the cerebellar hemispheres were viewed as involved in the control of limb movements, while the vermis was associated with control of axial muscles (Manni

and Petrosini, 2004). However, other studies have suggested that the cerebellum has a fractured somatotopic organization, with multiple scattered representations of a single body part that overlap with different body regions (Manni and Petrosini, 2004; Schlerf et al., 2010; Mottolese et al., 2013). We observed activation of the ipsilateral cerebellar hemisphere during head tasks, with spread into the vermis and overlap with areas activated in hand tasks. The relatively broad activations of the cerebellum associated with head and hand tasks may reflect the cerebellar fractured somatotopic organization and do not support the view of the hemispheres as exclusively responsible for the control of limb movements.

2.5.5. Limitations and future studies

Our study had some shortcomings that should be acknowledged. The first involves the known limitations of fMRI. The spatial resolution of fMRI does not allow reliable identification of small subcortical structures important for head movements such as the interstitial nucleus of Cajal (Fukushima, 1987; Klier et al., 2002; Farshadmanesh et al., 2008). Also, the imaging parameters used for functional scans led to an incomplete coverage of the inferior posterior cerebellum, so no conclusions can be made about this region. Another limitation is that the proposed protocol did not allow dissociation of motor signals from proprioceptive signals during isometric tasks. This caveat is relevant to all studies of motor tasks, since it is challenging to eliminate somatosensory signals generated from movement itself. Another limitation of our study is that the amount of force exerted during isometric tasks was not measured or controlled. Even though subjects were asked to perform submaximal isometric hand and neck contractions, the force exerted during tasks may have varied, which can affect the magnitude and extent of brain activations (van Duinen et al., 2008). Additionally, our study was focused on horizontal head rotation and, thus, the findings may not be

applicable to head movements in other directions. Finally, our studies did not allow testing whether isometric head rotations evoke similar patterns of activity as actual head movements. Nevertheless, the chosen tasks represent a reasonable strategy for investigating changes in brain function related to head motor control in humans.

2.5.6. Conclusions

These findings provide new information regarding the neural control of head movements in humans. Our results suggest that isometric tasks may provide a suitable method for investigating head movements to bypass the normal limitations of holding the head still during brain imaging. We conclude that head movements in humans are controlled bilaterally in the precentral gyrus, but with contralateral predominance. The study also provides evidence for the role of the cerebellum and basal ganglia in head tasks.

Chapter 3: Imaging neuroanatomical substrates for head movements in cervical dystonia*

3.1. Introduction

Head movements can be impaired or abnormal in several conditions affecting the brain or the musculoskeletal system. Head movements may appear to be disrupted or elicited inappropriately in a range of clinical disorders, such as head tremor, dystonia, tics, epilepsy, Tourette's syndrome, cerebral palsy, vestibular dysfunction, congenital muscular torticollis, and orthopedic problems involving the vertebral spine and shoulders. This chapter is focused on abnormal head movements caused by dystonia of the neck, which is known as cervical dystonia (CD).

3.1.1. Dystonia

Dystonia is currently defined as "movement disorder characterized by sustained or intermittent muscle contractions causing abnormal, often repetitive, movements, postures, or both" (Albanese et al., 2013). Further characteristics of dystonia include patterned, twisting or tremulous movements. Symptoms are often initiated or worsened by voluntary action and associated with overflow of muscle activation. They tend to abate during rest or relaxation.

Dystonic movements may emerge at any age, and in any region of the body. Some emerge abruptly and remain static, others are progressive or intermittent. In many cases, dystonic movements are slow and torsional. In some cases, however, dystonic movements may be rapid or jerky, or they lead to semi-rhythmical oscillations

**Parts of this chapter will be submitted as an original manuscript in a peer reviewed journal.*

resembling tremor (Fahn, 1984, 1989; Defazio et al., 2013b). If dystonic movements are the only clinical problem, the disorder is called *isolated dystonia*. However, they often are combined with other neurological or medical problems, and then are called *combined dystonia*. These many different clinical manifestations of dystonic movements are classified according to four dimensions (**Table 3.1**) that include the age at onset, the region of the body affected, their temporal aspects, and whether they are combined with additional clinical problems (Albanese et al., 2013).

Table 3.1: Classification of the dystonias according to clinical features

Dimension for classification	Subgroups
Age at onset	Infancy (birth to 2 years) Childhood (3-12 years) Adolescence (13-20 years) Early adulthood (21-40 years) Late adulthood (40 years and older)
Body distribution	Focal (one isolated region) Segmental (2 or more contiguous regions) Multifocal (2 or more non-contiguous regions) Hemidystonia (half the body) Generalized (trunk plus 2 other sites)
Temporal pattern	Disease course (static vs. progressive) Short-term variation (persistent, action-specific, diurnal, paroxysmal)
Associated features	Isolated (with or without tremor) Combined (with other neurological or systemic features)

In addition to the many varied clinical appearances of dystonic movements, there also are several different etiologies (Fung et al., 2013). The many causes are grouped according to whether there is evidence for a genetic or acquired cause, and whether there is evidence for any overt neuropathological defects in the nervous system (**Table 3.2**).

Table 3.2: Classification of the dystonias according to etiology

Dimension for classification	Subgroups
Nervous system pathology	Degenerative Structural (typically static) No evidence for degenerative or structural lesions
Heritability	Inherited (autosomal dominant, autosomal recessive, mitochondrial, etc…) Acquired (brain injury, drugs/toxins, vascular, neoplastic, etc…)
Idiopathic	Sporadic Familial

3.1.2. Cervical dystonia: clinical characteristics and epidemiology

Any skeletal muscle or combinations of muscles can be affected in dystonia. Focal involvement of neck muscles is known as cervical dystonia (CD) or spasmodic torticollis, which is associated with abnormal movements and postures of the head in any direction (Dauer et al., 1998; Jinnah et al., 2013). The head is typically tilted or turned to the right, left, upwards or downwards (**Figure 3.1**). The most common abnormality involves turning right or left in the horizontal plane (torticollis) (Jankovic et al., 2015). Disease progression is often characterized by spread of dystonia to muscles of the lower face, eyes and upper limbs.

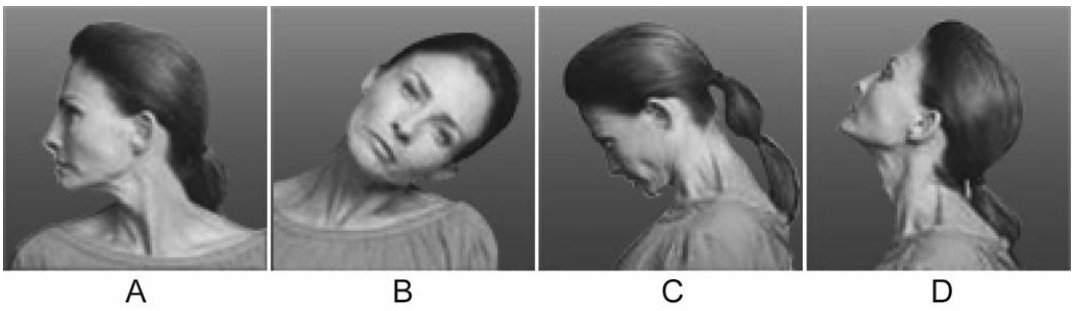

Figure 3.1: Types of cervical dystonia. Torticollis (A), laterocollis (B), anterocollis (C) and retrocollis (D). Modified from http://www.dysport.com/cervical-dystonia-tools-and-resources.

Most CD patients report temporary improvement of involuntary movements after using specific gestures known as sensory tricks, such as touching the lower face or

neck, and touching the posterior or superior part of the head (Tarsy and Simon, 2006; Patel et al., 2014). Interestingly, sensory tricks tend to be patient-specific, but they consist of a common strategy adopted by patients with different types of dystonia.

CD is the most common subtype of dystonia, with an estimated prevalence of about 23 to 182 per million worldwide (Nutt et al., 1988; Jankovic et al., 2007). It is more prevalent in women, with a mean age of onset of 40 years (Defazio et al., 2004; Defazio et al., 2007; Marras et al., 2007; Steeves et al., 2012; Defazio et al., 2013a). The abnormal head postures frequently interfere with the ability to engage in daily activities and are very stigmatizing, causing avoidance of social interaction. Consequently, CD has a significant negative impact on quality of life (Werle et al., 2014), comparable to what is reported by patients with multiple sclerosis, Parkinson's disease and stroke (Camfield et al., 2002).

Most cases of CD are classified as sporadic because a cause cannot be identified. In contrast, a cause is identifiable in acquired CD and may include medications, trauma, space-occupying lesions, and developmental or degenerative conditions. Botulinum toxin is the most effective treatment, with about 75% of patients showing improvements (Chan et al., 1991; Dauer et al., 1998; Crowner, 2007). Benefits from injections usually last for 3 to 4 months (Jinnah and Factor, 2015). Other treatment options are oral medications, neurosurgery, and rehabilitation, but there is limited evidence for the long-term benefits of these therapeutic modalities in isolated CD (Vidailhet et al., 2013; De Pauw et al., 2014; Jinnah and Factor, 2015).

3.1.3. Anatomical basis of CD

Although CD is the most common sporadic dystonia, conclusive evidence implicating specific regions of the central nervous system is lacking (Hedreen et al., 1988; McGeer and McGeer, 1988; Standaert, 2011). Historically, many studies of other

types of dystonia have implicated the basal ganglia (Berardelli et al., 1998; Hallett, 2006; Mink, 2006; Breakefield et al., 2008). This historical focus derives from a clinical neuroimaging case report of 28 patients with acquired hemidystonia in which the basal ganglia were more commonly affected than other brain regions (Marsden et al., 1985). Only two of the patients in this study had CD, which was associated with lesions of the caudate nucleus. A more recent study focusing on acquired CD found that the majority of lesions were in the posterior fossa (brainstem and cerebellum), and the remaining cases were equally distributed in the cervical spinal cord and basal ganglia (LeDoux and Brady, 2003). Abnormal vestibular function has also been implicated in CD (Munchau and Bronstein, 2001; Munchau et al., 2001; van Gaalen et al., 2012).

There are no accepted animal models of CD, but investigations in non-human primates, cats and rodents have indicated that abnormal function of the interstitial nucleus of Cajal and surrounding midbrain regions can lead to head postures resembling CD (Hassler and Hess, 1954; Foltz et al., 1959; Malouin and Bedard, 1982; Fukushima et al., 1987; Nakazawa et al., 1999; Matsumoto and Pouw, 2000; Klier et al., 2002; Evinger, 2005; Farshadmanesh et al., 2007; Farshadmanesh et al., 2008).

3.1.4. Neuroimaging studies in CD

Findings from neuroimaging investigations of individuals with CD are somewhat inconsistent (Neychev et al., 2011; Zoons et al., 2011). Imaging data in sporadic CD comes mainly from studies with positron emission tomography, voxel-based morphometry and diffusion tensor imaging (Neychev et al., 2011; Zoons et al., 2011). These studies have suggested abnormal metabolism, abnormal white and gray matter volumes and microstructural defects in multiple areas, including primary motor cortex (M1), premotor areas, somatosensory cortex, putamen, cerebellum, and thalamus. More recent studies have used resting-state functional imaging to investigate the

functional connectivity in CD, which is measured by the level of co-activation of separate brain regions at rest (van den Heuvel and Hulshoff Pol, 2010). These studies identified decreased functional connectivity in the basal ganglia and sensorimotor networks, whereas increased connectivity has been suggested for the executive function network (Delnooz et al., 2013a, b).

The few available functional magnetic resonance imaging (fMRI) studies in CD have tested brain activity during tasks with the hand rather than the head (**Table 3.3**) (de Vries et al., 2008; Obermann et al., 2008; Obermann et al., 2010; Opavsky et al., 2011; de Vries et al., 2012; Opavsky et al., 2012). CD patients showed increased activation in the caudate nucleus, putamen and thalamus when compared to controls during a grip force task (Obermann et al., 2008). Another study showed decreased activation in the premotor cortex, postcentral gyrus, and superior parietal and temporal cortices during imagined wrist movements in CD (de Vries et al., 2008). Interestingly, most of these studies have reported abnormal activation patterns in CD subjects compared to controls (de Vries et al., 2008; Obermann et al., 2008; Obermann et al., 2010), suggesting that this disorder may affect sensory and motor networks related to movements with unaffected muscles. Nonetheless, these studies do not provide information about brain activity directly related with head controls. Consequently, their relevance to understanding the pathogenesis of abnormal head movements, which is the main clinical problem in CD, is uncertain.

In summary, findings from different neuroimaging studies of CD point to abnormalities in several brain regions. Even though certain areas are implicated more frequently such as the basal ganglia, sensory and motor cortical areas, the lack of concordance in findings across different studies is noteworthy. The different areas identified may be due to the use of different methods. However, the lack of agreement between studies is evident even for modalities that measure a common biological

phenomenon such as brain activity, or even within a single type of imaging modality. Other reasons for inconsistencies may be the investigation of regions of interest vs. whole brain analysis, inclusion of a heterogeneous group of CD subjects or heterogeneity of individuals investigated among different studies, relatively small numbers of patients in some studies, use of different reference groups as control, and methodological differences in data acquisition and analyses.

Table 3.3: Task-based fMRI studies of CD

Cases/ Controls	Design/Task	Regions affected		ROI	Source
		Cortical	Subcortical		
8/9[A]	execution and motor imagery of hand flexion/ extension	Execution: ↓INS Imagery: ↓ S2, PM, sPar, sTL	Execution: ↓PUT	Whole brain	(de Vries et al., 2008)
9/14	execution of grip force task		↑CAUD, PUT, THAL	M1, BG, THAL	(Obermann et al., 2008)
17/17[B]	passive forearm movement	↑S1, S2, INS,CING	↑CBL	Whole brain	(Obermann et al., 2010)
7/9[C]	skilled hand motor task pre and post-BoNT[D]	CD pre-BoNT: ↓SM CD pre-BoNT vs. controls: ↑S2 CD pre vs. post-BoNT: ↓SMA, PMd	CD pre-BoNT: ↓Caud, GP, THAL CD post-BoNT vs. controls: ↓GP	Whole brain	(Opavsky et al., 2011)
7/9[C]	electrical stimulation of median nerve pre and post BoNT[D]	CD pre-BoNT vs. controls: ↓S2, INS CD pre vs. post-BoNT: ↑S2, INS, iPar		Whole brain	(Opavsky et al., 2012)
7/10[E]	motor imagery and execution of hand movements with or without TMS[F]	Execution with vs. without TMS, CD group: ↑iPar Execution with vs. without TMS, CDs vs. controls: ↓ ANG	Execution with vs. without TMS, CD group: ↑THAL	Whole brain	(de Vries et al., 2012)

[A]: Hand movements were clinically normal. The data shown represent results corrected for multiple comparisons.
[B]: CD subjects were investigated in the middle of their usual BoNT application interval to minimize movement artifacts in the scanner.
[C]: Rotational CD.
[D]: The tested extremity in all CD subjects was ipsilateral to the direction of the head deviation.
[E]: One subject had generalized dystonia with prominent CD; another subject had CD and spasmodic dysphonia.
[F]: TMS was applied over the left superior parietal cortex.

ANG, angular gyrus; BG, basal ganglia; BoNT, botulinum toxin; CAUD, caudate; CBL, cerebellum; CD, cervical dystonia; CING, cingulate gyrus; fMRI, functional magnetic resonance imaging; GP, globus pallidus; iPar, inferior parietal cortex; INS, insula; M1, primary motor cortex; NS, not significant; PMd, dorsal premotor area; PUT, putamen; ROI, regions of interest; S1, primary somatosensory area; S2, secondary somatosensory area; SM, sensorimotor cortex; SMA, supplementary motor area; sPar, superior parietal cortex; sTL, superior temporal lobe; THAL, thalamus; TMS, transcranial magnetic stimulation

3.1.5. Limitations of neuroimaging studies of CD

CD has been investigated with neuroimaging less frequently than other dystonias because these individuals have impaired ability for maintaining their head still and straight, as is required for brain scanning. The main movement impairment observed in CD, head movements, has not been tested with available imaging instruments in these subjects.

3.2. Objectives and significance

In our experiments in healthy volunteers, we demonstrated the feasibility of studying isometric head tasks with fMRI to delineate the neural substrates for normal head movements. The purpose of the following experiments was to determine the neural substrates for abnormal head movements in CD using similar methods.

Identifying the neuroanatomical substrates for abnormal head movements in CD is relevant for better understanding the pathogenesis of the main problem in this disorder. This information is also crucial for future studies focused on identifying the cause of the disease as well as the development of new therapeutic approaches for patients.

3.3. Materials and methods

3.3.1. Participants

All procedures were approved by the Emory University Institutional Review Board. CD participants were recruited by an experienced neurologist at the Movement Disorders Clinic at Emory University. Inclusion criteria consisted of a diagnosis of isolated CD with predominantly rotational abnormality (torticollis), absence of any apparent dystonia of the hands or other body parts, ability to straighten the head fully when lying relaxed, absence of tremor when lying relaxed, and absence of other

significant neurological diseases. The severity of dystonia was assessed with the Toronto Western Spasmodic Torticollis Rating Scale (TWSTRS) and Global Dystonia Rating Scale (GDRS) (Comella et al., 2003). Control subjects were the same group of healthy volunteers that participated in the experiments described in **Chapter 2**. Control participants were age-matched, neurologically normal and had the ability to perform head movements in all directions. Subjects were excluded if they had significant orthopedic problems of the cervical spine, head tremor or other abnormal movements when lying supine, significant neck pain, contraindications for MRI, or untreated psychiatric problems. All participants gave informed consent prior to enrollment in the study.

On the morning of scanning, participants were instructed to delay taking any of their usual oral medications until scans were completed. For those CD participants who were being treated with botulinum toxin, scanning was conducted just before the next scheduled injection to minimize treatment effects. We did not limit to participants not being treated with botulinum toxin because the vast majority of CD individuals receive these treatments, and excluding them would have yielded an atypical patient population.

We recruited 17 individuals with CD. One CD subject was excluded because of poor compliance with tasks. As a result, the final analyses were conducted with data from 17 controls (12 women, 5 men) and 16 participants with CD (9 women and 7 men). Mean age was 56.8±14.5 years (range 30-74 years) for the control group and 56.6±11.4 years (range 31-75 years) for CD. All CD subjects had rotational CD. Involuntary rotational movements were towards the right for 10 subjects and left for 6. Pure rotational torticollis is uncommon, so several participants also had additional horizontal (laterocollis) or vertical (anterocollis or retrocollis) movements, but none had dystonia of the limbs (**Table 3.4**).

Table 3.4: CD participants

ID	Disease duration (years)	Side of torticollis	Severity of torticollis (TWSTRS)	Other symptoms	Head tremor	Hand tremor	Motor severity score (TWSTRS)	GDRS (neck)	Time since BoNT (months)
1	5	R	Severe	latercollis (R)	No	No	18	4	NA
2	13	L	Moderate	retrocollis	Yes	Yes	20	7	2.5
3	3	L	Mild	anterocollis	No	No	12	4	3.4
4	15	R	Slight	latercollis (L)	Yes	No	18	4	4.4
5	2	L	Moderate	none	No	No	18	5	3.2
6	13	R	Mild	none	No	No	18	4	3.3
7	5	R	Slight	latercollis (R)	No	No	18	4	3.0
8	9	L	Slight	latercollis (R), lateral shift (R)	No	Yes	17	5	3.2
9	21	R	Mild	anterocollis	No	No	7	3	2.9
10	10	L	Slight	posterior shift	No	No	16	5	2.7
11	2	L	Mild	latercollis (R)	No	No	11	3	3.3
12	13	R	Mild	anterocollis	No	Yes	13	6	11.0
13	24	R	Moderate	retrocollis	Yes	No	15	6	2.8
14	26	R	Moderate	latercollis (R), anterocollis	Yes	No	23	8	4.7
15	7	R	Moderate	latercollis (L), anterocollis	No	No	18	7	26.0
16	8	R	Severe	none	Yes	No	16	8	3.0

BoNT, botulinum toxin treatment; GDRS, Global Dystonia Rating Scale; L, left; NA, not applicable; R, right; TWSTRS, Toronto Western Spasmodic Torticollis Rating Scale.

3.3.2. MR scanning

The procedures for MRI scanning were the same as described in **Chapter 2**, **section 2.3.2**.

3.3.3. Experimental design

The same experimental design was used for controls and CD participants. Details about the design were described in **Chapter 2**, **section 2.3.3** and **Figure 2.3**. CD subjects were carefully monitored during practice and scanning to ensure there were no involuntary movements of the head or other body parts.

3.3.4. Electromyography (EMG)

Methods and procedures for EMG recording and rating were the same as described in **Chapter 2**, **section 2.3.4**.

3.3.5. Head motion correction and analysis

The procedures to minimize head movements during scanning, head motion correction, and analysis of head movement followed the same steps as described in **Chapter 2**, **sections 2.3.5** and **2.3.6**. For the CD group, we recruited subjects capable of lying supine without head tremor and took special care to assure that they were relaxed with the head in the most comfortable position.

The threshold of 1.75 mm (half the size of a functional voxel) in any direction also was used as a criterion to exclude data from the final analyses in both groups.

3.3.6. Imaging data analysis

Imaging processing included the same procedures and methods as described in **Chapter 2**, **section 2.3.6**.

The imaging data analysis involved a two-stage whole-brain approach to examine the patterns of activation associated with head tasks in CD. First, we performed within-group analyses to identify the regions active during isometric head tasks in the control and CD groups separately, to delineate the distribution of activations. Next, we conducted between-group comparisons to directly identify significant differences between CD subjects and controls.

Statistical analyses of all imaging data involved use of the general linear model to assess the BOLD signal during active blocks in comparison to baseline, followed by group-level analyses treating participant as a random variable. Group activations during isometric tasks to either side were contrasted with the rest condition using a voxel-wise significance level of $p<0.05$, corrected for multiple comparisons with a 3D extension of the cluster-correction method of (Forman et al., 1995). Results were displayed on an averaged anatomical brain for each group as described in **Chapter 2**. MRI atlases were used for localization of activation maps with respect to 3-dimensional anatomy (Duvernoy, 1999; Schmahmann et al., 1999; Cho, 2010).

3.4. Results

3.4.1. Task confirmation

Participants were able to complete the tasks adequately as determined by observations during practice and EMG during scanning (**Table 3.5**). For 4 subjects (2 controls and 2 CDs), appropriate task performance was verified only manually during training because EMG could not be conducted for technical reasons. Qualitative EMG analysis revealed that controls and CD subjects were able to activate the appropriate muscles for each task on an average of 96.9 and 97.7 percent of all trials, respectively. In addition, the EMG data for the CD group indicated that involuntary head movements did not occur during scanning.

Table 3.5: Task confirmation with electromyography

Muscle	Task	Controls Active (%)	CD Active (%)
right ECU	wrist extension, right	99.0	100.0
left ECU	wrist extension, left	97.1	94.3
right SCM	head rotation, left	97.1	96.6
left SCM	head rotation, right	94.2	100.0

Muscle activity is shown as percent of trials in which there was obvious muscle activation in comparison to background. CD, cervical dystonia; ECU, extensor carpi ulnaris; SCM, sternocleidomastoid.

3.4.2. Head motion during scans

The distribution and amplitude of head motion were analyzed to ensure that subjects with CD did not have excessive head movements, and that isometric head tasks were not associated with increased head motion. For each subject, the analysis generated 1 measurement for each of the 6 movement parameters (3 planes of translation and 3 planes of rotation) associated with every brain volume collected, resulting in 106,488 data points for the whole sample. Using the threshold of 1.75 mm head motion in any plane (as described in **section 3.3.5**), we eliminated 1-3 blocks in 9 subjects (3 controls and 6 CD). This resulted in a total sample size of 33 subjects (17 controls and 16 CD), and a total of 91,452 data points for the final analysis.

After exclusion of data with excessive movements, we examined the distribution of total head motion measurements and their amplitudes in both control and CD groups **Figure 3.2**). This indicated that the vast majority of head motion fell below the movement cutoff of 1.75 mm in any plane in both groups (99.9% of total data points). To determine if head motion was different between CD and controls, an independent samples t-test was performed comparing total head motion (translation and rotation combined) between groups. This analysis showed that the amplitude of head movements was significantly greater in the CD group in comparison to controls ($t(91,450)=-48.08$, $p=0.00$, two-tailed). Although statistically significant because of the very large number of data points analyzed, the actual magnitude of the difference

between groups was quite small (average motion: CD = 0.28±0.27 mm, controls = 0.20 ± 0.23 mm). Importantly, head motion in both CD and control groups was within acceptable limits for most fMRI studies (Poldrack et al., 2011).

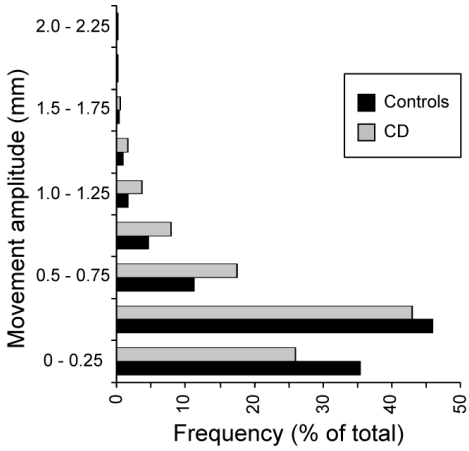

Figure 3.2: Distribution of head motion measurements and their amplitudes for control and cervical dystonia (CD) groups. The vast majority of head motion in both groups fell below acceptable limits for fMRI studies. The y axis represents the amplitude of each movement measured in mm. The x axis shows the distribution of head motion measurements as % of total values generated (Controls: n=17, total data points: 49,788; CD: n=16, total data points: 41,664). Measurements for translational and rotational movements were combined.

Next, we examined the distribution and average of head motion amplitude in the CD group during different tasks (rest periods, hand and head tasks) and in different planes (x, y and z) to verify if head motion was greater during a specific task or plane of motion. The results suggested that each condition and plane of movement demonstrated comparable head motion in the CD group (**Figure 3.3** and **Table 3.6**).

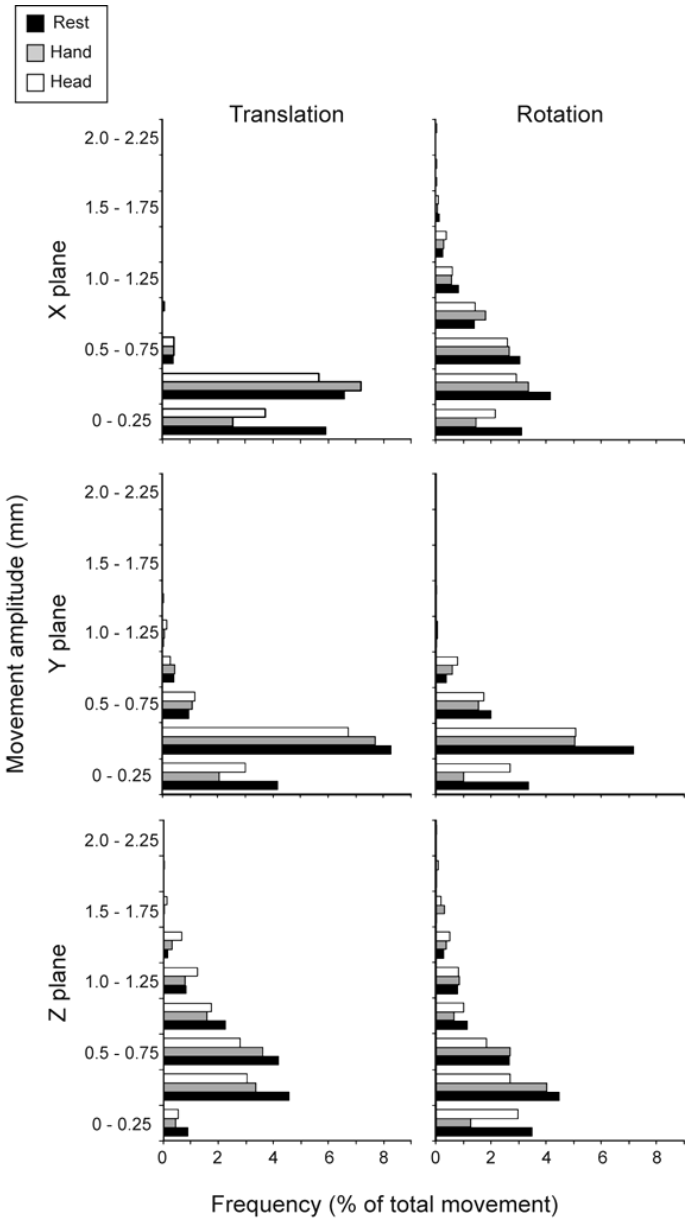

Figure 3.3: Head movements during rest, hand and head tasks in the CD group. The y axis represents the amplitude of each movement measured in mm. The x axis shows the distribution of head motion measurements as a percentage of total values generated (n=16 subjects, total data points: rest: 8,112; hand tasks: 6,360; head tasks: 6,360). Translational and rotational movements are shown for all 3 planes separately (x, y and z).

Table 3.6: Head motion during scans

Translation (mm)				Rotation (mm)			
Task	Plane	Mean	SD	Task	Plane	Mean	SD
	x	0.12	0.10		x	0.40	0.34
rest	y	0.16	0.15	rest	y	0.19	0.17
	z	0.36	0.24		z	0.34	0.29

Translation (mm)				Rotation (mm)			
Task	Plane	Mean	SD	Task	Plane	Mean	SD
	x	0.15	0.15		x	0.44	0.35
hand	y	0.17	0.16	hand	y	0.23	0.20
	z	0.46	0.32		z	0.42	0.37
	x	0.13	0.10		x	0.39	0.31
head	y	0.17	0.15	head	y	0.19	0.17
	z	0.38	0.26		z	0.39	0.34

SD, standard deviation.

3.4.3. Within-group analyses for control and CD participants

Findings for isometric hand and head tasks for the control group are described in **Chapter 2**, **sections 2.4.5-2.4.6**, and summarized in **Figures 2.8-2.9** and **Tables 2.4-2.6**.

Isometric hand tasks were evaluated first to provide a positive control and activation landmarks for subsequent comparison of head tasks. Isometric wrist extension with either hand among CD participants activated similar regions as controls, including the contralateral precentral gyrus in the hand knob (Yousry et al., 1997), the contralateral postcentral gyrus, bilateral supplementary motor area (SMA), bilateral basal ganglia, and ipsilateral cerebellum (**Figure 3.4-3.5** and **Table 3.7**). Activation in the left lateral/ventral precentral gyrus was observed in isometric tasks both with the right and the left hands.

Isometric head rotation to the right or left also produced overall patterns of activation similar to controls, with some exceptions (**Figure 3.4-5** and **Table 3.8**). Similarities included activation of bilateral SMA, basal ganglia, insula, frontal and parietal operculum, and ipsilateral cerebellum. Different than controls, CD participants activated the left medial precentral gyrus during head tasks to either side. In the control group, activation of the medial precentral gyrus during head tasks was either contralateral or bilateral. Furthermore, the activation of the medial precentral gyrus in CD seemed less prominent than in controls.

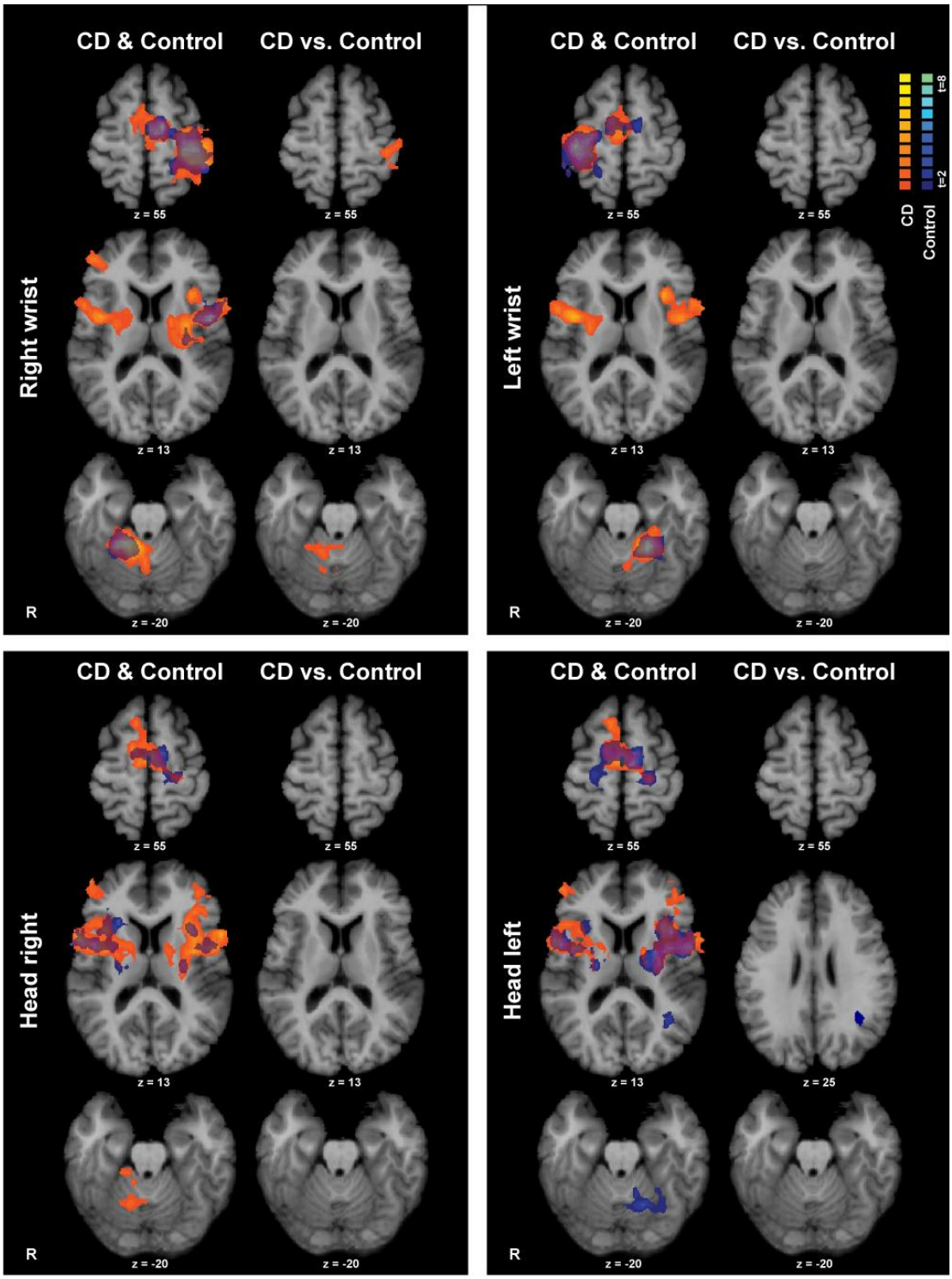

Figure 3.4: Within and between groups analyses of isometric hand and head tasks in comparison to rest for CD, controls, and CD versus controls. The left columns in each panel show individual group analyses overlaid as blue (control) and CD (orange). The right columns in each panel show the direct contrasts between groups. Activations were considered significant at $p<0.05$ (random effects analysis with cluster correction). Color t-scales for each group are shown on the upper right corner. CD, cervical dystonia; R, right; vs., versus.

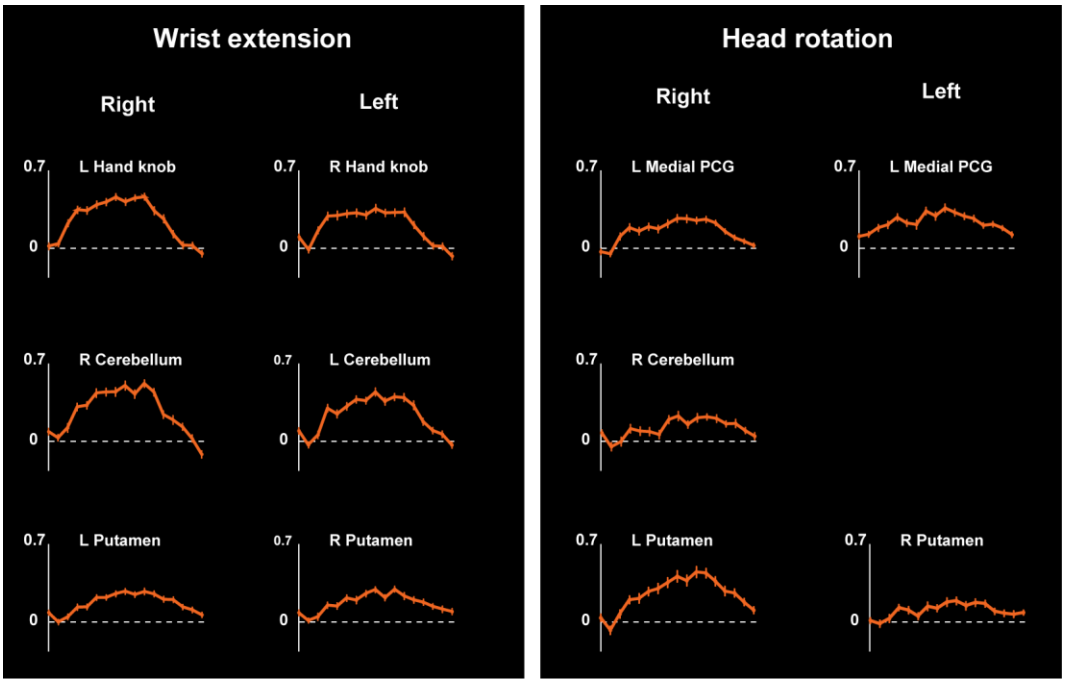

Figure 3.5: Blood oxygenation level dependent (BOLD) signal curves for selected sites for the within-group analysis in the CD group. BOLD signal curves show the average percent signal change over time for each task in comparison to baseline (y axis: % BOLD response; x axis: time measured in scans, from -1 to 15 scans). The dashed line shown in each curve represents 0% or baseline level for the BOLD response. CD, cervical dystonia; L, left; PCG, precentral gyrus; R, right.

Table 3.7: Talairach coordinates, maximum *t*-values (t_{max}) and *p*-values for within-group analysis of isometric hand tasks versus baseline in CD

Isometric task	Region	Hemi	x	y	z	t_{max}	*p*
Wrist extension, right	precentral gyrus, hand knob	L	-27	-28	52	8.79	0.00
	lateral/ventral precentral gyrus	L	-58	5	31	5.03	0.00
	SMA	L	-3	-13	61	5.14	0.00
	pre-SMA/middle cingulate gyrus	L	-3	-10	49	7.31	0.00
	pre-SMA	R	6	-4	49	3.70	0.00
	putamen	L	-30	-16	10	6.07	0.00
	putamen	R	27	-10	10	4.23	0.00
	globus pallidus	L	-18	-7	4	4.09	0.00
	globus pallidus	R	15	-10	4	3.31	0.00
	ventrolateral thalamus	L	-12	-19	4	4.04	0.00
	middle frontal gyrus	R	36	38	19	4.76	0.00
	anterior insula	L	-30	14	13	4.90	0.00
	mid-insula	L	-39	-4	13	4.82	0.00
	mid-insula	R	42	2	1	4.96	0.00
	frontal operculum	L	-48	-1	4	5.91	0.00
	frontal operculum	R	42	-4	10	5.03	0.00
	parietal operculum	L	-54	-34	31	6.55	0.00

Isometric task	Region	Hemi	x	y	z	t_{max}	*p*
Wrist extension, right (cont.)	parietal operculum	R	60	-19	25	5.82	0.00
	postcentral gyrus	L	-39	-34	46	7.84	0.00
	cerebellum, lobules III-V	R	15	-43	-20	8.94	0.00
	vermis, lobules V-VI	R	3	-55	-23	4.46	0.00
Wrist extension, left	precentral gyrus, hand knob	R	24	-28	61	5.96	0.00
	lateral/ventral precentral gyrus	L	-54	5	22	3.09	0.01
	SMA	R	3	-13	52	5.08	0.00
	pre-SMA/middle cingulate gyrus	R	6	-7	46	5.51	0.00
	putamen	R	27	-10	10	4.30	0.00
	globus pallidus	R	18	-5	1	3.48	0.00
	ventrolateral thalamus	R	15	-16	7	2.97	0.01
	anterior insula	L	-30	14	13	5.87	0.00
	mid-insula	R	39	-1	13	6.17	0.00
	mid-insula	L	-42	2	0	3.60	0.00
	frontal operculum	R	51	4	13	4.36	0.00
	frontal operculum	L	-45	-1	10	4.76	0.00
	parietal operculum	R	36	-25	22	5.54	0.00
	parietal operculum	L	-54	-22	22	4.77	0.00
	superior temporal gyrus	L	-51	2	1	6.74	0.00
	postcentral gyrus	R	36	-28	61	7.72	0.00
	postcentral gyrus	L	-39	-43	40	2.89	0.01
	cerebellum, lobules III-V	L	-12	-46	-17	9.22	0.00
	vermis, lobule V	L	-3	-58	-20	2.92	0.01

Hemi, hemisphere; L, left; R, right; SMA, supplementary motor area.

Table 3.8: Talairach coordinates, maximum *t*-values (t_{max}) and *p*-values for within-group analysis of isometric head tasks versus baseline in CD

Isometric task	Region	Hemi	x	y	z	t_{max}	*p*
Head rotation, right	medial precentral gyrus	L	-21	-25	55	3.07	0.01
	lateral/ventral precentral gyrus	L	-51	2	22	3.79	0.00
	lateral/ventral precentral gyrus	R	54	1	-37	4.35	0.00
	SMA	L	-3	-10	58	4.54	0.00
	SMA	R	3	-13	55	4.11	0.00
	pre-SMA	L	-3	-7	52	4.45	0.00
	pre-SMA	R	6	8	49	3.66	0.00
	anterior cingulate gyrus	R	4	14	31	3.08	0.01
	middle cingulate gyrus	L	-9	-1	40	3.16	0.01
	middle cingulate gyrus	R	13	11	37	3.26	0.01
	putamen	L	-27	-13	10	4.45	0.00
	putamen	R	24	-7	10	4.42	0.00
	globus pallidus	L	-15	2	4	3.46	0.00
	globus pallidus	R	15	-1	7	4.03	0.00
	ventrolateral thalamus	L	-15	-13	7	3.04	0.01
	superior frontal gyrus	L	-6	26	49	3.38	0.00
	middle frontal gyrus	L	-42	38	25	3.84	0.00

Isometric task	Region	Hemi	x	y	z	t_{max}	*p*
Head rotation, right (cont.)	middle frontal gyrus	R	39	44	19	4.21	0.00
	anterior insula	L	-30	14	13	5.25	0.00
	anterior insula	R	36	14	16	4.77	0.00
	mid-insula	L	-33	2	10	5.99	0.00
	mid-insula	R	39	-1	10	4.82	0.00
	frontal operculum	L	-45	11	4	7.26	0.00
	frontal operculum	R	54	5	16	6.74	0.00
	parietal operculum	L	-45	-37	31	3.47	0.00
	parietal operculum	R	54	-31	22	3.75	0.00
	postcentral gyrus	L	-57	-25	22	4.17	0.00
	postcentral gyrus	R	54	-19	22	3.91	0.00
	cerebellum, lobule III	R	21	-34	-20	3.26	0.01
	vermis, lobule V	R	0	-58	-17	3.09	0.01
	cerebellum, lobules V	R	15	-55	-17	3.21	0.01
	cerebellum, lobules V-VI	R	18	-49	-26	2.93	0.01
	dentate nucleus	R	12	-34	-29	5.65	0.00
Head rotation, left	medial precentral gyrus	L	-21	-25	55	3.47	0.00
	SMA	R	3	-13	55	4.93	0.00
	SMA	L	-6	-13	61	4.93	0.00
	pre-SMA	R	9	2	46	3.99	0.00
	middle cingulate gyrus	L	-9	-4	40	2.81	0.01
	putamen	R	24	-10	16	4.69	0.00
	putamen	L	-30	-10	7	4.01	0.00
	globus pallidus	R	18	-4	4	3.07	0.01
	globus pallidus	L	-21	-7	7	3.79	0.00
	ventrolateral thalamus	R	12	-10	4	2.61	0.02
	ventrolateral thalamus	L	-15	-7	10	4.99	0.00
	superior frontal gyrus	R	9	14	55	4.04	0.00
	middle frontal gyrus	R	36	41	22	4.98	0.00
	middle frontal gyrus	L	-36	26	31	4.90	0.00
	anterior insula	R	42	17	4	4.40	0.00
	anterior insula	L	-30	14	13	5.00	0.00
	mid-insula	R	36	-1	13	4.65	0.00
	mid-insula	L	-39	2	7	6.54	0.00
	frontal operculum	R	45	17	10	5.11	0.00
	frontal operculum	L	-51	-1	13	5.67	0.00
	parietal operculum	R	51	-28	34	4.47	0.00
	postcentral gyrus	R	54	-22	28	4.12	0.00

Hemi, hemisphere; L, left; R, right; SMA, supplementary motor area.

3.4.4. Between-groups comparisons for control and CD participants

Overall, visual comparisons of the areas of activation for both hand and head tasks suggested that CD participants activated broader areas in most regions (orange versus blue in **Figure 3.4**), including SMA, basal ganglia, ventrolateral thalamus, frontal

and parietal operculum, insula and cerebellum. To determine if the differences apparent in the within-group analyses were statistically significant, we directly compared the activation patterns between CD and control groups. Between-groups comparisons revealed statistically significantly differences only for right wrist extension and head rotation to the left (right columns in **Figure 3.4** and **Table 3.9**).

For isometric right wrist extension there was significantly greater activity in the CD group in comparison to controls in the contralateral hand knob extending into the postcentral gyrus, parietal operculum, ipsilateral cerebellar hemisphere, vermis, and pons. The BOLD signal curves for each group (**Figure 3.6**) further confirmed this difference. These results are consistent with previous fMRI studies of hand tasks in CD showing greater activation in motor and sensory areas (Zoons et al., 2011).

For isometric head rotation to the left, there was greater activity in controls in comparison to CD in two small regions in the temporo-parietal cortex: the ipsilateral angular gyrus and posterior middle temporal gyrus (**Figure 3.4** and **Table 3.9**). However, the BOLD signal curves for each group suggest that the difference between groups may not be biologically meaningful (**Figure 3.6**).

Table 3.9: Talairach coordinates, maximum *t*-values (t_{max}) and *p*-values for between-groups analyses of isometric tasks versus baseline in CD versus controls

Group	Isometric task	Region	Hemi	x	y	z	t_{max}	*p*
CD > Controls	Wrist extension, right	hand knob/ postcentral gyrus	L	-33	-28	43	4.40	0.00
		parietal operculum	L	-42	-43	43	3.25	0.00
		vermis, lobules IV-V	L	-3	-46	-23	2.93	0.01
		vermis, lobule V	L	3	-61	-17	3.03	0.01
		cerebellum, lobules V-VI	L	24	-43	-26	4.44	0.00
		cerebellum, lobule VI	L	18	-58	-29	2.79	0.01
		pons	L	9	-25	-26	2.41	0.02
		pons	L	15	-22	-23	3.08	0.00
Controls > CD	Head rotation, left	angular gyrus	L	-36	-52	25	2.82	0.01
		posterior MTG	L	-42	-64	16	2.60	0.01

Contrasts that did not reach statistical significance are not shown. CD, cervical dystonia; Hemi, hemisphere; L, left; MTG, middle temporal gyrus.

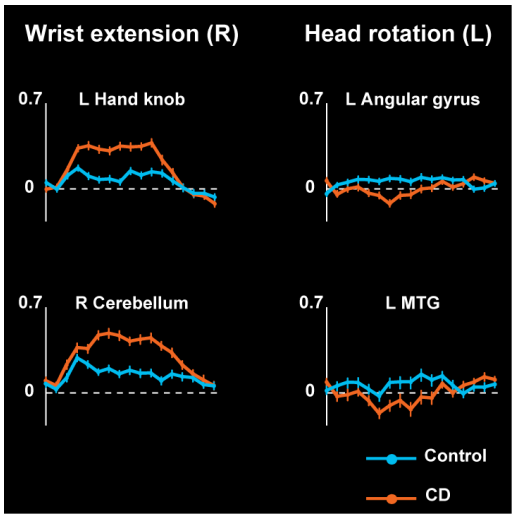

Figure 3.6: Blood oxygenation level dependent (BOLD) signal curves for selected sites for the between-groups analyses of CD (orange) versus controls (blue). BOLD signal curves show the average percent signal change over time for each task (y axis: % BOLD response; x axis: time measured in scans, from -1 to 15 scans). The dashed line shown in each curve represents 0% or baseline level for the BOLD response. CD, cervical dystonia; L, left; MTG, middle temporal gyrus; R, right.

The lack of statistical significance for isometric left wrist extension and head rotation to the right may be due to our stringent statistical thresholds used for data analysis. Indeed, the uncorrected maps showed areas of significantly different activation between CD and control groups for both contrasts. However, another possible explanation may be that combining individuals with right and left torticollis in the same group analysis produced excessively large variance in the data due to hemispheric asymmetries associated with head movement in the direction of torticollis. This latter possibility was further examined next.

3.4.5. Directional preference of torticollis

Involuntary head movements in CD occur in a consistently patterned direction for each individual (Shaikh et al., 2013). This directional preference may be associated with significant asymmetry of brain activity. Consequently, combining individuals with right or

left torticollis in the same group might result in increased variance and obscure any consistent abnormalities. Therefore, to address the hypothesis that the directional preference of head movements in CD might produce significant hemispheric asymmetries, we re-analyzed the CD data in two additional ways.

First, we divided the CD group in those with right (n=10) or left (n=6) torticollis and conducted a whole-brain analysis for each subgroup separately. These analyses showed that the CD data were driven largely by the results in the right torticollis subgroup (data not shown). This was expected, since there were a larger number of participants with right torticollis. We also performed an additional analysis to verify whether isometric head tasks in the direction of abnormal head movements evoked different activation patterns than head tasks in the opposite direction in each subgroup. This analysis was designed to more directly address our hypothesis that the directional preference of head movements in CD might produce significant hemispheric asymmetries during head tasks. With this purpose, we directly compared isometric head rotation to the torticollic and non-torticollic directions in both right and left torticollis subgroups. However, no statistical differences were observed for these contrasts (data not shown). Therefore, the strategy of dividing the CD group according to right or left torticollis did not reveal any further abnormalities, either because no such abnormalities exist, or because the numbers of cases with either right or left torticollis were too small to produce a statistically significant result.

As noted above, dividing the CD group into those with right or left torticollis addressed potential problems associated with asymmetric brain activations, but reduced statistical power for detecting abnormalities because the group sizes became much smaller. We therefore used a second strategy to address the potential consequences of directional bias in CD. This strategy involved digitally reversing the functional datasets of CD participants with left torticollis to match those with right torticollis. For the subjects

whose scans were flipped, we also digitally reversed the right/left orientations of each task. Data normalized in this manner are referred to hereafter as "CD_{NORM}".

Within-group analysis for the CD_{NORM} data did not considerably change the previously observed activation maps for hand tasks (**Figure 3.7** and **Table 3.10**, orange). For isometric head rotation in the direction of torticollis in comparison to baseline, there was bilateral (instead of ipsilateral in the non-normalized data) cerebellar activation (**Figure 3.7**, orange). No notable differences were observed for isometric head rotation in the non-torticollic direction in comparisons to baseline (compared to the non-normalized data). Direct comparisons between the control and CD_{NORM} groups also provided overall results similar to the non-normalized data for all tasks. These findings confirmed that flipping the imaging data and tasks for the CD participants with left torticollis did not result in profound distortion of the overall results, with only small changes in the final results that were likely due to statistical threshold effects.

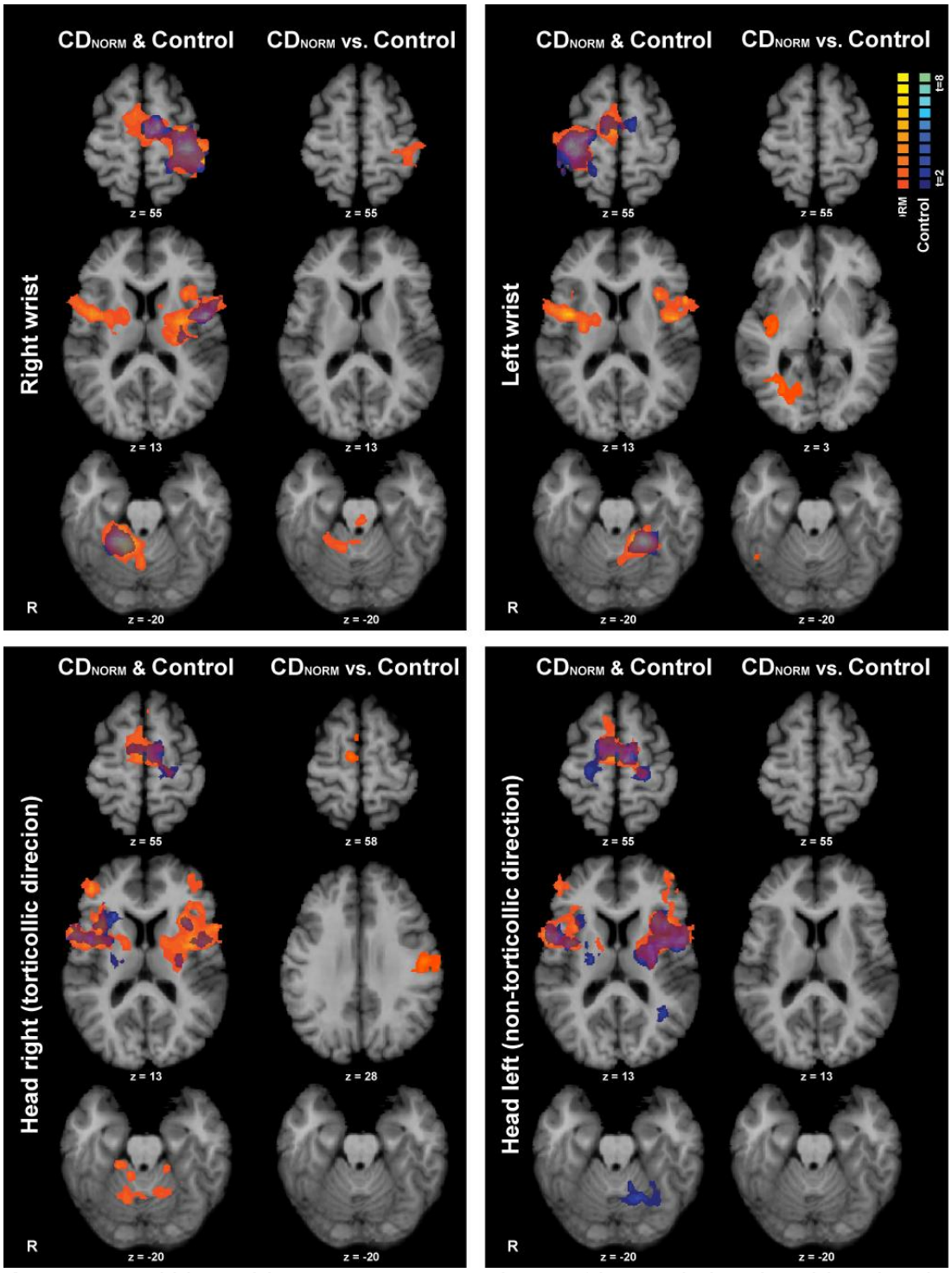

Figure 3.7: Within and between-groups analyses of isometric hand and head tasks in comparison to rest for CD_{NORM} and controls. The left columns in each panel show individual group analyses overlaid as blue (control) and CD_{NORM} (orange). The right columns in each panel show the direct contrasts between groups. Activations were considered significant at $p<0.05$ (random effects analysis with cluster correction). Color t-scales for each group are shown on the upper right corner. CD_{NORM}, cervical dystonia group normalized to side of torticollis; R, right.

Table 3.10: Talairach coordinates, maximum *t*-values (t_{max}) and *p*-values for between-groups analyses of isometric tasks versus baseline in CD_{NORM} versus controls

Group	Isometric task	Region	Hemi	x	y	z	t_{max}	*p*
CD_{NORM} > Controls	Wrist extension, right	hand knob/postcentral gyrus	L	-33	-31	46	4.27	0.00
		postcentral gyrus	R	39	-40	40	3.64	0.00
		frontal operculum	L	-48	-19	22	2.93	0.01
		vermis, lobules IV-V	L	-6	-52	-26	2.71	0.01
		cerebellum, lobules V-VI	R	24	-43	-26	4.62	0.00
		pons	L	-3	-25	-23	3.66	0.00
		pons	R	15	-22	-23	3.33	0.00
	Wrist extension, left	posterior insula	R	39	-16	7	3.79	0.00
		superior temporal gyrus	R	45	-22	10	3.20	0.00
		middle temporal gyrus	R	48	-58	-11	3.44	0.00
		inferior parietal gyrus	R	33	-58	-5	4.43	0.00
		middle occipital gyrus	R	21	-76	-2	4.01	0.00
	Head rotation, right	SMA	R	6	-13	58	3.88	0.00
		pre-SMA	R	9	-4	52	2.80	0.01
		postcentral gyrus	L	-48	-16	28	3.80	0.00
		middle frontal gyrus	L	-33	44	22	3.02	0.01
		inferior frontal gyrus	L	-39	38	-5	3.73	0.00

Contrasts that did not reach statistical significance are not shown. CD_{NORM}, cervical dystonia normalized to side of torticollis; PMd, dorsal premotor area; SMA, supplementary motor area.

Finally, we compared activation maps in the CD_{NORM} data for moving the head to the right (i.e., in the direction of torticollis) or left (direction opposite to torticollis). We hypothesized that these comparisons would enable us to address which regions drive the involuntary turning movements and which regions are invoked to oppose the involuntary movements. Comparing the activation patterns between the torticollic and non-torticollic directions in CD_{NORM} revealed that isometric head rotation in the direction opposite to torticollis was associated with greater activation in the contralateral postcentral gyrus, ipsilateral precentral sulcus and middle cingulate gyrus. In contrast, isometric head rotation in the direction of torticollis produced significant activation of the ipsilateral anterior cerebellum and vermis (**Figure 3.8-3.9** and **Table 3.11**). These results suggested that significant asymmetries of brain activity are associated with the torticollic and non-torticollic directions of head movements.

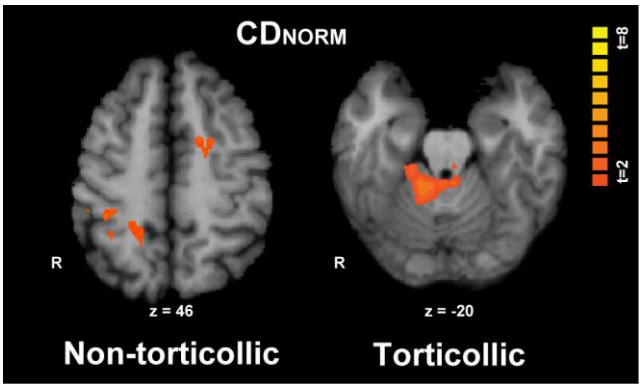

Figure 3.8: Non-torticollic and torticollic directions of isometric head rotation in CD_{NORM} (n=16). The image on the left shows regions with greater activation for the non-torticollic direction of head movement in comparison to the torticollic direction. These regions included the postcentral gyrus (right hemisphere), middle cingulate gyrus (left hemisphere) and precentral sulcus (not shown). The right image shows regions with greater activation for torticollic direction of head movement in comparison to the non-torticollic direction. These regions consisted of the ipsilateral cerebellum and contralateral pons. Areas with significant activation are shown in orange (p<0.05, random effects analysis with cluster correction). The color t-scale is shown on the upper right corner. CD_{NORM}, cervical dystonia group normalized to side of torticollis; R, right.

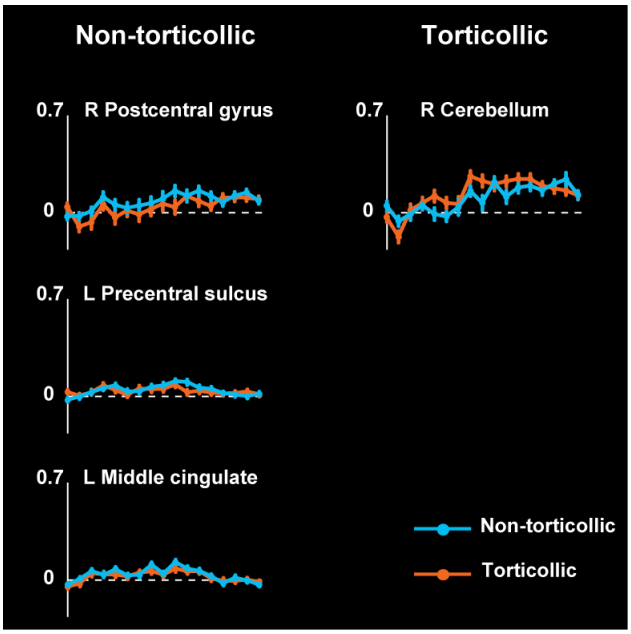

Figure 3.9: Blood oxygenation level dependent (BOLD) signal curves for selected sites for the contrasts between non-torticollic (blue) and torticollic (orange) directions of head movements in the CD_{NORM} group. BOLD signal curves show the average percent signal change over time for each task (y axis: % BOLD response; x axis: time measured in scans, from -1 to 15 scans). The dashed line shown in each curve represents 0% or baseline level for the BOLD response. CD_{NORM}, cervical dystonia normalized to side of torticollis; L, left; R, right.

Table 3.11: Talairach coordinates, maximum *t*-values (t_{max}) and *p*-values for within-group analysis of isometric head rotation to the torticollic direction versus the non-torticollic direction in CD_{NORM}

Isometric task	Region	Hemi	x	y	z	t_{max}	*p*
Non-torticollic >	postcentral gyrus	R	33	-37	46	3.67	0.00
Torticollic	postcentral gyrus	R	30	-46	52	3.67	0.00
	postcentral gyrus	R	30	-37	58	3.05	0.01
	precentral sulcus	L	-33	-10	34	3.80	0.00
	middle cingulate gyrus	L	-15	2	46	3.48	0.00
Torticollic >	vermis, lobule III-IV	R	3	-40	-20	3.63	0.00
Non-torticollic	vermis, lobule III-IV	L	-3	-40	-20	3.60	0.00
	cerebellum, lobules III-V	R	15	-40	-20	4.35	0.00
	pons	L	-3	-28	-17	2.54	0.02

CD_{NORM}, cervical dystonia normalized to side of torticollis; Hemi, hemisphere; L, left; R, right.

3.5. Discussion

Our studies involving a novel approach with isometric head tasks permitted the exploration of regional functional changes associated with abnormal head movements in CD. Overall, participants with CD showed similar regions of brain activation as controls. However, when the data were normalized according to the direction of torticollis (CD_{NORM}), the results suggested that moving the head in the direction of torticollis involved greater activation in the ipsilateral anterior cerebellum, whereas moving the head in the opposite direction was associated with greater activity in a few sensory and motor cortical regions. Collectively, these findings indicate potential cortical and subcortical areas that may be affected in CD, and imply significant asymmetries of brain activity associated with the torticollic and non-torticollic directions of head movements.

3.5.1. Neuroanatomical substrates for head movements in CD

All the available fMRI studies in CD have identified abnormal activations during different types of tasks with the upper limbs, such as grip force, passive forearm movement, and imagined wrist movements (**Table 3.3**) (de Vries et al., 2008; Obermann et al., 2008; Obermann et al., 2010; Opavsky et al., 2011, 2012). While these studies

provide evidence for abnormal brain activation in CD during tasks with a clinically normal body part, they do not teach us about the involuntary head movements observed in CD. By investigating isometric head rotation during fMRI, we were able to address some important issues regarding the neural control of head movements in CD.

Our studies suggested that isometric head rotation to either side may be associated with less prominent activation of the medial precentral gyrus in CD subjects (**Figure 3.4**). This limited activity was suggested by the within-group analyses, but not after statistical comparisons with the control group. Since previous fMRI studies in CD did not address brain activation patterns associated with head movements (Zoons et al., 2011), comparisons with our data for isometric head tasks is not possible. However, our experiments in controls revealed that the bilateral medial precentral gyrus has an important role in the performance of isometric head rotation (**Chapter 2**). Thus, one potential explanation is that the medial precentral gyrus plays a relatively less important role in head rotation in CD than in normal individuals. An alternative explanation could be that the medial precentral gyrus is chronically over-active in CD. If this is the case, then comparing head rotation tasks to the resting condition to assess the change in BOLD signal for each case may result in apparently lower activations because of a ceiling effect. This latter interpretation is more consistent with positron emission tomography (PET) studies implying enhanced cortical metabolic activity (Galardi et al., 1996; Magyar-Lehmann et al., 1997), and with transcranial magnetic stimulation (TMS) studies implying enhanced cortical excitability (Odergren et al., 1997; Hanajima et al., 1998) in persons with CD. Future PET imaging studies could investigate whether regional metabolism or cerebral blood flow in the medial precentral gyrus region is greater in CD in comparison to controls address this more directly. Another way to test this would be to compare active and resting motor thresholds of the medial precentral gyrus with TMS in CD and controls.

3.5.2. Direction of head movements and side of torticollis

One of the limitations inherent to neuroimaging studies is that it is challenging to distinguish cause from effect (Neychev et al., 2011). In other words, it is difficult to distinguish the brain region that may cause an abnormality from secondary effects. These secondary effects may reflect relatively short-term reactive changes in brain activity, such as the nearly instantaneous alterations in sensory feedback following an abnormal movement. Alternatively, they may reflect long-term adaptations to a chronically abnormal brain region, such as disuse atrophy.

We attempted to discriminate cause from effect by exploring the functional imaging data in relation to the direction of spontaneous abnormal rotations in the CD group. Because the involuntary movements in CD are chronically patterned in a single direction for each case, we reasoned that attempts to voluntarily turn the head might reveal hemispheric asymmetries associated with the abnormal movement. Presumably, voluntarily turning the head in the same direction as torticollis would require less volitional effort because of the inherent tendency of the involuntary mechanisms. This condition might point more specifically to the regions responsible for the abnormal movements.

To address this hypothesis, we analyzed the CD data in two additional ways. First, we separated the CD group into those with right or left torticollis. Data analysis of each subgroup separately or in comparison to controls did not reveal very informative results likely because of a low statistical power. Next, we normalized the data according to the side of torticollis in all subjects (CD_{NORM}). Interestingly, the CD_{NORM} data revealed that isometric head rotation in the direction torticollis in comparison to the opposite direction involved prominent activity of the ipsilateral anterior cerebellum, which plays a key role in motor control and in the modulation of cortical excitability (Coffman et al., 2011; Manto et al., 2012; Bostan et al., 2013), and has been implicated as playing a

causal role in dystonia (Neychev et al., 2011; Avanzino and Abbruzzese, 2012; Filip et al., 2013; Prudente et al., 2014). Thus our results suggest the cerebellum may be the primary driver of abnormal head rotation in CD.

Conversely, turning the head opposite to the direction of torticollis would presumably require more volitional effort to antagonize the inherent tendency of the involuntary mechanisms in CD. It may also be associated with more prominent sensory feedback from proprioceptors in muscles that fail to relax. Consistent with this idea, analysis of CD_{NORM} revealed significant activation in the contralateral postcentral gyrus, the ipsilateral middle cingulate gyrus and precentral sulcus. The primary somatosensory area is located in the postcentral gyrus, and it is important for processing of sensory information from the contralateral side of the body. The middle cingulate gyrus is activated primarily in relation to movement execution, while the regions surrounding the precentral sulcus are mainly involved in motor planning (Picard and Strick, 2001). Thus, our results suggest that moving the head opposite to the pathological direction involved increased somatosensory and motor processing. If this is the case, then the increased cortical activation reflects a compensatory adaptation to the involuntary rotational movements.

Although it is impossible to distinguish cause and effect from our imaging data, we can build a speculative model that could be tested in future studies. In this model, abnormal asymmetric function originating from the cerebellum and its brainstem connections is responsible constant involuntary rotation of the head. These abnormal movements are then partly counteracted by forebrain mechanisms that attempt to correct the abnormal head posture. Thus the dynamic position of the head observed in CD may reflect an interaction between two mechanisms involved in motor control; a pathological one and a compensatory one. This proposed mechanism is identical to that known to cause gaze-evoked eye nystagmus, where abnormal slow drifting movements

of the eyes from a target caused by cerebellar dysfunction are constantly being corrected by rapid saccades mediated by forebrain structures (Shaikh et al., 2013).

3.5.3. Wrist movements in CD

Even though our main purpose was to delineate the neuroanatomical substrates for head movements in CD, we included isometric wrist movements as a positive control condition since hand tasks have been extensively studied in normal and CD populations. We observed increased activation in the CD group in comparison to controls in the contralateral pre- and postcentral gyri (hand knob vicinity), parietal operculum, ipsilateral cerebellum, vermis and pons during isometric right wrist extension (**Figure 3.4**). These findings suggested abnormal processing in the motor network during movements with clinically normal muscles. This is consistent with investigations showing a similar phenomenon in CD and other focal dystonias (Zoons et al., 2011; Jinnah et al., 2013; Lehericy et al., 2013). Furthermore, these results imply a more general central nervous system defect that may be clinically evident only in a single body region.

3.5.4. Limitations

Although our results provide novel insights into patterns of brain activity associated with head movements in CD, some limitations must be noted.

First, neuroimaging studies rarely allow the discrimination of cause from effect, as noted above. Thus any interpretations regarding causal mechanisms must be considered speculative. Further studies that involve manipulation of the proposed sites in humans and animals are needed. Longitudinal and intervention studies in patients, as well as experimental manipulations in animals, may help clarify this issue. A related problem is that the abnormal head movements in CD are largely involuntary, while intentional isometric contractions are voluntary. Thus the results presented here are

likely to reflect an interaction between voluntary and involuntary brain mechanisms, and it is not feasible to conclusively distinguish which brain regions contribute to the different mechanisms.

A third limitation is that fMRI is not ideal for detecting changes in relatively small brain regions that have been proposed to play a role in the abnormal head movements of CD, such as the interstitial nucleus of Cajal (Klier et al., 2002), superior colliculus (Holmes et al., 2012), or red nucleus (Nakazawa et al., 1999). On a related note, the imaging parameters used in our studies determined that coverage of the brain extended from the cortex through most of the cerebellum, but the very caudal regions of the cerebellum and brainstem fell outside of the imaging window. Therefore, no comments can be made regarding involvement of those regions.

A fourth limitation is that apparent differences between CD subjects and controls were observed for the within-groups analyses of brain activity, but most of these differences failed to achieve statistical significance in between-groups analyses. The most likely explanation for this discrepancy is that the magnitude of differences between CD and controls was small, so they did not survive the stringent statistical comparisons that required a voxel-wise significance level of $p<0.05$, corrected for multiple comparisons. In fact, significant group differences could be revealed with less stringent statistical comparisons without cluster-correction. The ideal study would require a much larger group of CD subjects, all with pure rotational torticollis to one side, but recruiting such a population is not feasible because CD is so rare. In this regard, it is worth emphasizing that our study is one of the largest fMRI studies of CD to be conducted, with the most uniform population of subjects with pure CD with a mostly rotational head abnormality.

A final limitation was that we were able to monitor the EMG activity of only two pairs of muscles during the isometric tasks, i.e., the bilateral SCM and ECU. While the

EMG recordings were appropriate for verifying task performance, we did not investigate the role of other muscles with synergistic or antagonistic actions for each task. Considering that dystonic patients often show overflow of activity to muscles not primarily involved in a movement (Albanese et al., 2013; Jinnah and Factor, 2015), it would have been interesting to measure the EMG activity of other muscles, such as those involved in stabilizing the shoulders and trunk, and neck muscles important for head movements in other directions. Nonetheless, the use of EMG during fMRI scanning is technically challenging and it requires a number of safety precautions (van Rootselaar et al., 2008; van der Meer et al., 2010; Noth et al., 2012). Thus, the mere fact that we used EMG represents an improvement in comparison to prior neuroimaging studies of CD.

3.5.5. Conclusions and future directions

By investigating a task directly related to the involuntary movements observed in CD, our findings have pointed to cortical and subcortical areas that may be involved in the abnormal head movements observed in CD.

There was limited activation in the medial precentral gyrus in the CD group, a region we demonstrated that is relevant for isometric head rotation in normal individuals. This finding suggested that CD participants had impaired voluntary control of the isometric head tasks, which is consistent with the involuntary head movements that are characteristic of this disorder. Future investigations in humans with CD should explore the role of the medial precentral gyrus in head movements in other directions and other types of CD. Moreover, follow-up neuroimaging studies may use the medial precentral gyrus as a region of interest for investigations of brain metabolism, blood flow, structural and functional connectivity.

Our studies have also provided a valuable experimental paradigm that can be used by others to address questions relevant to CD and other dystonias. For instance, future studies using a similar design can be conducted to investigate hand dystonia and directly compare the results with CD subjects. This would be relevant to study simultaneously two distinct types of dystonia during performance of tasks unrelated to symptoms and tasks that trigger dystonia, providing clearer evidence about the brain regions associated with causal or compensatory mechanisms. Additionally, future investigations may also examine isometric tasks involving other body parts to study movements directly relevant to other dystonias, such as an isometric foot task in foot dystonia.

Our studies represent an improvement from prior fMRI investigations of CD. In comparison to previous investigations, we investigated an unusually homogeneous group and a large sample size. Not only did we limit to isolated CD, but we focused on rotational CD because different types of head directions may yield different results. Furthermore, we focused on isometric head rotation in our experiments, since this was the most prominent problem for the CD group. Finally, we employed a novel analytical approach to address the possibility that the directional pattern of involuntary head movements in CD might produce significant hemispheric asymmetries. Normalizing the CD data to direction of torticollis revealed that CD participants demonstrated prominent activation in the ipsilateral anterior cerebellum during the performance of isometric head rotation to the side of torticollis. In contrast, isometric head rotation in the opposite direction induced greater activity in isolated cortical regions involved in sensory and motor processing. This suggests that the abnormal head movements observed in CD may be largely driven by subcortical pathways, while voluntary mechanisms from cortical areas are elicited to correct the abnormal head postures. This combination of subcortical abnormalities and voluntary readjustments may ultimately result in the

unstable head positions observed in CD. Other regions such as the basal ganglia may also be involved in driving or compensating for the abnormal head movements in CD. Nonetheless, this hypothesis provides important clues for potential targets for future investigations in humans, as well as candidate regions for experimental manipulations in animals.

Chapter 4: Neuropathology of cervical dystonia*

4.1. Introduction

Neuropathological studies can be very helpful for identifying regions of brain abnormality associated with a neurological disorder. They are especially useful when multiple brain areas are known to control a specific function, yet the abnormality may be limited to only one of these. A well known example is Parkinson's disease, a disorder characterized by different kinds of movement impairments, such as slowness, tremor and limited motion. Many brain regions may contribute to these movement impairments, but neuropathological studies have isolated the source of the problem to nigrostriatal dopamine neurons. Therefore, neuropathology investigations provide valuable tools for pointing towards brain regions that may be involved in human disease.

The neuropathology of cervical dystonia (CD) has not been well characterized (Neychev et al., 2011; Standaert, 2011). A review of the literature disclosed only 15 autopsy reports for CD, and no consistent neuropathological changes were noted (**Table 4.1**). With only one exception, all of these reports were conducted more than 2 decades ago, and did not include immunohistochemical methods for detecting specific pathological processes. Additionally, most studies included fewer than 3 cases, and comparisons to healthy controls were often lacking. The failure to detect overt changes has contributed to the belief that there are no neuropathological defects in sporadic CD. However, additional studies with modern stains and quantitative methods are needed.

* Contents of this chapter were published as a peer reviewed manuscript in the journal *Experimental Neurology*. Reference: Prudente *et al.,* Exp Neurol. 2013; 241: 95-104.

Table 4.1: Postmortem studies of cases with CD

Onset	Age at death	Sex	Body region affected	Brain regions investigated	Pathological findings	Source
23	24	M	neck	BG, MB/BS, CBL	loss of neurons, gliosis, multiple lacunes in PUT, substantia innonimata; perivascular lymphocytic infiltration suggestive of vasculitis	(Foerster, 1933)
21	25	F	neck	CTX, THAL, CAUD, PUT, GP, SN, CBL	cell loss in CTX; cell loss in the molecular and Purkinje cell layers in CBL; diffuse perivascular lymphocytic infiltration and meningeal thickening consistent with chronic encephalitis	(Grinker and Walker, 1933)
43	90	M	neck, tongue, forearm, hand, fingers	CTX, GP, CAUD, PUT, THAL, SN, RN	atrophy of CAUD and PUT; cell shrinkage in CAUD, PUT and GP bilaterally, with vacuolization, pyknotic nuclei, neuronophagia, gliosis, and presence of lipoid pigment; cell loss in GP	(Alpers and Drayer, 1937)
59	65	F	neck	CTX, THAL, GP, CAUD, PUT, CBL (vermis, hemispheres and peduncles), MB, NBM, RN, SN, INC, pons, medulla, SC	normal	(Tarlov, 1970)
NA	NA	NA	neck	upper pons	normal	(Tarlov, 1970)
56	62	F	neck, upper and lower face	BG, SC, BS, CBL, cerebrum	normal	(Garcia-Albea et al., 1981)
NA	50	F	neck	NA	normal	(Zweig et al., 1986)

Onset	Age at death	Sex	Body region affected	Brain regions investigated	Pathological findings	Source
61	68	F	upper face, larynx, neck	CTX, HIP, CAUD, PUT, GP, hypothalamus, THAL, MB, pons, medulla, CBL	normal	(Jankovic et al., 1987)
47	50	F	neck	HIP, amygdala, GP, CAUD, PUT, basal forebrain, THAL, STN, BS, CBL	normal	(Zweig et al., 1988)
<33	68	M	upper and lower face, neck	HIP, amygdala, CAUD, PUT, ACC, GP, THAL, STN, CBL, SN, LC, NBM, raphe, PPN, medulla, CN III, CN IV	depigmentation in SN, LC; NFT in NBM; neuronal loss in SN, raphe, PPN, LC; astrocytosis in SN	(Zweig et al., 1988)
59	68	F	neck, lower face	CTX, CAUD, PUT, GP, NBM, THAL, STN, RN, SN,LC, raphe, inferior olive, SC (cervical and thoracic)	normal	(Gibb et al., 1988)
54	72	F	neck, face	PAG, PPN, RF, CNF, GP, CAUD, PUT, HIP, CTX (anterior frontal, parietal, temporal)	diffuse gliosis in GP; patchy gliosis in CAUD, PUT; signs of AD, Lewy bodies in BS	(Holton et al., 2008)
46	79	F	neck, lower face, hand	same as above	cystic infarct in CAUD; diffuse gliosis in GP; patchy gliosis in CAUD, PUT; small vessel disease in BG	(Holton et al., 2008)
47	65	M	axial, larynx	same as above	diffuse gliosis in GP; patchy gliosis in CAUD, PUT; mild small vessel disease	(Holton et al., 2008)

Onset	Age at death	Sex	Body region affected	Brain regions investigated	Pathological findings	Source
73	80	F	neck	same as above	diffuse gliosis in GP; patchy gliosis in CAUD, PUT	(Holton et al., 2008)

This table includes only cases originally described or typically cited as examples of sporadic or idiopathic dystonia. Segmental and multifocal dystonia cases were included if dystonia of the neck also was a prominent feature of the disorder. ACC, nucleus accumbens; AD, Alzheimer's disease; BG, basal ganglia; BS, brainstem; CAUD, caudate; CD, cervical dystonia; CNF, cuneiform nucleus; CN III, cranial nerve III; CN IV, cranial nerve IV; CBL, cerebellum, CTX, cerebral cortex; GP, globus pallidus; HIP, hippocampus; ID, identifier; INC, interstitial nucleus of Cajal; MB, midbrain; NA, not available; NFT, neurofibrillary tangles; NBM, nucleus basalis of Meynert; PAG, periaqueductal gray; PPN, pedunculopontine nucleus; PUT, putamen; RF, reticular formation; RN, red nucleus; SC, spinal cord; STN, subthalamic nucleus; THAL, thalamus.

Despite the absence of overt structural defects, functional imaging techniques have revealed areas of abnormality in sporadic CD. Positron emission tomography (PET) imaging of regional blood flow or glucose metabolism have shown abnormal patterns of activity involving cortical motor areas, the basal ganglia, thalamus, and cerebellum (Stoessl et al., 1986; Galardi et al., 1996; Magyar-Lehmann et al., 1997). Other imaging studies have raised the possibility of subtle architectural disturbances in these regions. Voxel-based morphometric studies of MRI scans from affected individuals have shown abnormal white and gray matter volumes in the cerebral cortex, basal ganglia, cerebellum, and thalamus (Draganski et al., 2003; Egger et al., 2007; Obermann et al., 2007; Draganski et al., 2009; Walsh et al., 2009). Diffusion tensor MRI also has shown abnormal fractional anisotropy in white matter tracts within the prefrontal cortex, basal ganglia, thalamus and corpus callosum, a measure that reflects microstructural anomalies (Colosimo et al., 2005; Bonilha et al., 2007; Fabbrini et al., 2008; Bonilha et al., 2009). Finally, investigations in animals have suggested that abnormal function of several brain regions can lead to abnormal head movements resembling CD (Evinger, 2005). Thus, findings from these investigations raise the possibility that subtle anatomical defects occur within specific brain regions in CD.

4.2. Objectives and significance

The purpose of the following experiments was to search for subtle histopathological abnormalities in postmortem brain tissue of individuals with CD in comparison to age-matched controls. We used the findings from imaging and animal studies as a guide to delineate potential neuropathological changes in sporadic CD. Identifying the regions of the brain that may cause CD is important for a better understanding of pathogenesis of the disorder and for rational design of new treatment strategies.

4.3. Materials and methods

4.3.1. Autopsy material

The National Institute of Child Health and Development Brain and Tissue Bank for Developmental Disorders at the University of Maryland was searched for autopsy specimens of subjects with CD. Twenty cases of possible sporadic CD were reviewed with approval by the Institutional Review Board of the Johns Hopkins University. Among these, 14 had histories compatible with sporadic CD according to current criteria, but only 4 had sufficient tissue of good quality for study (CD1-4). Tissue from 2 additional cases (CD5 and CD6) became available after the initial screening study and was included in the second part of the study. Because these samples came from a public brain bank, systematic sampling of multiple regions for stereological studies was not feasible, and clinical information was sometimes limited. Tissue from normal controls was obtained from the Johns Hopkins Brain Resource Center and the Emory Alzheimer's Disease Research Center.

Formalin-preserved tissue was methodically sampled with regions of interest based on recent human imaging investigations, animal studies, and findings from acquired CD. The regions sampled included the somatosensory cortex, caudate nucleus, putamen, globus pallidus, midbrain (including substantia nigra, red nucleus, interstitial nucleus of Cajal), brainstem, cerebellar hemispheres and vermis, and deep cerebellar nuclei. Tissue was embedded in paraffin and sectioned at 10 µm.

4.3.2. Genetic testing

Genotyping was performed on unstained sections from all CD cases and controls. Tested sections were from the cerebral cortex, midbrain, basal ganglia or cerebellum. Brain tissue was scraped from slides and transferred to microcentrifuge tubes. DNA was extracted with the Classic™ Genomic DNA Isolation Kit (Lamda Biotech, St. Louis, MO) and examined for sequence variants in exon 5 of *TOR1A* and all exons and introns of *THAP1* in 2 independent

runs involving sections from different brain regions, with Sanger sequencing as described previously (Xiao et al., 2009; Xiao et al., 2010).

4.3.3. Histological procedures

The staining battery was designed to detect inclusion bodies, in view of studies of other forms of dystonia (McNaught et al., 2004). Stains for degenerative processes were included in view of the association between CD and degenerative Parkinsonian disorders (Boesch et al., 2002; Papapetropoulos and Singer, 2006). Stains for inflammatory processes were included because of prior associations of focal dystonia with autoimmune diseases (Moore et al., 1986; Rajagopalan et al., 1989; Deitiker et al., 2011). Staining methods included hematoxylin/eosin (H&E), cresyl violet, Hirano silver, and immunohistochemistry. For immunohistochemistry, sections were stained for neuronal markers (parvalbumin, calbindin, calretinin), markers for intracellular inclusions (IC2 for polyglutamine sequences, TAR DNA binding protein 43, ubiquitin), neuroglial markers (glial fibrillary acidic protein, human leukocyte antigen-DR and ionized calcium binding adapter molecule 1), and cluster of differentiation 3, a T-cell marker. Sections first were heated at 37°C overnight, then heated to 60°C for 1 hr and deparaffinized. For antigen retrieval, sections were boiled in distilled water for 7 min. Nonspecific binding was blocked with 5% goat serum in phosphate-buffered saline, containing 0.4% Triton X-100 for 1 hr at room temperature. Slides were incubated with primary antibody overnight at room temperature and then with secondary antibody for 1 hr. Sections then were incubated with streptavidin-peroxidase complex and developed for 5 min with diaminobenzidine, and counterstained with cresyl violet.

4.3.4. Two-stage analysis

In the first stage of the analysis, an experienced neuropathologist examined the first 4 brains for overt changes. This subjective assessment revealed frequent ubiquitin-positive

inclusions in melanized nigral neurons and a patchy loss of cerebellar Purkinje cells. In the second stage of the study, material from the original 4 brains plus 2 additional brains that became available after the initial study were analyzed. The two main subjective findings identified in stage one were quantified and compared to age-matched controls by a microscopist blinded to phenotype. Tissue from 12 controls was investigated for the analysis of nigral inclusions, and 13 controls were studied for the Purkinje cells analysis. Quantification of the number of nigral inclusions and Purkinje cells was performed using Stereo Investigator (MicroBrightField, Inc., Williston, VT, USA). Two ubiquitin-stained sections from different regions of the substantia nigra were randomly selected for counting intranuclear inclusions for each case. Two H&E-stained sections from different regions of the cerebellum were randomly selected for Purkinje cell counts for each case.

4.3.5. Statistical analyses

To examine the association between CD and the number of nigral intranuclear inclusions, two statistical approaches were used. In one approach, the analysis was based on the proportion of cells with at least one inclusion. A logistic regression model was fitted to the proportion of cells with inclusions, and both age and group (CD or control) were analyzed as explanatory variables. To adjust for the correlation among neuronal cells within a given case, the Williams weighting option was used as implemented in SAS PROC LOGISTIC (SAS Institute Inc., Cary, NC, USA), which assumed an exchangeable correlation structure. The above approach had the limitation that it ignored information about the number of inclusions per cell. To use this cell-specific information, we considered an alternative approach based on the number of inclusions (ranging from 0 to 6) for each neuron. A log-linear regression model was fitted for the number of inclusions, and age and group were analyzed as explanatory variables. The generalized estimating equation method (Liang and Zeger, 1986) was used to adjust for intra-individual correlation among the cells.

Purkinje cell loss was investigated by examining linear Purkinje cell density measured as the number of cells/mm of Purkinje cell layer. Fitted linear regression models employing the generalized estimating equation approach were used to examine the association between CD and Purkinje cell density, with adjustments for age and the intra-individual correlation of Purkinje cell density measurements (Liang and Zeger, 1986). In this model, Purkinje cell density was the response variable and both age and group (CD or control) were explanatory variables. Residual plots were used to determine if there were departures from model assumptions, such as evidence of nonlinearity or non-constant variance.

A linear regression analysis using the generalized estimating equation approach also was conducted to investigate the association between the occurrence of *THAP1* sequence variants and Purkinje cell density, adjusted for age and group. In all regression analyses described, two persons with ages reported as “over 80” were assigned arbitrarily the age of 85.

4.4. Results

4.4.1. Samples

The CD cases consisted of 5 women and 1 man (**Table 4.2**). Mean age at onset was 45±10.7 years, and mean age at death was 70.0±10.4 years. Mean duration of CD was 25±15.3 years. Post-mortem intervals ranged from 5 to 25 hours. None of the 6 CD cases examined had clinical histories of prolonged agonal states with hypoxia, nor histories of taking drugs known to cause neuropathological changes. In stage 2 of the study, findings from CD individuals were compared to 16 age-matched controls (average age at death of 69.5±9.8 years, **Table 4.2**).

Although none of the CD cases had a family history of dystonia, all were examined for mutations associated with DYT1 and DYT6 dystonia. There were no c.904_906delGAG mutations or other variants in exon 5 of *TOR1A*. In contrast, 2 single nucleotide sequence variants in the non-coding region of *THAP1* (c.71+9C>A and c.268-31A>G) were identified in

both cases and controls (**Table 4.2**). The intron 1 variant (c.71+9C>A) was found in 3 CD cases. The intron 2 variant (c.268-31A>G) was found in 2 CD cases and 1 control. The c.268-31A>G variant is novel, but the c.71+9C>A variant has been reported (Xiao et al., 2010; LeDoux et al., 2012).

Table 4.2: Clinical information for CD cases and controls

ID	Diagnosis	Sex	Age at onset	Age at death	PMI	Cause of death	Family history	*THAP1* gene
CD1	CD, BL, FD	F	39	60	18	COD	negative	c.71+9C>A, het
CD2	CD	F	53	75	20	COD	NA	c.268-31A>G, het
CD3	CD, BL	M	52	58	5	temporal glioma	negative	c.71+9C>A, hom c.268-31A>G, hom
CD4	CD	F	40	65	25	CVD	negative	c.71+9C>A, het
CD5	CD, FHD	F	29	82	6	COD	negative	normal
CD6	CD, NT, HT	F	57	80	22	respiratory arrest	NT	normal
N1	normal	M	NR	55	NA	lung carcinoma	NA	normal
N2	normal	M	NR	59	NA	multiple sclerosis, stroke	NA	normal
N3	normal	M	NR	60	NA	cardiopulmonary arrest	NA	normal
N4	normal	F	NR	61	NA	cardiac failure	NA	normal
N5	normal	M	NR	62	NA	carcinoma of lymph nodes, liver, lung	NA	normal
N6	normal	F	NR	62	NA	leiomyosarcoma	NA	normal
N7	normal	M	NR	64	NA	lung carcinoma	NA	c.268-31A>G, het
N8	normal	M	NR	70	NA	nasopharyngeal carcinoma, leukemia	NA	normal
N9	normal	F	NR	74	NA	aortic aneurysm	NA	normal
N10	normal	F	NR	76	NA	lung carcinoma, aortic aneurysm	NA	normal
N11	normal	M	NR	76	NA	cardiac arrest	NA	normal
N12	normal	M	NR	77	NA	pneumonia	NA	c.71+9C>A, hom
N13	normal	M	NR	84	NA	bronchopneumonia, rheumatoid myocarditis	NA	normal
N14	normal	F	NR	80+	NA	NA	NA	normal
N15	normal	M	NR	80+	NA	NA	NA	normal
N16	normal	M	NR	69	NA	aortic aneurysm	NA	normal

Information was obtained from the University of Maryland Brain and Tissue Bank for Developmental Disorders, Johns Hopkins Brain Resource Center and the Emory Alzheimer's Disease Research Center. Age is expressed in years. BL, blepharospasm; CD, cervical dystonia; COD, "complication of disorder"; CVD, cardiovascular disease; F, female; FD, facial dystonia; FHD, focal hand dystonia; HT, hand tremor; hom, homozygous; het, heterozygous; ID, identifier; M, male; NA, not available; NR, not relevant; NT, neck tremor; PMI, post-mortem interval in hours. The glioma in CD3 was restricted to the temporal lobe on one side of the brain.

4.4.2. Screening phase

Tissue quality for all CD cases chosen for the final examinations showed good preservation and no signs of prolonged hypoxia before death.

The most salient findings in the midbrain included focal areas of gliosis, satellitosis (accumulation of glial cells around neurons), and frequent ubiquitin-positive intranuclear inclusions in the substantia nigra (**Figure 4.1**). These small and homogeneous round inclusions resembled Marinesco bodies, a common finding in melanin-pigmented neurons in the substantia nigra pars compacta and locus ceruleus of normal aged humans (Yuen and Baxter, 1963).

Findings in the cerebellum included focal areas of Bergmann gliosis, patchy loss of Purkinje cells, and torpedo bodies in the granule cell layer (**Figure 4.2**). Torpedo bodies are axonal swellings of Purkinje cells that are thought to be a non-specific result of abnormal accumulation of cellular constituents (Mann et al., 1980; Louis et al., 2009). No consistent abnormalities were seen in regions implicated in recent imaging and animal studies including the cerebral cortex, basal ganglia, interstitial nucleus of Cajal, red nucleus or pons. Findings for each case are summarized in **Table 4.3**.

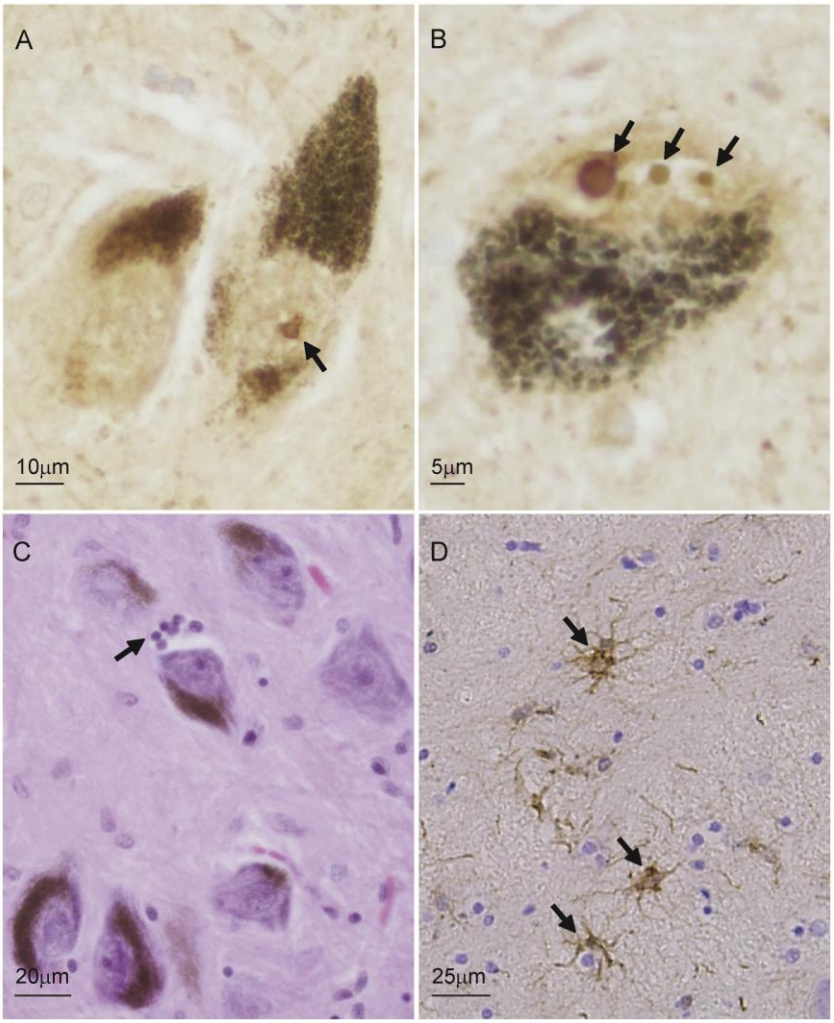

Figure 4.1: Histopathology in the midbrain. Panels A-B show typical ubiquitin-positive inclusions in the substantia nigra (Marinesco bodies). Nigral neurons with one or multiple inclusions were observed (black arrows). Panel C shows an example of satellitosis (arrow) around a dopaminergic neuron in the substantia nigra. Panel D shows increased number and activation of astrocytes (gliosis, arrows) in a midbrain section of a cervical dystonia case. Panels A-B: ubiquitin immunostaining; Panel C: hematoxylin and eosin; Panel D: glial fibrillary acidic protein.

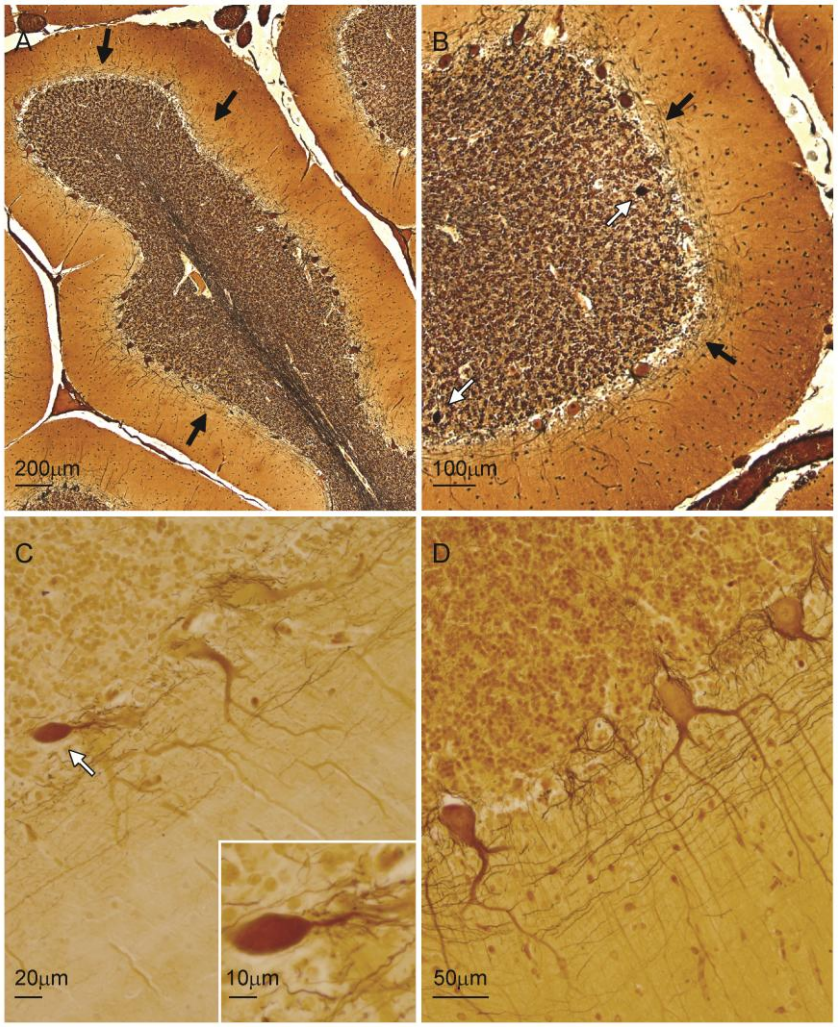

Figure 4.2: Histopathology in the cerebellum. Panels A-B shows areas with patchy loss of Purkinje cells, as indicated by the black arrows. Torpedo bodies (white arrows) can be identified in Panels B-C. Panel D shows a typical Purkinje cell layer with morphologically normal cell bodies. Panels A-D: silver impregnation.

Table 4.3: Main findings of the subjective screening study

ID	BS	MB	INC	RN	BG	CBL	CTX
CD1	normal	gliosis, ballooned neurons, satellitosis, uINI in SN	normal	normal	arrested migration of neuroblasts	gliosis, slight microgliosis, cell loss in dentate nucleus	normal
CD2	normal	corpora amylacea, isolated axonal swellings, satellitosis, uINI in SN	normal	normal	hyalinosis and mineralization (GP)	frequent torpedo bodies, patchy loss of Purkinje cells	normal
CD3	uINI (LOC)	slight microgliosis, slight satellitosis, patchy microgliosis in TG, uINI in SN	normal	normal	satellitosis	patchy microgliosis in peduncle, gliosis around Purkinje cells, slight satellitosis, Bergmann gliosis, torpedo bodies, patchy loss of Purkinje cells	normal
CD4	normal	isolated axonal swellings, clusters of oligodendrocytes, focal astrogliosis, satellitosis, uINI in SN	normal	normal	hemosiderin loaded macrophages	corpora amylacea, Bergmann gliosis in vermis, frequent torpedo bodies, patchy loss of Purkinje cells	normal

Tissue from cases CD5 and CD6 was not analyzed during the initial screening study. BG, basal ganglia (caudate, putamen, globus pallidus); BS, brainstem; CBL, cerebellum; CTX, cerebral cortex; GFAP, glial fibrillary acidic protein; GP, globus pallidus; ID, identifier; INC, interstitial nucleus of Cajal; LOC, locus ceruleus; MB, midbrain; RN, red nucleus; SN, substantia nigra; TG, tegmentum; uINI, ubiquitinated intranuclear inclusions.

4.4.3. Quantification phase

Ubiquitin-positive intranuclear inclusions in the substantia nigra were quantified in 6 CD individuals and 12 controls (**Table 4.4**). The number of melanized neurons available for counting ranged from 139 to 1393. The number of inclusions in individual melanized neurons ranged from 0 to 6. Among CD cases, 8% of the cells counted had at least one inclusion, as compared to 11% of cells counted in the control group. The mean ± standard deviation for the total number of inclusions indentified was 35.8±25.2 for the CD group and 63.0±81.3 for the controls. The logistic regression analysis indicated that neither group (Wald test: W=0.44; 1 df; p=0.51) nor age (Wald test: W=1.41; 1 df; p=0.24) was a significant predictor of the proportion of cells with inclusions. The estimated intra-individual correlation was r=0.06 among the cells counted. Further analysis included an investigation of the association between number of inclusions per cell, group and age. Log-linear regression analysis based on the number of inclusions (ranging from 0 to 6) per cell failed to converge to a solution, owing to numerical difficulties. As an alternative, computationally simpler approach, a square root transformation was applied to the inclusion counts in order to stabilize their variances, and a linear regression model was fitted using the generalized estimating equation method. The results of this cell-specific regression analysis showed that neither group (Wald test: W=0.89; 1 df; p=0.37) nor age (Wald test: W=-0.74; 1 df; p=0.46) was a significant predictor of the number of inclusions. The quantitative study therefore failed to confirm any abnormality of nigral inclusions in the CD brains.

Table 4.4: Number of nigral inclusions in melanized neurons in the substantia nigra

ID	Total cell count	Total number of cells w/ inclusions	Proportion of cells with inclusions (%)	Number of cells with 1 to 6 inclusions per cell					
				1	2	3	4	5	6
CD1	698	58	8.3	28	12	12	5	0	1
CD2	407	12	2.9	6	3	2	1	0	0
CD3	263	8	3.0	5	0	2	1	0	0
CD4	396	31	7.8	16	12	1	1	1	0
CD5	365	72	19.7	37	24	9	2	0	0
CD6	531	34	6.4	24	8	2	0	0	0
N2	262	43	16.4	29	8	4	2	0	0
N3	197	0	0.0	0	0	0	0	0	0
N5	139	3	2.2	2	0	1	0	0	0
N6	727	53	7.3	40	10	3	0	0	0
N7	141	8	5.7	2	4	2	0	0	0
N8	705	15	2.1	10	4	1	0	0	0
N9	1393	252	18.1	130	71	32	16	3	0
N10	200	47	23.5	28	17	2	0	0	0
N12	980	199	20.3	78	52	40	21	7	1
N14	353	7	2.0	6	0	0	1	0	0
N15	355	35	9.9	21	9	4	1	0	0
N16	504	94	18.7	53	21	12	7	0	1

Ubiquitin-positive intranuclear inclusions in the substantia nigra were quantified in 6 CD individuals and 12 controls. The number of inclusions in each melanized neurons ranged from 0 to 6. Logistic regression analysis indicated that neither group nor age was a significant predictor of the proportion of cells with inclusions, or the number of inclusions per cell. ID, identifier.

Main subjective findings in the cerebellum included loss of Purkinje cells, areas of focal gliosis and torpedo bodies. Due to difficulties in quantifying gliosis and the low frequency of torpedo bodies, the only variable analyzed was Purkinje cells. The linear density of Purkinje cells was measured in two separate cerebellar sections from each of 6 CD individuals and 13 controls (**Figure 4.2A**). The CD group had an average linear density of 2.26±0.48 cells/mm, whereas controls had an average linear density of 2.70±0.58 cells/mm. Regression analysis indicated that CD was significantly associated with lower linear density of Purkinje cells (Wald test: W=-2.06; 1 df; $p<0.05$). The estimated intra-individual correlation was r=0.73 for the linear density of Purkinje cell measurements. Age was not a significant predictor of Purkinje cell linear density ($p=0.72$). Moreover, dropping age from the model did not affect the fitted regression

coefficient for group, indicating that age was not a confounding variable. Residual plots did not reveal any apparent departures from model assumptions. These results confirm a lower linear density of Purkinje cells in CD brains in comparison with controls.

Independent from patient group (CD vs. controls), samples with a *THAP1* sequence variant had a lower linear density of Purkinje cells (2.14±0.54 cells/mm) compared to *THAP1* negative cases (2.75±0.48 cells/mm) as revealed by linear regression analysis (Wald test: W=-2.00; 1 df; $p<0.05$; **Figure 4.2B**). The controls with *THAP1* sequence variants (N7 and N12) fell at the lower limits of normal for linear density. The unexpected finding of *THAP1* sequence variants in the control group led to a more detailed investigation of the available medical records. N7 had no neurological problems, but N12 had a history of hand tremors. The neuropathological evaluation of N12 was not consistent with Parkinson's disease, but available records were insufficient to determine if the tremors were consistent with dystonic or essential tremor.

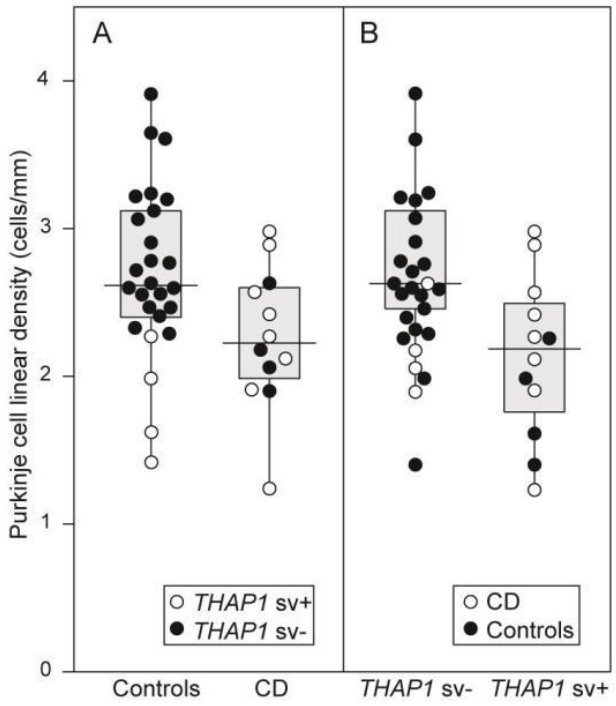

Figure 4.3: Box and whisker plot comparing Purkinje cell linear density in 6 cervical dystonia (CD) cases and 13 controls. In this type of plot, the upper and lower limits of the box show the upper and lower quartiles of the data, with the horizontal line in between showing the median. The whiskers show the entire data range, and circles depict each data point. Two independent sections for each subject were analyzed, and all 12 points for the CD group and 26 for the controls are shown. Regression analysis indicated that CD was significantly associated with lower density of Purkinje cells at $p<0.05$ (A). Regression analysis also revealed that cases with a *THAP1* sequence variant (*THAP1* sv+) had a significantly lower linear density of Purkinje cells compared to *THAP1* negative cases at $p<0.05$ (*THAP1* sv-) (B). In A, open and closed circles represent the data for *THAP1* positive and negative cases within each group. In B, open and closed circles represent the data for CD and controls within each *THAP1* group.

4.5. Discussion

The experiments described provide neuropathological findings from the largest cohort of CD patients ever evaluated. Guided by recent findings from human neuroimaging studies and animal models, this investigation provides a more thorough and quantitatively rigorous evaluation than previously available. In the more traditional subjective phase of these studies when 4 CD brains were available, two changes

appeared salient. The CD brains appeared to have a relatively large number of Marinesco bodies in the substantia nigra. The CD brains also appeared to show reduced cerebellar Purkinje neurons, along with related findings of increased torpedo bodies and focal regions of gliosis. Extensive stains failed to reveal any consistent defects in the basal ganglia, cerebral cortex, red nucleus, or interstitial nucleus of Cajal. The absence of consistent structural defects in these regions was disappointing, considering that these areas have been implicated in multiple prior studies relevant to CD (Carpenter et al., 1958; Malouin and Bedard, 1982; Fukushima, 1987; Walker et al., 1990; Neychev et al., 2011). In the second quantitative phase of our studies, the reduced number of Purkinje neurons was confirmed, but the increase in nigral inclusions was not. Although we did not intend to address neuropathology associated with *THAP1* sequence variants, an incidental finding was a significantly lower linear density of Purkinje cells among cases harboring such variants, regardless of whether they had CD or not. The results are valuable for three main reasons. First, they highlight some general weaknesses in the way that human neuropathological studies for dystonia have been conducted, and they lead to suggestions for potential solutions. Second, they question recent classifications of dystonia that propose to discriminate acquired from sporadic forms by the presence or absence of neuropathological correlates. Third, they highlight limitations inherent to all studies that involve attempts at clinico-pathological correlations, including dystonia.

4.5.1. Limitations of human neuropathology

While it may initially seem surprising that no prior study has identified the changes described in the current studies, an analysis of the prior reports reveals several explanations. One reason is that there are only 15 reported cases, with most studies including only 1-2 cases, making it difficult to appreciate subtle defects (Foerster, 1933;

Grinker and Walker, 1933; Alpers and Drayer, 1937; Garcia-Albea et al., 1981; Jankovic et al., 1987). Moreover, all prior studies relied exclusively on subjective impressions of a neuropathologist, with no quantification of suspected abnormalities, eliminating the possibility of identifying subtle quantitative differences. Additionally, several of these reports included cases with clinical or neuropathological findings suggesting acquired CD (**Table 4.1**), and others combined different types of dystonias, presuming a common neuropathological substrate (Gibb et al., 1988; Zweig et al., 1988; Holton et al., 2008). By mixing different disorders in the same study, any potentially consistent defect limited to sporadic CD becomes difficult to discern. With a single exception (Holton et al., 2008), all prior reports were published more than two decades ago; and they did not include special methods such as immunohistochemistry with the power to detect specific neuropathological processes.

Perhaps the most serious shortcoming of prior studies is that many focused only on specific regions of interest. As summarized in a recent review (Neychev et al., 2011), the belief that all forms of dystonia arise from dysfunction of the basal ganglia has dominated scientific thought for decades, despite accumulating evidence that other brain regions are involved. Some of the prior autopsy studies highlighted abnormalities in the striatum and/or globus pallidus in tissue of CD individuals (Foerster, 1933; Alpers and Drayer, 1937; Holton et al., 2008). However, brain regions other than the basal ganglia were often not analyzed in detail, so it is possible that additional defects in other areas were overlooked. Furthermore, several prior studies of CD did not address the cerebellum (Alpers and Drayer, 1937; Tarlov, 1970; Zweig et al., 1986; Gibb et al., 1988; Holton et al., 2008). Among the few studies that reported a broader analysis in cases of probable sporadic CD, one described patchy loss of Purkinje cells, but quantitative comparisons to controls were lacking (Garcia-Albea et al., 1981). As a result, the authors interpreted these findings as incidental.

Wherever possible, we aimed to avoid the limitations of prior studies. To avoid problems associated with mixing different forms of dystonia together, we focused on cases with isolated sporadic CD. Cases of acquired CD were excluded. Although dystonia outside of the neck region was allowed, CD was the main clinical problem. We also employed an extensive battery of histological stains sensitive for detecting inclusion bodies, degeneration, or inflammatory processes. We also took advantage of evidence from modern human neuroimaging studies and animal studies to guide selection of brain regions. The Marinesco bodies in the substantia nigra initially were intriguing, in view of evidence that they may be more frequent in dopamine-related disorders (Beach et al., 2004), combined with evidence of dysfunction of dopamine pathways in dystonia (Perlmutter and Mink, 2004; Wichmann, 2008; Zhao et al., 2008). The cerebellar defects also were intriguing, in view of recent studies suggesting abnormal cerebellar Purkinje neuron activity in dystonia (Pizoli et al., 2002; Neychev et al., 2008; Chen et al., 2009). As a final step, we sought to confirm subjective findings with rigorous quantitative methods. We were unable to confirm an increase in Marinesco bodies, highlighting the weakness in relying on subjective impressions. However, we were able to confirm a reduction in the linear density of cerebellar Purkinje neurons. Purkinje neurons densities in CD overlapped with those of controls (**Figure 4.2**), explaining how such a defect might be overlooked in prior studies.

After the histopathology was completed, molecular studies were conducted to identify sequence variants associated with DYT1 and DYT6 dystonia. Although none had the GAG deletion of DYT1 dystonia, 4 cases and 2 controls unexpectedly were found to harbor sequence variants in *THAP1*. The spectrum of *THAP1* mutations responsible for causing DYT6 dystonia is heterogeneous and not yet fully defined (Xiao et al., 2010; LeDoux et al., 2012; Paudel et al., 2012). The c.71+9C>A variant was first reported by Xiao and colleagues (Xiao et al., 2010) with an allele frequency of 7/2420 in

mainly adult-onset sporadic dystonia and 1/1200 in matched controls. A follow-up investigation revealed that this variant is likely to be pathological (Vemula et al., 2014). The c.268-31A>G variant is novel. In comparison to previous work using DNA derived from whole blood (Xiao et al., 2010), the relatively high frequency of *THAP*1 variants in the post-mortem samples examined in this study suggests the possibility that *THAP*1 is prone to somatic mutations (Kennedy et al., 2012). Nonetheless, *THAP1* sequence variants appear to be associated with significantly lower linear density of Purkinje cells regardless of the existence of CD, a finding consistent with observations that Purkinje cells express the highest levels of this gene in the brain (LeDoux et al., 2012). The existence of *THAP1* sequence variants in 2 controls led to questions regarding whether they should be included in the final analysis, especially since one clinically had overt tremor. However, eliminating these controls *improved* the strength of the association between lower Purkinje cell density and CD, because both of these controls fell at the lowest limits of the control group (**Figure 4.3**). These findings emphasize the importance of molecular diagnosis in both cases and controls.

Despite an improved study design, our study still had several shortcomings. We examined only 6 CD brains. Based on the results we obtained for Purkinje cell linear density, a power analysis indicates the need for 15 CD cases for a confirmatory follow-up study. Because CD is so rare, obtaining this many cases could take many years without a large-scale cooperative effort. The rarity of CD and the small number of brains evaluated also creates a risk of missing subtle changes elsewhere in the brain, but were not sufficiently obvious to be detected in the screening neuropathological portion of our study. Many histological findings were not quantified, so it remains possible that significant changes exist in brain regions other than the cerebellum.

Another limitation of our study was that it involved tissue available through a public brain bank, where precise selection of matched brain regions was not feasible.

Tissue selection is important, because different body regions are represented somatotopically in many brain regions, including the cerebellum. Notably, tissue from different regions of the cerebellum were not available for analysis. It also was not possible to compare the corresponding right and left sides of the brain, which may be important for a disorder such as CD, where the head and neck are consistently turned or tilted in one direction. A related limitation was the paucity of detailed clinical information, such as the direction of head movements, which could be important for interpreting asymmetrical findings in the brain, or presence of tremor, which is associated with neuropathological findings similar to those reported here (Louis et al., 2006; Louis and Vonsattel, 2008; Shill et al., 2008; Louis et al., 2009; Louis et al., 2011).

A final limitation was the inability to include truly stereological methods for counting inclusions and cells. Truly unbiased stereological studies of human autopsy material are rarely feasible because of specific requirements including sectioning of the entire region of interest, systematic random sampling through the tissue, and particularly the requirement for random planes of section (Kristiansen and Nyengaard, 2012). Finally, despite a comprehensive battery of stains, none was sensitive for the detection of changes in the fine structure of neurons, such as dendrites. Most of these limitations are a common problem in autopsy studies and they might be solved by the establishment of a centralized brain bank, where the collection and processing of clinical information together with post-mortem brains could be standardized. Any follow-up study also would have to account for *THAP1* sequence variants, and ideally incorporate new evidence regarding which of these variants may be pathogenic.

4.5.2. Relevance for classifying the dystonias

The results of these studies are directly relevant to efforts that classify the many different dystonias by etiology. Traditionally, idiopathic and acquired dystonias are

distinguished largely based on whether the clinical phenotype is pure or mixed with non-dystonic features. However, some investigators have suggested that the distinction also includes the occurrence of histopathogical defects (Neychev et al., 2011). For example, some authors have described idiopathic dystonia as a "neurofunctional disorder" because of the absence of apparent neurodegeneration (Breakefield et al., 2008). Others have similarly stated that idiopathic dystonia is characterized by "abnormal functioning of a structurally-normal appearing brain" (Tanabe et al., 2009). Several additional authors have implied that idiopathic dystonias are defined in part by the absence of neuropathological abnormalities (De Carvalho Aguiar and Ozelius, 2002; Nemeth, 2002; Schwarz and Bressman, 2009).

The current studies showing a lower linear density of Purkinje neurons in the cerebellum in CD demonstrate that neuropathological changes may be revealed in dystonia when appropriate methods are applied. In fact, prior studies of human DYT1 generalized dystonia have shown perinuclear inclusions in the brainstem, although frank cell loss was not apparent (McNaught et al., 2004). Histological studies of animal models of DYT1 dystonia also have revealed subtle changes of the structure of the dendrites of cerebellar Purkinje neurons (Zhang et al., 2011) or size of midbrain dopamine neurons (Song et al., 2012). Finally, modern human neuroimaging studies of CD have repeatedly provided evidence for microstructural defects (Neychev et al., 2011; Zoons et al., 2011). In view of these findings, it seems likely that additional neuropathological changes will be uncovered. If this is the case, then reliance on the presence or absence of neuropathological abnormalities to discriminate idiopathic from acquired dystonia becomes increasingly problematic.

4.5.3. Inferring causation from clinico-pathological studies

Results from clinico-pathological studies inevitably lead to questions regarding a causal link between the clinical features and the histopathological defects. The results presented here are correlative and cannot establish a causal link between CD and a lower linear density of Purkinje neurons. In fact, Purkinje cell loss is a non-specific finding that is associated with a variety of conditions. Purkinje cell loss is typical of a large group of disorders known as the spinocerebellar ataxias (Yang et al., 2000; Sarna and Hawkes, 2003). However, Purkinje cell loss sometimes is associated with other degenerative disorders such as Parkinson's disease (Takada et al., 1993; Wenning et al., 1996) or Alzheimer's disease (Sarna and Hawkes, 2003; Mavroudis et al., 2010). Purkinje cell loss also occurs in non-degenerative disorders including essential tremor (Louis et al., 2006; Louis and Vonsattel, 2008; Louis et al., 2011), hypoxia/ischemia (Sarna and Hawkes, 2003; Kern and Jones, 2006), traumatic brain injury (Sarna and Hawkes, 2003; Park et al., 2007), autism (Sarna and Hawkes, 2003; Kern and Jones, 2006), a variety of drugs and toxins (Sarna and Hawkes, 2003), and even normal aging (Sarna and Hawkes, 2003; Zhang et al., 2010). Cerebellar Purkinje neurons therefore seem unusually vulnerable to many biological processes.

It is important to note that our cases had a relatively narrow age range that statistically did not contribute to Purkinje cell density, none had clinical histories of using drugs known to affect Purkinje neurons, none had evidence of another neurodegenerative disease or trauma, and tissue quality was good with no evidence of prolonged hypoxia before death. Thus, it is unlikely that Purkinje cell loss resulted from these other conditions. However, the association of Purkinje neuron loss with other disorders emphasizes that the lower linear density of Purkinje neurons found in CD is not specific to this disorder, and probably not responsible for causing dystonic symptoms.

The relationships between CD and essential tremor are important to consider. Clinically, up to two thirds of patients with CD have a tremor that resembles essential tremor (Jankovic et al., 1991; Pal et al., 2000), and recent studies have suggested that CD and essential tremor may share similar genetic substrates (Hedera et al., 2010). The neuropathology of essential tremor is similar to our findings, with subtle reductions in the linear density of Purkinje neurons, prominent torpedo bodies, and focal areas of Bergmann gliosis (Louis et al., 2006; Louis and Vonsattel, 2008; Shill et al., 2008; Louis et al., 2009; Louis et al., 2011). In view of the many relationships between CD and essential tremor, it is perhaps not surprising that they may share some similar pathological features. In essential tremor, the loss of Purkinje neurons may not cause tremor, but instead may reflect a pathological neurophysiological process involving aberrant oscillatory activity in circuits that involve the cerebellum, thalamus, and motor cortex (Raethjen and Deuschl, 2012). The reduction in the linear density of Purkinje neurons in CD may similarly reflect abnormal cerebellar physiology, although the nature of the physiological changes probably differs from essential tremor. Animal studies have suggested that abnormal bursting patterns of cerebellar Purkinje neurons may underlie dystonia, and this abnormal bursting may predispose to torpedo body formation, gliosis, and loss of these neurons (LeDoux and Lorden, 2002; Chen et al., 2009). Thus a reduction in Purkinje cell density is neither specific nor causal in CD, but may instead provide a clue to an abnormal physiology. This interpretation is consistent with recent genetic studies suggesting that CD may result from mutations affecting Purkinje neuron function (Xiao et al., 2012).

Chapter 5: Summary and final conclusions*

5.1. Overview

The findings from **Chapters 2-4** begin to fill critical gaps in the understanding of normal and abnormal head movements in humans. Our results indicate that isometric tasks provide a suitable method for investigating head movements with functional magnetic resonance imaging (fMRI). They open the door to using brain imaging to identify brain regions involved with head movements in any direction, both in normal and diseased populations. Furthermore, the neuroimaging and neuropathology studies focused on cervical dystonia (CD) added valuable information to our knowledge of brain regions responsible for this poorly understood disorder.

In **Chapter 2**, we described the patterns of brain activity associated with isometric head rotation that were investigated with fMRI in healthy volunteers (Prudente et al., 2015). Isometric wrist extension activated similar brain regions as prior studies have reported for actual hand movements. Isometric head rotation significantly activated the bilateral precentral gyrus, but with contralateral predominance. Activation of the precentral gyrus in each hemisphere was observed both medial and lateral to the hand area. The medial precentral focus was activated only during head tasks, whereas the lateral precentral focus was active during both hand and head tasks. These results suggest that the medial precentral gyrus has a more specific role in generating head movements, while the lateral precentral focus may be involved in any isometric task, either monitoring movement or stabilizing the body. Other regions involved in head movements

* Contents of this chapter were published as a peer commentary in the journal *Neuroscience*. Reference: Prudente *et al.,* Neurosci. 2014; 260: 23-35.

were also indicated by our studies, such as the supplementary motor area, insula, putamen, and ipsilateral cerebellum. These findings help to clarify the location of the neck region in the motor homunculus and reconcile prior conflicting results in the field.

The fMRI studies in CD described in **Chapter 3** represent the first task-based neuroimaging investigation of head movements in this population. Isometric head rotation in the CD group produced less prominent activation of the medial precentral gyrus, the same region identified as important for isometric head rotation in normal individuals. Additionally, CD subjects had an overall broader activation of cortical and subcortical areas during head and hand isometric tasks, but direct comparisons between controls and CD did not reveal statistically significant differences. Perhaps the most relevant findings derived from the analyses of CD data normalized to the side of torticollis. This novel analytical strategy indicated that isometric head rotation in the direction of torticollis is associated with more activation in the ipsilateral cerebellum, whereas moving the head in the opposite direction is associated with more activity in sensory and motor cortical areas. Although prior studies had never considered the impact of the direction of abnormal movements in CD in imaging studies, our findings are perhaps not surprising. The importance of laterality has been well accepted in imaging studies of the limbs. No one would ever consider combining results from one limb affected by writer's cramp or stroke with the unaffected limb to be a reasonable strategy. The same applies for CD, even though the head is a single structure that moves as one unit.

The investigation of postmortem brain samples of CD individuals and controls described in **Chapter 4** represented the largest autopsy study of dystonia using quantitative and immunostaining methods. Guided by findings from animal models and imaging studies in humans, several brain regions were examined with an extensive battery of histopathological stains in a two-stage study design (Prudente et al., 2015).

The initial subjective neuropathological assessment revealed only two regions with relatively consistent changes. The substantia nigra had frequent ubiquitin-positive intranuclear inclusions known as Marinesco bodies. Additionally, the cerebellum showed patchy loss of Purkinje cells, areas of focal gliosis and torpedo bodies. Other brain regions showed minor or inconsistent changes. In the second stage of the analysis, quantitative studies confirmed a significantly lower Purkinje cell density in CD. Our interpretation is that the reduction in the linear density of Purkinje neurons in CD may reflect abnormal cerebellar physiology, and this may predispose to torpedo body formation, gliosis, and subtle loss of Purkinje neurons. Furthermore, the results indicate that subtle neuropathological changes may be revealed in CD when appropriate methods are applied.

Overall, the fMRI results combined with the neuropathology findings provide convergent evidence that the cerebellum is involved in head movements, and that abnormal cerebellar function may be associated with CD. Consistent with these findings, several investigations in animals and humans have implicated the cerebellum in different types of dystonias (Neychev et al., 2011; Filip et al., 2013; Prudente et al., 2014). In this chapter, we explore how the cerebellum may be involved in CD and speculate about which neural pathways may mediate the abnormal head movements observed in the disorder. We will focus on five main questions:

- What does greater cerebellar fMRI activation mean?
- Is cerebellar involvement due to degeneration or abnormal function?
- Is there any other evidence of cerebellar dysfunction in CD?
- How can dysfunction of the cerebellum lead to abnormal head movements in CD?
- How can the results be used to guide future studies?

5.2. What does greater cerebellar fMRI activation mean?

The most relevant finding of our fMRI studies in CD was the greater activity in the cerebellum during isometric head rotation in the direction of torticollis when compared to head rotation to the opposite side. However, how can greater fMRI activation in the cerebellum be related to abnormal head movements in CD?

The neurophysiological processes that drive the cerebellar blood oxygenation level dependent (BOLD) signal are not fully understood. In the cerebral cortex, activity-dependent energy use and the BOLD signal are thought to be mainly driven by the postsynaptic effects of glutamate caused by excitatory inputs to a cortical region (Arthurs and Boniface, 2002; Heeger and Ress, 2002). Thus, to understand the source of the cerebellar BOLD signal, it is important to understand how much energy is demanded by neural processes within the cerebellum.

Stimulation of mossy and climbing fibers in rodents leads to time-locked increases in blood flow in the cerebellar cortex (Mathiesen et al., 2000). Granule cells use 67% of the energy, most of which is consumed by the process of relaying mossy fiber input in the cerebellar cortex (Diedrichsen et al., 2010). Studies in rodents have shown that 18% of the energy in the cerebellar cortex is consumed by Purkinje cells (Thomsen et al., 2004). Furthermore, stimulation of parallel fibers in rats increases blood flow and tissue oxygen in the cerebellar cortex (Diedrichsen et al., 2010). If the proportional increases of blood flow and energy use observed in the cerebral cortex hold for the cerebellum, those numbers suggest that increased activity in the mossy and parallel fiber systems contributes most to the BOLD signal. Therefore, increased fMRI activation in the cerebellum is likely driven by increased signaling in the cerebellar cortex (Diedrichsen et al., 2010).

Considering the intrinsic and extrinsic cerebellar connections, we can speculate that the increased cerebellar BOLD signal observed in our fMRI experiments was a

result of increased signaling in granule and Purkinje cells, which in turn led to augmented inhibition of the deep cerebellar nuclei. The final result would be decreased or altered cerebellar output to the ventrolateral thalamus and other subcortical areas receiving inputs from the cerebellum, such as the red nucleus, vestibular nuclei, reticular formation, inferior olive, superior colliculus and interstitial nucleus of Cajal.

Altered activation of the ventrolateral thalamus by the deep cerebellar nuclei would lead to abnormal excitation of the cerebral cortex, especially in the primary motor cortex (M1). As a result, abnormal signals would be transmitted from M1 to cervical neck motor neurons through the corticospinal and corticobulbar tracts, which may explain the impaired voluntary control of neck muscles observed in CD. Similarly, distorted cerebellar output to the other efferent connections of the cerebellum may ultimately lead to abnormal activation of several direct subcortical pathways to cervical motor neurons. These pathways include the vestibulospinal, reticulospinal, tectospinal, interstitiospinal and fastigiospinal tracts (Fukushima, 1987; Peterson, 2004). Altered output to these subcortical pathways may lead to abnormal activation of neck motor neurons and induce altered activity of cervical muscles in individuals with CD.

Although available data regarding the sources of cerebellar BOLD signal provide a model for the neurophysiological processes underlying increased fMRI activation in the cerebellum, we cannot determine the cause of this increased BOLD signal in our experiments. In individuals with CD the source of increased signaling in the cerebellar cortex may be due to altered function of any region that sends projections through the mossy or climbing fiber systems, intrinsic abnormalities of granule cells, or altered function of Purkinje cells. Interestingly, in **Chapter 4** we observed decreased density of Purkinje cells associated with signs of Purkinje cell injury in CD cases. Therefore, based on the neuropathology data, we hypothesize that the greater BOLD signal during head

rotation in the direction of torticollis in comparison to the opposite direction represented abnormal function of the remaining Purkinje cells in participants with CD.

5.3. Is cerebellar involvement due to degeneration or abnormal function?

In **Chapter 4**, we identified a lower density of Purkinje cells in CD brains in comparison to age-matched controls. These findings lead to the pertinent question of whether cerebellar involvement in CD is due to neurodegeneration in the cerebellum. Considering that evidence of degeneration of the cerebellum or any other brain regions has not been reported in sporadic dystonias, we propose that the subtle Purkinje cell loss observed in CD cases does not represent a cause for the disorder. Instead, we propose that Purkinje cell function in CD is chronically abnormal and the loss of these neurons is a consequence of their distorted function.

Overt lesions of the cerebellum detectable with imaging methods are those that involve loss of cerebellar tissue, such as stroke, and they usually cause ataxia, not dystonia. But what might be the outcome of lesions that are irritative and distort cerebellar output instead? It has been proposed that dystonia can result from lesions of the cerebellum that distort cerebellar output (Neychev et al., 2011). Such “lesions” may result from local irritation, such as hemorrhage, or functional derangements due to compressive effects of mass lesions. Such “lesions” may also be primarily functional, with no overt anatomical abnormality.

A simple and well-documented illustration of this point involves the consequences of lesions in M1. Destructive lesions with loss of cortical function in M1 result in weakness or paralysis. On the other hand, irritative lesions causing distorted cortical output cause epileptic seizures. Irritative lesions often are not visible with routine clinical imaging studies. In some cases the responsible lesions can be revealed with detailed histological studies. In other cases, the “lesion” is based on a functional defect.

Thus, lesions of M1 can cause different motor phenotypes, depending on the nature of the lesion and its consequences. This phenomenon is not unique to the cerebral cortex, but also is known to occur in most other regions of the nervous system. Therefore, it is possible that distorted cerebellar output instead of loss of function may result in dystonia, not ataxia (**Figure 5.1**).

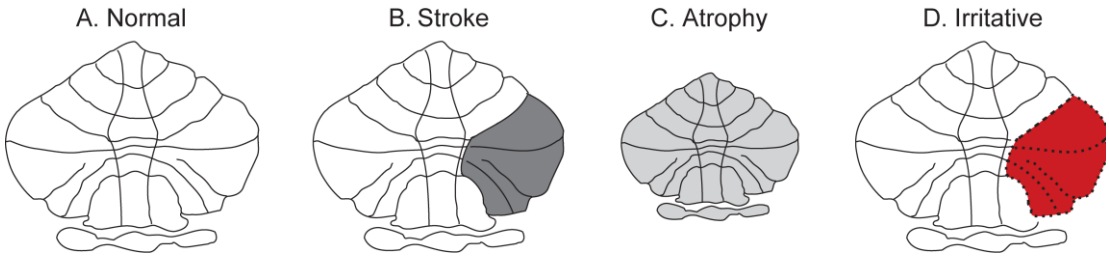

Figure 5.1: Lesions of the cerebellum may cause different phenotypes depending on the nature of the lesion and its consequences. Normal cerebellar structure and output from the cerebellum result in normal patterns of movements (A). Decreased cerebellar output due to cerebellar stroke (B) or atrophy (C) may cause ataxia. In contrast, irritative lesions causing distorted cerebellar output (represented in red) may lead to dystonia (D).

The hypothesis of distortion of cerebellar output is consistent with prior literature indicating that cerebellar lesions occasionally may cause dystonia (Neychev et al., 2011). Such lesions are more likely to be space-occupying lesions such as tumors that compress and distort surrounding cerebellar functions, or hemorrhages that cause a local irritative focus. This hypothesis also is consistent with observations that the vast majority of function-based imaging studies of human dystonia, such as positron emission tomography (PET) studies of fluorodeoxyglucose or blood flow, have revealed increases in cerebellar activity, not decreases (Neychev et al., 2011). Furthermore, the hypothesis is consistent with the strong relationship between dystonia and tremor, because tremor also is viewed as functional distortion of cerebellar processing.

It also is important to acknowledge a phenomenon in studies that attempt to link focal lesions with dystonia. Following an acute insult to the nervous system such as stroke, dystonia rarely emerges immediately. Instead, it typically emerges after a delay of several weeks or years (Saint Hilaire et al., 1991; Ghika et al., 1994; He et al., 1995; Scott and Jankovic, 1996; Palfi et al., 2000; Kim, 2001). This delay argues that the lesion itself cannot be causing dystonia by loss of function from the damaged region. Instead, dystonia must arise from some secondary adaptive response to the lesion. The location of this adaptive response is unknown. It may occur in nearby undamaged structures, or it may occur in more remote regions. Thus the lesion method, while used extensively to establish structure-function relationships in clinical neurology, has an unexplained limitation in studies of dystonia. However, studies addressing potential adaptive changes in the brain that occur with the development of dystonia could provide powerful clues to the real source of the problem.

The distinction between lesions that cause distorted function versus loss of function is also consistent with multiple animal studies showing that dystonia arises from distorted cerebellar output due to abnormal increase in Purkinje cell firing or abnormal bursting patterns, rather than loss of output (LeDoux et al., 1993; LeDoux et al., 1995; LeDoux et al., 1998; Pizoli et al., 2002; Xiao and Ledoux, 2005; Calderon et al., 2011; Alvarez-Fischer et al., 2012; Fan et al., 2012; Raike et al., 2012; Raike et al., 2015). For instance, generalized dystonia in the *dt* mutant rat arises from abnormal Purkinje neuron output (LeDoux et al., 1993; LeDoux et al., 1995). Paroxysmal dystonia in *tottering* mutant mice similarly arises from dysfunctional Purkinje neurons (Campbell and Hess, 1999; Campbell et al., 1999; Neychev et al., 2008; Raike et al., 2013). Importantly, removal of the cerebellum or selective genetic deletion of Purkinje neurons eliminates dystonia in those models (LeDoux et al., 1993; LeDoux et al., 1995; Campbell and Hess, 1999; Campbell et al., 1999; Neychev et al., 2008; Raike et al., 2013), suggesting that

the abnormal firing of Purkinje cells caused the aberrant movements, not cell death. Interestingly, some of these studies have suggested that the abnormal bursting patterns of cerebellar Purkinje neurons may predispose to torpedo body formation and gliosis (LeDoux and Lorden, 2002; Chen et al., 2009; Raike et al., 2015), similar to the findings observed in our neuropathology investigation of human tissue.

In summary, we propose that CD does not result from degeneration of Purkinje cells. Instead, loss of these neurons may be an indirect sign of their chronically abnormal electrophysiological activity. Furthermore, if Purkinje neurons have abnormally increased activity in CD as is suggested by some rodent models of dystonia, then the inhibitory output to the deep cerebellar nuclei will be enhanced, leading to decreased activation of these nuclei and, in turn, decreased output from the cerebellum to the thalamus and several brainstem areas. Decreased activation of regions receiving efferent connections from the cerebellum can ultimately alter the control of neck muscles through several pathways and lead to abnormal head movements in CD.

5.4. Is there any other evidence of cerebellar dysfunction in CD?

There has been increasing appreciation that the cerebellum is involved in dystonias (Neychev et al., 2011; Avanzino and Abbruzzese, 2012; Sadnicka et al., 2012; Filip et al., 2013), but what is the evidence suggesting that the cerebellum plays a role specifically in CD?

5.4.1. Evidence from human studies

Clinical imaging studies using computed tomography and structural MRI have linked CD with focal lesions of cerebellar circuits (LeDoux and Brady, 2003; Kumandas et al., 2006; Zadro et al., 2008; Neychev et al., 2011). A diffusion tensor imaging (DTI) study in individuals with craniocervical dystonia (dystonia of facial and neck muscles

combined) indicated abnormal cerebellar microstructure and fiber organization, especially in the anterior cerebellum and vermis (Prell et al., 2013). Another DTI study showed that persons with CD had decreased axonal fiber organization in the superior cerebellar peduncles, which carry the output fibers from the cerebellum to the thalamus and brainstem (Blood et al., 2012). Voxel-based morphometry studies in CD have demonstrated both increases and decreases in cerebellar grey matter volume, including the anterior cerebellum (Draganski et al., 2003; Obermann et al., 2007; Zoons et al., 2011; Prell et al., 2013; Piccinin et al., 2014b). PET studies have indicated increased glucose metabolism in the bilateral cerebellar hemispheres (Galardi et al., 1996). Increased fMRI activation bilaterally in the cerebellum during a unilateral passive forearm task has also been reported (Obermann et al., 2010). Collectively, these imaging investigations suggest abnormal structure and function of the cerebellum and its connections in CD.

It has been proposed that cerebellar dysfunction underlies defects in sensorimotor integration or maladaptive plasticity in CD and other dystonias (Neychev et al., 2011; Quartarone and Hallett, 2013). Human physiological studies have revealed subclinical abnormalities of eyeblink conditioning in CD (Tolosa et al., 1988; Teo et al., 2009; Hoffland et al., 2013). Eyeblink conditioning is thought to be an intrinsic function of the cerebellum, and thus cannot be readily ascribed to dysfunction of other brain regions (Gerwig et al., 2007; Avanzino and Abbruzzese, 2012).

Some surgical studies also suggest involvement of the cerebellum, since dentatectomy (Hitchcock, 1973; Davis, 2000) or deep brain stimulation of regions of the thalamus receiving cerebellar afferents can relieve dystonia in some cases (Fukaya et al., 2007; Goto et al., 2008; Morishita et al., 2010; Hedera et al., 2013). There is also anecdotal evidence of beneficial effects of deep brain stimulation of the cerebellum in a case of axial dystonia. Additionally, noninvasive stimulation of the cerebellum has

shown to lead to temporary improvements of symptoms in a few cases of focal hand dystonia and CD (Hoffland et al., 2013; Bradnam et al., 2014; Koch et al., 2014; Bharath et al., 2015).

5.4.2. Evidence from animal studies

There is evidence from multiple animal models that abnormal activity of the cerebellum may lead to dystonia. Abnormal movements of the head and neck resembling CD have been reported following experimental manipulations in nonhuman primates (**Table 5.1**) (Foltz et al., 1959; Malouin and Bedard, 1982; Klier et al., 2002; Holmes et al., 2012). Even though those studies did not involve direct manipulations of the cerebellum, they explored several subcortical areas that have direct connections with the cerebellum. Perhaps the strongest evidence of cerebellar involvement in dystonia comes from studies in rodents, as described in section 5.3 (LeDoux et al., 1993; LeDoux et al., 1995; LeDoux et al., 1998; Pizoli et al., 2002; Xiao and Ledoux, 2005; Calderon et al., 2011; Alvarez-Fischer et al., 2012; Fan et al., 2012; Raike et al., 2012). Importantly, twisted postures and movements of the head have been reported in some of these models (**Table 5.2**) (LeDoux et al., 1998; Pizoli et al., 2002; Alvarez-Fischer et al., 2012; Fan et al., 2012; Raike et al., 2012), further suggesting that abnormal cerebellar function may lead to CD.

Table 5.1: Some primate studies reported to show dystonic movements of the head

Species	Region targeted	Manipulation	Motor phenotype	References
Macaca mulatta	red nucleus	electrolytic lesion	torticollis	(Carpenter, 1956)
Macaca mulatta	reticular formation	electrolytic lesion	torticollis	(Foltz et al., 1959)
Macaca mulatta, Theropithecus gelada, Pan troglodytes	vestibular nuclei	physical lesion	torticollis, nystagmus	(Tarlov, 1969)
Macaca mulatta	tegmentum	electrolytic lesion	torticollis	(Malouin and Bedard, 1982)
Macaca fascicularis	substantia nigra, globus pallidus	bicuculline, muscimol	torticollis, limb dystonia	(Burbaud et al., 1998)
Macaca fascicularis, Macaca mulata	interstitial nucleus of Cajal	muscimol	torticollis	(Klier et al., 2002; Farshadmanesh et al., 2007)
Macaca nemestrina	substantia nigra	bicuculline, muscimol	torticollis	(Dybdal et al., 2012)
Macaca mulatta	substantia nigra, superior colliculus	muscimol	torticollis	(Holmes et al., 2012)

The term *torticollis*, which literally means *twisted neck*, historically was used often as a synonym for cervical dystonia.

Table 5.2: Some smaller mammals reported to have abnormal or dystonic movements of the head

Type of dystonia modeled	Species	Cause	Type of model	Motor phenotype	References
cervical	cat	electrical stimulation, kainic acid, or 6OHDA in midbrain	phenotypic	sustained abnormal head/neck postures	(Malouin and Bedard, 1982, 1983)
cervical	cat	bicuculline in putamen	phenotypic	sustained abnormal head/neck postures	(Yamada et al., 1995)
cervical	cat	electrical stimulation of globus pallidus	phenotypic	sustained abnormal head/neck postures	(Filion and Hebert, 1983)
cervical	rat	sigma receptor ligand in red nucleus	phenotypic	abnormal head/neck postures	(Matsumoto et al., 1990; Nakazawa et al., 1999)
focal	mouse	electrical stimulation or kainic acid injection into cerebellum	phenotypic	sustained but reversible abnormal postures of the trunk, limbs, neck or face	(Raike et al., 2012)
generalized	mouse or rat	electrical stimulation or kainic acid injection into cerebellum	phenotypic	sustained but reversible abnormal postures of the trunk, limbs, neck and face	(Pizoli et al., 2002; Alvarez-Fischer et al., 2012; Raike et al., 2012)
paroxysmal	mouse	*tottering* or *rocker* mutants of (*Cacna1a* gene)	phenotypic	attacks of transient twisting or abnormal postures of the trunk, neck, limbs and/or face	(Shirley et al., 2008)
paroxysmal	hamster	unknown gene	phenotypic	attacks of transient twisting or abnormal postures of the trunk, neck, limbs and/or face	(Loscher et al., 1989)

6OHDA, 6-hydroxydopamine.

5.5. How can dysfunction of the cerebellum lead to abnormal head movements in CD?

In order to propose a model to explain how the cerebellum may be linked to the abnormal head movements observed in CD, it is useful to briefly review the anatomical structure and connections of the cerebellum with other brain regions.

5.5.1. Intrinsic cerebellar anatomy

The cerebellar cortex is structurally organized in three layers. The outermost or molecular layer of the cerebellar cortex contains the cell bodies of inhibitory interneurons, the stellate and basket cells, dispersed among the axons of granule cells and dendrites of Purkinje cells. The axons of the granule cells in this layer run parallel to the long axis of the cerebellar folia and therefore are called parallel fibers. Beneath the molecular layer is the Purkinje cell layer, consisting of a single layer of Purkinje cell bodies. Purkinje neurons have large cell bodies and dendritic arborizations that extend upward into the molecular layer. Their axons project into the underlying white matter to the deep cerebellar or vestibular nuclei and provide the sole output of the cerebellar cortex. This output is entirely inhibitory and mediated by the neurotransmitter gamma-aminobutyric acid (GABA). Lastly, the innermost or granular layer contains a vast number of granule cells, which release the neurotransmitter glutamate and, thus, are considered excitatory. Also in this layer are a few inhibitory Golgi interneurons.

5.5.2. Cerebellar connections

The cerebellum has afferent and efferent connections with several brain regions (Fukushima, 1987; Manni and Petrosini, 2004; Apps and Garwicz, 2005; Ramnani, 2006; Glickstein and Doron, 2008; Apps and Hawkes, 2009; Manto et al., 2012; Bostan et al., 2013). There are two main types of afferent inputs to the cerebellum: mossy fibers and

climbing fibers. All efferent connections from the cerebellum originate from the deep cerebellar nuclei and project to the ventrolateral thalamus and multiple brainstem nuclei. The deep cerebellar nuclei are comprised by the fastigial nucleus, interposed nuclei (emboliform and globose), and the dentate nucleus.

Mossy fibers enter the cerebellum via the middle and inferior cerebellar peduncles and terminate as excitatory synapses on the dendrites of granule cells. There are several sources of inputs to mossy fibers, the largest of which are the pontine nuclei, which in turn receive extensive projections from the cerebral cortex and spinal cord. In non-human primates, the densest cortico-pontine projections arise in the precentral gyrus, and there are also less prominent projections from dorsal areas of the prefrontal cortex (Ramnani, 2006; Bostan et al., 2013). Other sources of mossy fibers include the vestibular nerve and nuclei, the reticular formation, the spinal cord, and feedback from deep cerebellar nuclei. These fibers carry sensory information from the periphery as well as information from the cerebral cortex (Apps and Garwicz, 2005; Manto et al., 2012).

Climbing fibers are the neuronal projections from the inferior olivary nucleus to the cerebellum. These axons pass through the pons and enter the cerebellum via the inferior cerebellar peduncle where they form excitatory synapses with the deep cerebellar nuclei and Purkinje cells. Each climbing fiber forms synapses with 1-10 Purkinje cells, whereas each Purkinje cell receives input from a single climbing fiber. This highly specific connectivity of the climbing fiber system contrasts with the massive convergence and divergence of the mossy and parallel fibers. Inferior olivary neurons that give rise to climbing fibers convey somatosensory, visual, or motor information from various sources, such as the spinal cord, vestibular system, red nucleus, superior colliculus, reticular formation and sensory and motor cortices. Climbing fiber activation

is thought to serve as a motor error signal sent to the cerebellum, and is an important signal for motor timing and coordination (Manto et al., 2012).

The outputs from the cerebellum originate from the deep cerebellar nuclei and leave the cerebellum through the superior cerebellar peduncle. The fastigial nucleus is the most medially located of the cerebellar nuclei. It receives input from the vermis and from cerebellar afferents that carry vestibular, proximal somatosensory, auditory, and visual information. There have been reports of projections from the fastigial nucleus to the vestibular nuclei, the reticular formation, interstitial nucleus of Cajal (INC) and spinal cord (Fukushima, 1987). The interposed nuclei comprise the emboliform nucleus and the globose nucleus, which are situated lateral to the fastigial nucleus. They receive input from the intermediate zone and from cerebellar afferents that carry spinal, somatosensory, auditory, and visual information. The interposed nuclei project to the contralateral red nucleus from which originates the rubrospinal tract. The dentate nucleus is the largest and the most lateral of the cerebellar nuclei. It receives inputs from the cerebellar hemispheres and afferents that carry information from the cerebral cortex via the pontine nuclei. It projects to the contralateral red nucleus and the ventrolateral thalamic nucleus. Importantly, the ventrolateral thalamus projects to the premotor cortex and M1 and contributes to motor planning and descending output to muscles via the corticospinal tract. Thus, the cerebellar projection to the thalamus has important modulatory influence over cortical motor areas.

Finally, it is important to consider the anatomical connections of the cerebellum and basal ganglia. Subcortical pathways of communication linking those regions have been identified by tract tracing studies in both rodents and non-human primates (Ichinohe et al., 2000; Hoshi et al., 2005; Bostan et al., 2010; Bostan and Strick, 2010; Bostan et al., 2013). In primates, it has been shown that the cerebellar dentate nuclei have disynaptic connections with the striatum through the ventroanterior and/or

ventrolateral thalamus (Hoshi et al., 2005). These projections to the striatum originate from motor and non-motor domains in the dentate nuclei, and they terminate in regions of the putamen and caudate known to be within the “sensorimotor” and “associative” pathways of the basal ganglia (Hoshi et al., 2005). A trisynaptic connection between the dentate nuclei and the globus pallidus externus has also been reported (Bostan et al., 2013). On the other hand, studies in primates have also identified projections from the subthalamic nucleus to the pontine nuclei, which in turn send afferents to the cerebellar cortex through the mossy fibers (Bostan et al., 2010). These connections originate from motor and non-motor domains within the subthalamic nucleus, and they terminate in motor and non-motor regions of the cerebellar cortex. Altogether, these findings indicate that the cerebellum and the basal ganglia have reciprocal connections carrying motor and non-motor information, and, therefore, the cerebellum can influence the function of the basal ganglia and vice versa.

5.5.3. Cerebellar dysfunction and abnormal head movements

Considering the cerebellar connections described above, abnormal function of the cerebellum can indirectly influence the descending control over motor neurons innervating cervical muscles via several pathways (**Figure 5.2**). Here I propose two pathways by which abnormal cerebellar function could lead to abnormal head movements in CD.

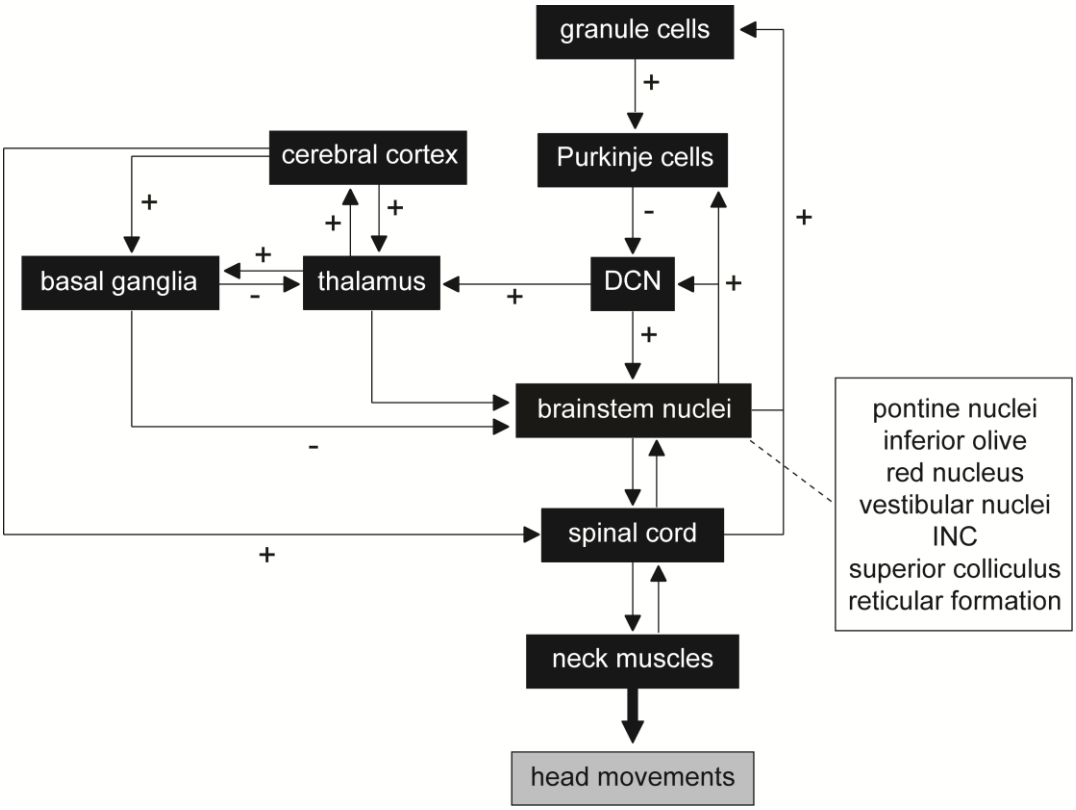

Figure 5.2: Anatomical connections of the cerebellum. Plus signs represent excitatory connections and negative signs represent inhibitory connections. CF, climbing fibers; INC, interstitial nucleus of Cajal; MF, mossy fibers.

The first pathway involves the indirect efferent connection of the cerebellum with the cerebral cortex (**Figure 5.2**), more specifically with M1. The cerebellar dentate nucleus projects to the ventrolateral thalamus, which in turn sends direct connections to M1. The axons of neurons from M1 project to different levels of the spinal cord form the corticospinal tract, and they are thought to be involved in the control of voluntary movements. Similarly, the corticobulbar tract is formed by the projections from M1 to cranial nerve nuclei in the brainstem. The corticospinal and corticobulbar tracts control the activation of motor neurons for neck muscles. As result, the cerebellum can influence activity in muscles controlling head movements by indirect modulation of the excitability of the corticospinal/corticobulbar tracts. Hence, if cerebellar function is

abnormal in CD, as suggested by our fMRI and neuropathology findings, then the aberrant head postures and movements may occur due to faulty signals about head position from the cerebellum to M1 through the cerebello-thalamo-corticospinal pathway. Data supporting this hypothesis come from studies showing cerebellar modulation of M1 excitability using noninvasive stimulation methods in healthy individuals and in a few cases of focal dystonia, including CD (Ugawa et al., 1995; Brighina et al., 2009; Grimaldi et al., 2013; Koch et al., 2014; Celnik, 2015). Additionally, neuroimaging investigations in persons with CD and other dystonias have suggested structural and functional abnormalities of the cerebello-thalamo-cortical networks (Neychev et al., 2011; Zoons et al., 2011).

Some types of movement, such as basic reflexes or postural control, may not require cortical involvement, raising the possibility that the cortex may not be required as the final pathway for CD. Thus, another potential pathway that could influence activation of motor neurons controlling neck muscles is the direct connection between the deep cerebellar nuclei and brainstem areas (**Figure 5.2**). For example, the cerebellar fastigial nucleus sends projections to the interstitial nucleus of Cajal, which is located in the midbrain (Fukushima et al., 1977; Fukushima et al., 1979a; Fukushima et al., 1979b). The interstitial nucleus of Cajal has been proposed to serve a central role in the control of head movements by integrating afferents from the cerebral cortex, cerebellum, vestibular system, basal ganglia and neck proprioceptors (Fukushima, 1987). It has direct efferents to motor neurons of the cervical spinal cord, placing it in a position where it could directly disrupt head control without involvement of the cerebral cortex. Consequently, it is possible that abnormal cerebellar output to the interstitial nucleus of Cajal could induce altered function in this area and, in turn, lead to abnormal head postures and movements in CD. Supporting this hypothesis, pharmacological and electrophysiological manipulations of this region provoke abnormalities of head control

resembling CD both in humans and primates (Sano et al., 1970; Vasin et al., 1985; Klier et al., 2002; Klier et al., 2007; Farshadmanesh et al., 2008; Loher and Krauss, 2009).

A point that deserves consideration is how the pathways described may affect the activity of both alpha and gamma motor neurons. Alpha motor neurons innervate extrafusal muscle fibers, which provide the force for muscle contraction. Gamma motor neurons innervate the ends of intrafusal fibers and help maintain the tension of muscle spindles to keep them sensitive to changes in muscle length. The activity of alpha and gamma motor neurons must be synchronized in order to allow coordinated movements to be generated. This synchronization, known as alpha-gamma coactivation, maintains muscle spindle length when the muscle actively contracts. Alpha-gamma coactivation occurs because most sources of input to alpha motor neurons have collaterals that project to gamma motor neurons. Thus, whenever motor commands are sent by descending pathways to alpha motor neurons, the appropriate compensating commands also are sent to gamma motor neurons. As a result, it is important to keep in mind that the cerebellum and the pathways described may be involved in CD and other dystonias by modulating the activation of alpha *and/or* gamma motor neurons. A few studies have hypothesized that abnormal sensitivity of muscle spindles could be involved in dystonia (Kaji et al., 1995; Grunewald et al., 1997; Rosales and Dressler, 2010). Tonic vibration of neck muscles, which is thought to primarily affect muscle spindle afferents, induces abnormal head orientation responses in persons with CD (Anastasopoulos et al., 1997; Lekhel et al., 1997). Similar findings of abnormal movements after vibration of dystonic muscles have also been reported for arm muscles (Kaji et al., 1995; Grunewald et al., 1997). There is as yet, however, no conclusive evidence regarding whether changes in fusimotor sensitivity and activation in dystonia represent a cause or a consequence of the disorder.

Finally, it is important to note that the pathways described were based on the hypothesis of the cerebellum as the source of the problem in CD. However, based on our fMRI and neuropathology data, it is not possible to determine whether abnormal cerebellar function is a cause or a consequence of the abnormal movements observed in CD. Thus, an alternative hypothesis could be that abnormal function of any region that has connections with the cerebellum can modify cerebellar signaling and, consequently, modulate the neural outputs to cervical muscles through the pathways described above. For instance, several studies have proposed that CD and other dystonias are caused by deficits in sensorimotor integration (Grunewald et al., 1997; Kanovsky, 2002; Tinazzi et al., 2003; Neychev et al., 2011; Quartarone and Hallett, 2013). The cerebellum plays an essential role in the central integration of movement performance through feed-forward and feedback mechanisms. As such, it continuously receives inputs from motor planning areas (cerebral cortex and basal ganglia), muscle spindles and proprioceptors about the planning and progression of any given movement. Therefore, faulty afferent inputs from any of those sources could lead to abnormal activation of cervical muscles.

5.6. How can the results be used to guide future studies?

In view of the findings from **Chapters 2-4**, we conclude the cerebellum is involved in normal head movements, and that abnormal cerebellar function may be associated with CD. Even though the results do not prove a causal relationship between distorted function of the cerebellum and CD, they provide a framework that may guide future investigations focused on the mechanisms of the disorder or new treatment strategies for patients:

- Future imaging studies could examine head movements in other directions both in healthy individuals and in persons with CD.

- Neuroimaging investigations focused on CD could examine individuals with similar patterns of abnormal head movements to avoid the normalization methods required in our studies.
- Neurophysiology investigations and even surgical interventions could examine the effects of stimulating the cerebellum ipsilateral to the side of torticollis to try to alleviate symptoms in patients with CD.
- Future neuropathology studies could investigate a larger sample of CD cases, perform a quantitative analysis of cerebellar torpedoes, examine different regions of the cerebellum, or compare the findings with other types of dystonia.
- Animal studies could target specifically the anterior cerebellum using chemical, electrical or genetic manipulations to test whether abnormal activity in this region can lead to distorted head postures and movements.
- Investigations in animals could explore specific pathways to determine whether the abnormal inputs to cervical muscles in CD travel through the thalamo-corticospinal, interstitiospinal, rubrospinal, fastigiospinal or other pathways.
- Animal studies could test the effects of manipulating the alpha/gamma system to examine whether abnormal gamma sensitivity is a cause or consequence of dystonia.
- Future investigations focused on the neurochemical properties of the cerebellum may point to alternative pharmacological targets for CD.

In summary, our work has provided fruitful ideas for follow up investigations that will contribute even further for the understanding of normal and abnormal head movements in humans.

References

Alarcon F, Zijlmans JC, Duenas G, Cevallos N (2004). Post-stroke movement disorders: report of 56 patients. J Neurol Neurosurg Psychiatry 75:1568-1574.

Albanese A, Bhatia K, Bressman SB, Delong MR, Fahn S, Fung VS, Hallett M, Jankovic J, Jinnah HA, Klein C, Lang AE, Mink JW, Teller JK (2013). Phenomenology and classification of dystonia: A consensus update. Mov Disord 28:863-873.

Alpers BJ, Drayer CS (1937). The organic background of some cases of spasmodic torticollis: report of case with autopsy. Am J Med Sci 193:378-384.

Alvarez-Fischer D, Grundmann M, Lu L, Samans B, Fritsch B, Moller JC, Schaefer MK, Hartmann A, Oertel WH, Bandmann O (2012). Prolonged generalized dystonia after chronic cerebellar application of kainic acid. Brain Res 1464:82-88.

Anagnostou E, Paraskevas GP, Spengos K, Vassilopoulou S, Zis V, Vassilopoulos D (2011). Same or opposite? Association of head-movement weakness with limb paresis in stroke. Neurologist 17:309-311.

Anastasopoulos D, Bhatia K, Bisdorff A, Bronstein AM, Gresty MA, Marsden CD (1997). Perception of spatial orientation in spasmodic torticollis. Part I: The postural vertical. Mov Disord 12:561-569.

Apps R, Garwicz M (2005). Anatomical and physiological foundations of cerebellar information processing. Nat Rev Neurosci 6:297-311.

Apps R, Hawkes R (2009). Cerebellar cortical organization: a one-map hypothesis. Nat Rev Neurosci 10:670-681.

Arthurs OJ, Boniface S (2002). How well do we understand the neural origins of the fMRI BOLD signal? Trends Neurosci 25:27-31.

Avanzino L, Abbruzzese G (2012). How does the cerebellum contribute to the pathophysiology of dystonia? Basal Ganglia 2:231-235.

Balagura S, Katz RG (1980). Undecussated innervation to the sternocleidomastoid muscle: a reinstatement. Ann Neurol 7:84-85.

Beach TG, Walker DG, Sue LI, Newell A, Adler CC, Joyce JN (2004). Substantia nigra Marinesco bodies are associated with decreased striatal expression of dopaminergic markers. J Neuropathol Exp Neurol 63:329-337.

Beevor CE (1909). Remarks on the paralysis of the movements of the trunk in hemiplegia, and the muscles which are affected. Br Med J 1:881-885.

Bender MB, Shanzer S, Wagman IH (1964). On the physiologic decussation concerned with head turning. Confin Neurol 24:169-181.

Benecke R, Meyer BU, Schonle P, Conrad B (1988). Transcranial magnetic stimulation of the human brain: responses in muscles supplied by cranial nerves. Exp Brain Res 71:623-632.

Berardelli A, Priori A, Inghilleri M, Cruccu G, Mercuri B, Manfredi M (1991). Corticobulbar and corticospinal projections to neck muscle motoneurons in man. A functional study with magnetic and electric transcranial brain stimulation. Exp Brain Res 87:402-406.

Berardelli A, Rothwell JC, Hallett M, Thompson PD, Manfredi M, Marsden CD (1998). The pathophysiology of primary dystonia. Brain 121 (Pt 7):1195-1212.

Bharath RD, Biswal BB, Bhaskar MV, Gohel S, Jhunjhunwala K, Panda R, George L, Gupta AK, Pal PK (2015). Repetitive transcranial magnetic stimulation induced modulations of resting state motor connectivity in writer's cramp. Eur J Neurol 22:796-e754.

Bizzi E, Schiller PH (1970). Single unit activity in the frontal eye fields of unanesthetized monkeys during eye and head movement. Exp Brain Res 10:150-158.

Blood AJ, Kuster JK, Woodman SC, Kirlic N, Makhlouf ML, Multhaupt-Buell TJ, Makris N, Parent M, Sudarsky LR, Sjalander G, Breiter H, Breiter HC, Sharma N (2012). Evidence for altered Basal Ganglia-brainstem connections in cervical dystonia. PLoS One 7:e31654.

Boesch SM, Wenning GK, Ransmayr G, Poewe W (2002). Dystonia in multiple system atrophy. J Neurol Neurosurg Psychiatry 72:300-303.

Bonilha L, de Vries PM, Hurd MW, Rorden C, Morgan PS, Besenski N, Bergmann KJ, Hinson VK (2009). Disrupted thalamic prefrontal pathways in patients with idiopathic dystonia. Parkinsonism Relat Disord 15:64-67.

Bonilha L, de Vries PM, Vincent DJ, Rorden C, Morgan PS, Hurd MW, Besenski N, Bergmann KJ, Hinson VK (2007). Structural white matter abnormalities in patients with idiopathic dystonia. Mov Disord 22:1110-1116.

Bostan AC, Strick PL (2010). The cerebellum and basal ganglia are interconnected. Neuropsychol Rev 20:261-270.

Bostan AC, Dum RP, Strick PL (2010). The basal ganglia communicate with the cerebellum. Proc Natl Acad Sci U S A 107:8452-8456.

Bostan AC, Dum RP, Strick PL (2013). Cerebellar networks with the cerebral cortex and basal ganglia. Trends in cognitive sciences.

Bradnam LV, Frasca J, Kimberley TJ (2014). Direct current stimulation of primary motor cortex and cerebellum and botulinum toxin a injections in a person with cervical dystonia. Brain Stimul 7:909-911.

Breakefield XO, Blood AJ, Li Y, Hallett M, Hanson PI, Standaert DG (2008). The pathophysiological basis of dystonias. Nat Rev Neurosci 9:222-234.

Brighina F, Romano M, Giglia G, Saia V, Puma A, Giglia F, Fierro B (2009). Effects of cerebellar TMS on motor cortex of patients with focal dystonia: a preliminary report. Exp Brain Res 192:651-656.

Burbaud P, Bonnet B, Guehl D, Lagueny A, Bioulac B (1998). Movement disorders induced by gamma-aminobutyric agonist and antagonist injections into the internal globus pallidus and substantia nigra pars reticulata of the monkey. Brain Res 780:102-107.

Calderon DP, Fremont R, Kraenzlin F, Khodakhah K (2011). The neural substrates of rapid-onset dystonia-parkinsonism. Nat Neurosci 14:357-365.

Camfield L, Ben-Shlomo Y, Warner TT (2002). Impact of cervical dystonia on quality of life. Mov Disord 17:838-841.

Campbell DB, Hess EJ (1999). L-type calcium channels contribute to the tottering mouse dystonic episodes. Mol Pharmacol 55:23-31.

Campbell DB, North JB, Hess EJ (1999). Tottering mouse motor dysfunction is abolished on the Purkinje cell degeneration (pcd) mutant background. Exp Neurol 160:268-278.

Carpenter MB (1956). A study of the red nucleus in the rhesus monkey; anatomic degenerations and physiologic effects resulting from localized lesions of the red nucleus. J Comp Neurol 105:195-249.

Carpenter MB, Brittin GM, Pines J (1958). Isolated lesions of the fastigial nuclei in the cat. J Comp Neurol 109:65-89.

Celnik P (2015). Understanding and modulating motor learning with cerebellar stimulation. Cerebellum 14:171-174.

Chan J, Brin MF, Fahn S (1991). Idiopathic cervical dystonia: clinical characteristics. Mov Disord 6:119-126.

Chen G, Popa LS, Wang X, Gao W, Barnes J, Hendrix CM, Hess EJ, Ebner TJ (2009). Low-frequency oscillations in the cerebellar cortex of the tottering mouse. J Neurophysiol 101:234-245.

Cho ZH (2010). 7.0 Tesla MRI brain atlas: in vivo atlas with cryomacrotome correlation, 1st Edition. New York: Springer.

Coffman KA, Dum RP, Strick PL (2011). Cerebellar vermis is a target of projections from the motor areas in the cerebral cortex. PNAS 108:16068-16073.

Colosimo C, Pantano P, Calistri V, Totaro P, Fabbrini G, Berardelli A (2005). Diffusion tensor imaging in primary cervical dystonia. J Neurol Neurosurg Psychiatry 76:1591-1593.

Comella CL, Leurgans S, Wuu J, Stebbins GT, Chmura T (2003). Rating scales for dystonia: a multicenter assessment. Mov Disord 18:303-312.

Criswell E, Cram R (2010). Cram's Introduction to Surface Electromyography, 2 Edition: Jones & Bartlett Publishers.

Crowner BE (2007). Cervical dystonia: disease profile and clinical management. Phys Ther 87:1511-1526.

Dauer WT, Burke RE, Greene P, Fahn S (1998). Current concepts on the clinical features, aetiology and management of idiopathic cervical dystonia. Brain 121 (Pt 4):547-560.

Davis R (2000). Cerebellar stimulation for cerebral palsy spasticity, function, and seizures. Arch Med Res 31:290-299.

De Carvalho Aguiar PM, Ozelius LJ (2002). Classification and genetics of dystonia. Lancet Neurol 1:316-325.

De Pauw J, Van der Velden K, Meirte J, Van Daele U, Truijen S, Cras P, Mercelis R, De Hertogh W (2014). The effectiveness of physiotherapy for cervical dystonia: a systematic literature review. J Neurol.

de Vries PM, de Jong BM, Bohning DE, Hinson VK, George MS, Leenders KL (2012). Reduced parietal activation in cervical dystonia after parietal TMS interleaved with fMRI. Clin Neurol Neurosurg 114:914-921.

de Vries PM, Johnson KA, de Jong BM, Gieteling EW, Bohning DE, George MS, Leenders KL (2008). Changed patterns of cerebral activation related to clinically normal hand movement in cervical dystonia. Clin Neurol Neurosurg 110:120-128.

Defazio G, Berardelli A, Hallett M (2007). Do primary adult-onset focal dystonias share aetiological factors? Brain 130:1183-1193.

Defazio G, Abbruzzese G, Livrea P, Berardelli A (2004). Epidemiology of primary dystonia. Lancet Neurol 3:673-678.

Defazio G, Jankovic J, Giel JL, Papapetropoulos S (2013a). Descriptive Epidemiology of Cervical Dystonia. Tremor Other Hyperkinet Mov (N Y) 3.

Defazio G, Gigante AF, Abbruzzese G, Bentivoglio AR, Colosimo C, Esposito M, Fabbrini G, Guidubaldi A, Girlanda P, Liguori R, Marinelli L, Morgante F, Santoro L, Tinazzi M, Livrea P, Berardelli A (2013b). Tremor in primary adult-onset dystonia: prevalence and associated clinical features. J Neurol Neurosurg Psychiatry 84:404-408.

Deitiker PR, Oshima M, Jankovic J, Duane DD, Aoki KR, Atassi MZ (2011). Association of HLA Class II alleles and haplotypes with cervical dystonia: HLA DR13-DQ6 (DQB1*0604) homozygotes are at greatly increased risk of cervical dystonia in Caucasian Americans. Autoimmunity 44:167-176.

Delnooz CC, Pasman JW, Beckmann CF, van de Warrenburg BP (2013a). Task-free functional MRI in cervical dystonia reveals multi-network changes that partially normalize with botulinum toxin. PLoS One 8:e62877.

Delnooz CC, Pasman JW, Beckmann CF, van de Warrenburg BP (2013b). Altered striatal and pallidal connectivity in cervical dystonia. Brain Struct Funct.

DeToledo JC, Dow R (1998). Sternomastoid function during hemispheric suppression by amytal: insights into the inputs to the spinal accessory nerve nucleus. Mov Disord 13:809-812.

Diedrichsen J, Verstynen T, Schlerf J, Wiestler T (2010). Advances in functional imaging of the human cerebellum. Curr Opin Neurol 23:382-387.

Draganski B, Thun-Hohenstein C, Bogdahn U, Winkler J, May A (2003). "Motor circuit" gray matter changes in idiopathic cervical dystonia. Neurol 61:1228-1231.

Draganski B, Schneider SA, Fiorio M, Kloppel S, Gambarin M, Tinazzi M, Ashburner J, Bhatia KP, Frackowiak RS (2009). Genotype-phenotype interactions in primary dystonias revealed by differential changes in brain structure. Neuroimage 47:1141-1147.

Duvernoy HM (1999). The human brain. Surface, blood supply and three-dimensional sectional anatomy., 2 Edition. New York: Springer.

Dybdal D, Forcelli PA, Dubach M, Oppedisano M, Holmes A, Malkova L, Gale K (2012). Topography of dyskinesias and torticollis evoked by inhibition of substantia nigra pars reticulata. Mov Disord.

Egger K, Mueller J, Schocke M, Brenneis C, Rinnerthaler M, Seppi K, Trieb T, Wenning GK, Hallett M, Poewe W (2007). Voxel based morphometry reveals specific gray matter changes in primary dystonia. Mov Disord 22:1538-1542.

Elsley JK, Nagy B, Cushing SL, Corneil BD (2007). Widespread presaccadic recruitment of neck muscles by stimulation of the primate frontal eye fields. J Neurophysiol 98:1333-1354.

Evinger C (2005). Animal models of focal dystonia. NeuroRx 2:513-524.

Fabbrini G, Pantano P, Totaro P, Calistri V, Colosimo C, Carmellini M, Defazio G, Berardelli A (2008). Diffusion tensor imaging in patients with primary cervical dystonia and in patients with blepharospasm. Eur J Neurol 15:185-189.

Fahn S (1984). The varied clinical expressions of dystonia. Neurol Clin 2:541-554.

Fahn S (1989). Clinical variants of idiopathic torsion dystonia. J Neurol Neurosurg Psychiatry Suppl:96-100.

Fan X, Hughes KE, Jinnah HA, Hess EJ (2012). Selective and sustained alpha-amino-3-hydroxy-5-methyl-4-isoxazolepropionic acid receptor activation in cerebellum induces dystonia in mice. J Pharmacol Exp Ther 340:733-741.

Farshadmanesh F, Klier EM, Chang P, Wang H, Crawford JD (2007). Three-dimensional eye-head coordination after injection of muscimol into the interstitial nucleus of Cajal (INC). J Neurophysiol 97:2322-2338.

Farshadmanesh F, Chang P, Wang H, Yan X, Corneil BD, Crawford JD (2008). Neck muscle synergies during stimulation and inactivation of the interstitial nucleus of Cajal (INC). J Neurophysiol 100:1677-1685.

Filion M, Hebert R (1983). Redundancy in ascending and descending pathways mediating head turning elicited by entopenducular stimulation in the cat. Neuroscience 10:169-176.

Filip P, Lungu OV, Bares M (2013). Dystonia and the cerebellum: A new field of interest in movement disorders? Clin Neurophysiol 124:1269-1212-1276.

Foerster O (1933). Mobile spasm of the neck muscles and its pathological basis. J Comp Neurol 58:725-735.

Foltz EL, Knopp LM, Ward AA, Jr. (1959). Experimental spasmodic torticollis. J Neurosurg 16:55-67.

Forman SD, Cohen JD, Fitzgerald M, Eddy WF, Mintun MA, Noll DC (1995). Improved assessment of significant activation in functional magnetic resonance imaging (fMRI): use of a cluster-size threshold. Magn Reson Med 33:636-647.

Fukaya C, Katayama Y, Kano T, Nagaoka T, Kobayashi K, Oshima H, Yamamoto T (2007). Thalamic deep brain stimulation for writer's cramp. J Neurosurg 107:977-982.

Fukushima K (1987). The interstitial nucleus of Cajal and its role in the control of movements of head and eyes. Prog Neurobiol 29:107-192.

Fukushima K, Hirai N, Rapoport S (1979a). Direct excitation of neck flexor motoneurons by the interstitiospinal tract. Brain Res 160:358-362.

Fukushima K, Peterson BW, Wilson VJ (1979b). Vestibulospinal, reticulospinal and interstitiospinal pathways in the cat. Prog Brain Res 50:121-136.

Fukushima K, Fukushima J, Terashima T (1987). The pathways responsible for the characteristic head posture produced by lesions of the interstitial nucleus of Cajal in the cat. Exp Brain Res 68:88-102.

Fukushima K, Peterson BW, Uchino Y, Coulter JD, Wilson VJ (1977). Direct fastigiospinal fibers in the cat. Brain Res 126:538-542.

Fung VS, Jinnah HA, Bhatia K, Vidailhet M (2013). Assessment of patients with isolated or combined dystonia: An update on dystonia syndromes. Mov Disord 28:889-898.

Galardi G, Perani D, Grassi F, Bressi S, Amadio S, Antoni M, Comi GC, Canal N, Fazio F (1996). Basal ganglia and thalamo-cortical hypermetabolism in patients with spasmodic torticollis. Acta Neurol Scand 94:172-176.

Gandevia SC, Applegate C (1988). Activation of neck muscles from the human motor cortex. Brain 111 (Pt 4):801-813.

Garcia-Albea E, Franch O, Munoz D, Ricoy JR (1981). Brueghel's syndrome, report of a case with postmortem studies. J Neurol Neurosurg Psychiatry 44:437-440.

Gerardin E, Lehericy S, Pochon JB, Tezenas du Montcel S, Mangin JF, Poupon F, Agid Y, Le Bihan D, Marsault C (2003). Foot, hand, face and eye representation in the human striatum. Cereb Cortex 13:162-169.

Gerwig M, Kolb FP, Timmann D (2007). The involvement of the human cerebellum in eyeblink conditioning. Cerebellum 6:38-57.

Ghika J, Ghika-Schmid F, Bogousslasvky J (1998). Parietal motor syndrome: a clinical description in 32 patients in the acute phase of pure parietal strokes studied prospectively. Clin Neurol Neurosurg 100:271-282.

Ghika J, Bogousslavsky J, Henderson J, Maeder P, Regli F (1994). The "jerky dystonic unsteady hand": a delayed motor syndrome in posterior thalamic infarctions. J Neurol 241:537-542.

Gibb WR, Lees AJ, Marsden CD (1988). Pathological report of four patients presenting with cranial dystonias. Mov Disord 3:211-221.

Glickstein M, Doron K (2008). Cerebellum: connections and functions. Cerebellum 7:589-594.

Goebel R, Esposito F, Formisano E (2006). Analysis of functional image analysis contest (FIAC) data with brainvoyager QX: From single-subject to cortically aligned group general linear model analysis and self-organizing group independent component analysis. Hum Brain Mapp 27:392-401.

Goonetilleke SC, Gribble PL, Mirsattari SM, Doherty TJ, Corneil BD (2011). Neck muscle responses evoked by transcranial magnetic stimulation of the human frontal eye fields. The European journal of neuroscience 33:2155-2167.

Goto S, Shimazu H, Matsuzaki K, Tamura T, Murase N, Nagahiro S, Kaji R (2008). Thalamic Vo-complex vs pallidal deep brain stimulation for focal hand dystonia. Neurology 70:1500-1501.

Grimaldi G, Argyropoulos GP, Boehringer A, Celnik P, Edwards MJ, Ferrucci R, Galea JM, Groiss SJ, Hiraoka K, Kassavetis P, Lesage E, Manto M, Miall RC, Priori A, Sadnicka A, Ugawa Y, Ziemann U (2013). Non-invasive Cerebellar Stimulation-a Consensus Paper. Cerebellum.

Grinker RR, Walker AE (1933). The pathology of spasmodic torticollis with a note on respiratory failure from anesthesia in chronic encephalitis. J Nerv Ment Dis 78:630-637.

Grunewald RA, Yoneda Y, Shipman JM, Sagar HJ (1997). Idiopathic focal dystonia: a disorder of muscle spindle afferent processing? Brain 120 (Pt 12):2179-2185.

Hallett M (2006). Pathophysiology of dystonia. J Neural Transm Suppl:485-488.

Hanajima R, Ugawa Y, Terao Y, Sakai K, Furubayashi T, Machii K, Uesugi H, Mochizuki H, Kanazawa I (1998). Cortico-cortical inhibition of the motor cortical area projecting to sternocleidomastoid muscle in normals and patients with spasmodic torticollis or essential tremor. Electroencephalogr Clin Neurophysiol 109:391-396.

Hassler R, Hess WR (1954). [Experimental and anatomical findings in rotatory movements and their nervous apparatus]. Arch Psychiatr Nervenkr Z Gesamte Neurol Psychiatr 192:488-526.

He F, Zhang S, Qian G, Zhang C (1995). Delayed dystonia with striatal CT lucencies induced by a mycotoxin (3-nitropropionic acid). Neurology 45:2178-2183.

Hedera P, Phibbs FT, Fang JY, Cooper MK, Charles PD, Davis TL (2010). Clustering of dystonia in some pedigrees with autosomal dominant essential tremor suggests the existence of a distinct subtype of essential tremor. BMC Neurol 10:66.

Hedera P, Phibbs FT, Dolhun R, Charles PD, Konrad PE, Neimat JS, Davis TL (2013). Surgical targets for dystonic tremor: Considerations between the globus pallidus and ventral intermediate thalamic nucleus. Parkinsonism Relat Disord 19:684-686.

Hedreen JC, Zweig RM, DeLong MR, Whitehouse PJ, Price DL (1988). Primary dystonias: a review of the pathology and suggestions for new directions of study. Adv Neurol 50:123-132.

Heeger DJ, Ress D (2002). What does fMRI tell us about neuronal activity? Nat Rev Neurosci 3:142-151.

Hitchcock E (1973). Dentate lesions for involuntary movement. Proc Royal Soc Med 66:877-879.

Hoffland BS, Kassavetis P, Bologna M, Teo JT, Bhatia KP, Rothwell JC, Edwards MJ, van de Warrenburg BP (2013). Cerebellum-dependent associative learning deficits in primary dystonia are normalized by rTMS and practice. Eur J Neurosci.

Holmes AL, Forcelli PA, DesJardin JT, Decker AL, Teferra M, West EA, Malkova L, Gale K (2012). Superior colliculus mediates cervical dystonia evoked by inhibition of the substantia nigra pars reticulata. J Neurosci 32:13326-13332.

Holton JL, Schneider SA, Ganesharajah T, Gandhi S, Strand C, Shashidharan P, Barreto J, Wood NW, Lees AJ, Bhatia KP, Revesz T (2008). Neuropathology of primary adult-onset dystonia. Neurol 70:695-699.

Hoshi E, Tremblay L, Feger J, Carras PL, Strick PL (2005). The cerebellum communicates with the basal ganglia. Nat Neurosci 8:1491-1493.

Ichinohe N, Mori F, Shoumura K (2000). A di-synaptic projection from the lateral cerebellar nucleus to the laterodorsal part of the striatum via the central lateral nucleus of the thalamus in the rat. Brain Res 880:191-197.

Isa T, Sasaki S (2002). Brainstem control of head movements during orienting; organization of the premotor circuits. Prog Neurobiol 66:205-241.

Jankovic J, Svendsen CN, Bird ED (1987). Brain neurotransmitters in dystonia. N Engl J Med 316:278-279.

Jankovic J, Tsui J, Bergeron C (2007). Prevalence of cervical dystonia and spasmodic torticollis in the United States general population. Parkinsonism Relat Disord 13:411-416.

Jankovic J, Leder S, Warner D, Schwartz K (1991). Cervical dystonia: clinical findings and associated movement disorders. Neurol 41:1088-1091.

Jankovic J, Adler CH, Charles D, Comella C, Stacy M, Schwartz M, Manack Adams A, Brin MF (2015). Primary results from the Cervical Dystonia Patient Registry for Observation of OnabotulinumtoxinA Efficacy (CD PROBE). J Neurol Sci 349:84-93.

Jinnah HA, Factor SA (2015). Diagnosis and treatment of dystonia. Neurol Clin 33:77-100.

Jinnah HA, Berardelli A, Comella C, Defazio G, Delong MR, Factor S, Galpern WR, Hallett M, Ludlow CL, Perlmutter JS, Rosen AR (2013). The focal dystonias: Current views and challenges for future research. Mov Disord 28:926-943.

Kaji R, Rothwell JC, Katayama M, Ikeda T, Kubori T, Kohara N, Mezaki T, Shibasaki H, Kimura J (1995). Tonic vibration reflex and muscle afferent block in writer's cramp. Ann Neurol 38:155-162.

Kang SY, Ma HI, Lee MJ, Kwon SB, Jung S, Kim YJ, Hwang SH (2011). Ipsilateral tilt and contralateral sensory change of neck in cortical infarction. J Clin Neurol 7:156-158.

Kanovsky P (2002). Dystonia: a disorder of motor programming or motor execution? Mov Disord 17:1143-1147.

Keisker B, Hepp-Reymond MC, Blickenstorfer A, Kollias SS (2010). Differential representation of dynamic and static power grip force in the sensorimotor network. Eur J Neurosci 31:1483-1491.

Kennedy SR, Loeb LA, Herr AJ (2012). Somatic mutations in aging, cancer and neurodegeneration. Mechanisms of ageing and development 133:118-126.

Kern JK, Jones AM (2006). Evidence of toxicity, oxidative stress, and neuronal insult in autism. Journal of toxicology and environmental health Part B, Critical reviews 9:485-499.

Kim JS (2001). Delayed onset mixed involuntary movements after thalamic stroke. Brain 124:299-309.

Klier EM, Wang H, Crawford JD (2007). Interstitial nucleus of cajal encodes three-dimensional head orientations in Fick-like coordinates. J Neurophysiol 97:604-617.

Klier EM, Wang H, Constantin AG, Crawford JD (2002). Midbrain control of three-dimensional head orientation. Science 295:1314-1316.

Koch G, Porcacchia P, Ponzo V, Carrillo F, Caceres-Redondo MT, Brusa L, Desiato MT, Arciprete F, Di Lorenzo F, Pisani A, Caltagirone C, Palomar FJ, Mir P (2014). Effects of Two Weeks of Cerebellar Theta Burst Stimulation in Cervical Dystonia Patients. Brain Stimul.

Kristiansen SL, Nyengaard JR (2012). Digital stereology in neuropathology. APMIS : acta pathologica, microbiologica, et immunologica Scandinavica 120:327-340.

Kumandas S, Per H, Gumus H, Tucer B, Yikilmaz A, Kontas O, Coskun A, Kurtsoy A (2006). Torticollis secondary to posterior fossa and cervical spinal cord tumors: report of five cases and literature review. Neurosurg Rev 29:333-338.

LeDoux MS, Lorden JF (2002). Abnormal spontaneous and harmaline-stimulated Purkinje cell activity in the awake genetically dystonic rat. Exp Brain Res 145:457-467.

LeDoux MS, Brady KA (2003). Secondary cervical dystonia associated with structural lesions of the central nervous system. Mov Disord 18:60-69.

LeDoux MS, Lorden JF, Ervin JM (1993). Cerebellectomy eliminates the motor syndrome of the genetically dystonic rat. Exp Neurol 120:302-310.

LeDoux MS, Lorden JF, Meinzen-Derr J (1995). Selective elimination of cerebellar output in the genetically dystonic rat. Brain Res 697:91-103.

LeDoux MS, Hurst DC, Lorden JF (1998). Single-unit activity of cerebellar nuclear cells in the awake genetically dystonic rat. Neuroscience 86:533-545.

LeDoux MS, Xiao J, Rudzinska M, Bastian RW, Wszolek ZK, Van Gerpen JA, Puschmann A, Momcilovic D, Vemula SR, Zhao Y (2012). Genotype-phenotype correlations in THAP1 dystonia: Molecular foundations and description of new cases. Parkinsonism Relat Disord 18:414-425.

Lehericy S, Tijssen MA, Vidailhet M, Kaji R, Meunier S (2013). The anatomical basis of dystonia: Current view using neuroimaging. Mov Disord 28:944-957.

Lekhel H, Popov K, Anastasopoulos D, Bronstein A, Bhatia K, Marsden CD, Gresty M (1997). Postural responses to vibration of neck muscles in patients with idiopathic torticollis. Brain 120 (Pt 4):583-591.

Lemon RN (2008). Descending pathways in motor control. Annu Rev Neurosci 31:195-218.

Liang KY, Zeger SL (1986). Longitudinal data analysis using generalized linear models. Biometrika 73:13-22.

Loher TJ, Krauss JK (2009). Dystonia associated with pontomesencephalic lesions. Mov Disord 24:157-167.

Loscher W, Fisher JE, Jr., Schmidt D, Fredow G, Honack D, Iturrian WB (1989). The sz mutant hamster: a genetic model of epilepsy or of paroxysmal dystonia? Mov Disord 4:219-232.

Louis ED, Vonsattel JP (2008). The emerging neuropathology of essential tremor. Mov Disord 23:174-182.

Louis ED, Yi H, Erickson-Davis C, Vonsattel JP, Faust PL (2009). Structural study of Purkinje cell axonal torpedoes in essential tremor. Neurosci Lett 450:287-291.

Louis ED, Vonsattel JP, Honig LS, Ross GW, Lyons KE, Pahwa R (2006). Neuropathologic findings in essential tremor. Neurol 66:1756-1759.

Louis ED, Faust PL, Ma KJ, Yu M, Cortes E, Vonsattel JP (2011). Torpedoes in the cerebellar vermis in essential tremor cases vs. controls. Cerebellum 10:812-819.

Magyar-Lehmann S, Antonini A, Roelcke U, Maguire RP, Missimer J, Meyer M, Leenders KL (1997). Cerebral glucose metabolism in patients with spasmodic torticollis. Mov Disord 12:704-708.

Malouin F, Bedard PJ (1982). Frontal torticollis (head tilt) induced by electrolytic lesion and kainic acid injection in monkeys and cats. Exp Neurol 78:551-560.

Malouin F, Bedard PJ (1983). Evaluation of head motility and posture in cats with horizontal torticollis. Exp Neurol 81:559-570.

Mann DM, Stamp JE, Yates PO, Bannister CM (1980). The fine structure of the axonal torpedo in Purkinje cells of the human cerebellum. Neurol Res 1:369-378.

Manni E, Petrosini L (2004). A century of cerebellar somatotopy: a debated representation. Nat Rev Neurosci 5:241-249.

Manon-Espaillat R, Ruff RL (1988). Dissociated weakness of sternocleidomastoid and trapezius muscles with lesions in the CNS. Neurology 38:796-797.

Manto M, Bower JM, Conforto AB, Delgado-Garcia JM, da Guarda SN, Gerwig M, Habas C, Hagura N, Ivry RB, Marien P, Molinari M, Naito E, Nowak DA, Oulad Ben Taib N, Pelisson D, Tesche CD, Tilikete C, Timmann D (2012). Consensus paper: roles of the cerebellum in motor control--the diversity of ideas on cerebellar involvement in movement. Cerebellum 11:457-487.

Marras C, Van den Eeden SK, Fross RD, Benedict-Albers KS, Klingman J, Leimpeter AD, Nelson LM, Risch N, Karter AJ, Bernstein AL, Tanner CM (2007). Minimum incidence of primary cervical dystonia in a multiethnic health care population. Neurology 69:676-680.

Marsden CD, Obeso JA, Zarranz JJ, Lang AE (1985). The anatomical basis of symptomatic hemidystonia. Brain 108 (Pt 2):463-483.

Mastaglia FL, Knezevic W, Thompson PD (1986). Weakness of head turning in hemiplegia: a quantitative study. J Neurol Neurosurg Psychiatry 49:195-197.

Mathiesen C, Caesar K, Lauritzen M (2000). Temporal coupling between neuronal activity and blood flow in rat cerebellar cortex as indicated by field potential analysis. J Physiol 523 Pt 1:235-246.

Matsumoto RR, Pouw B (2000). Correlation between neuroleptic binding to sigma(1) and sigma(2) receptors and acute dystonic reactions. Eur J Pharmacol 401:155-160.

Matsumoto RR, Hemstreet MK, Lai NL, Thurkauf A, De Costa BR, Rice KC, Hellewell SB, Bowen WD, Walker JM (1990). Drug specificity of pharmacological dystonia. Pharmacol Biochem Behav 36:151-155.

Mavroudis IA, Fotiou DF, Adipepe LF, Manani MG, Njau SD, Psaroulis D, Costa VG, Baloyannis SJ (2010). Morphological changes of the human purkinje cells and deposition of neuritic plaques and neurofibrillary tangles on the cerebellar cortex of Alzheimer's disease. Am J Alzheimers Dis Other Demen 25:585-591.

Mayka MA, Corcos DM, Leurgans SE, Vaillancourt DE (2006). Three-dimensional locations and boundaries of motor and premotor cortices as defined by functional brain imaging: a meta-analysis. Neuroimage 31:1453-1474.

McGeer EG, McGeer PL (1988). The dystonias. Can J Neurol Sci 15:447-483.

McNaught KS, Kapustin A, Jackson T, Jengelley TA, Jnobaptiste R, Shashidharan P, Perl DP, Pasik P, Olanow CW (2004). Brainstem pathology in DYT1 primary torsion dystonia. Ann Neurol 56:540-547.

Mink JW (2006). Abnormal circuit function in dystonia. Neurology 66:959.

Moore AP, Behan PO, Behan WM (1986). Lymphocyte subset abnormalities in patients with spasmodic torticollis. Acta Neurol Scand 74:371-378.

Morishita T, Foote KD, Haq IU, Zeilman P, Jacobson CE, Okun MS (2010). Should we consider Vim thalamic deep brain stimulation for select cases of severe refractory dystonic tremor. Stereotact Funct Neurosurg 88:98-104.

Mottolese C, Richard N, Harquel S, Szathmari A, Sirigu A, Desmurget M (2013). Mapping motor representations in the human cerebellum. Brain 136:330-342.

Munchau A, Bronstein AM (2001). Role of the vestibular system in the pathophysiology of spasmodic torticollis. J Neurol Neurosurg Psychiatry 71:285-288.

Munchau A, Corna S, Gresty MA, Bhatia KP, Palmer JD, Dressler D, Quinn NP, Rothwell JC, Bronstein AM (2001). Abnormal interaction between vestibular and voluntary head control in patients with spasmodic torticollis. Brain 124:47-59.

Nakazawa M, Kobayashi T, Matsuno K, Mita S (1999). Possible involvement of a sigma receptor subtype in the neck dystonia in rats. Pharmacol Biochem Behav 62:123-126.

Nambu A (2011). Somatotopic organization of the primate basal ganglia. Front Neuroanat 5:26.

Naumann M, Magyar-Lehmann S, Reiners K, Erbguth F, Leenders KL (2000). Sensory tricks in cervical dystonia: perceptual dysbalance of parietal cortex modulates frontal motor programming. Ann Neurol 47:322-328.

Nemeth AH (2002). The genetics of primary dystonias and related disorders. Brain 125:695-721.

Neychev VK, Fan X, Mitev VI, Hess EJ, Jinnah HA (2008). The basal ganglia and cerebellum interact in the expression of dystonic movement. Brain 131:2499-2509.

Neychev VK, Gross RE, Lehericy S, Hess EJ, Jinnah HA (2011). The functional neuroanatomy of dystonia. Neurobiol Dis 42:185-201.

Noth U, Laufs H, Stoermer R, Deichmann R (2012). Simultaneous electroencephalography-functional MRI at 3 T: an analysis of safety risks imposed by performing anatomical reference scans with the EEG equipment in place. J Magn Reson Imaging 35:561-571.

Nutt JG, Muenter MD, Aronson A, Kurland LT, Melton LJ, 3rd (1988). Epidemiology of focal and generalized dystonia in Rochester, Minnesota. Mov Disord 3:188-194.

Obermann M, Vollrath C, De Greiff A, Gizewski ER, Diener HC, Hallett M, Maschke M (2010). Sensory disinhibition on passive movement in cervical dystonia. Mov Disord 25:2627-2633.

Obermann M, Yaldizli O, De Greiff A, Lachenmayer ML, Buhl AR, Tumczak F, Gizewski ER, Diener HC, Maschke M (2007). Morphometric changes of sensorimotor structures in focal dystonia. Mov Disord 22:1117-1123.

Obermann M, Yaldizli O, de Greiff A, Konczak J, Lachenmayer ML, Tumczak F, Buhl AR, Putzki N, Vollmer-Haase J, Gizewski ER, Diener HC, Maschke M (2008). Increased basal-ganglia activation performing a non-dystonia-related task in focal dystonia. Eur J Neurol 15:831-838.

Obrador S (1953). Clinical observations on the representation of the neck movements within the primary motor cortex. Electroencephalogr Clin Neurophysiol 5:611-612.

Odergren T, Rimpilainen I (1996). Activation and suppression of the sternocleidomastoid muscle induced by transcranial magnetic stimulation. Electroencephalogr Clin Neurophysiol 101:175-180.

Odergren T, Rimpilainen I, Borg J (1997). Sternocleidomastoid muscle responses to transcranial magnetic stimulation in patients with cervical dystonia. Electroencephalogr Clin Neurophysiol 105:44-52.

Opavsky R, Hlustik P, Otruba P, Kanovsky P (2011). Sensorimotor network in cervical dystonia and the effect of botulinum toxin treatment: a functional MRI study. J Neurol Sci 306:71-75.

Opavsky R, Hlustik P, Otruba P, Kanovsky P (2012). Somatosensory cortical activation in cervical dystonia and its modulation with botulinum toxin: an fMRI study. Int J Neurosci 122:45-52.

Pal PK, Samii A, Schulzer M, Mak E, Tsui JK (2000). Head tremor in cervical dystonia. CJNS 27:137-142.

Palfi S, Leventhal L, Goetz CG, Hantraye T, Roitberg BZ, Sramek J, Emborg M, Kordower JH (2000). Delayed onset of progressive dystonia following subacute 3-nitropropionic acid treatment in Cebus apella monkeys. Mov Disord 15:524-530.

Pantano P, Totaro P, Fabbrini G, Raz E, Contessa GM, Tona F, Colosimo C, Berardelli A (2011). A transverse and longitudinal MR imaging voxel-based morphometry study in patients with primary cervical dystonia. AJNR Am J Neuroradiol 32:81-84.

Papapetropoulos S, Singer C (2006). Cervical dystonia as a presenting symptom of Parkinson's disease. Parkinsonism Relat Disord 12:514-516.

Park E, Ai J, Baker AJ (2007). Cerebellar injury: clinical relevance and potential in traumatic brain injury research. Prog Brain Res 161:327-338.

Patel N, Hanfelt J, Marsh L, Jankovic J (2014). Alleviating manoeuvres (sensory tricks) in cervical dystonia. J Neurol Neurosurg Psychiatry.

Paudel R, Hardy J, Revesz T, Holton JL, Houlden H (2012). Review: Genetics and neuropathology of primary pure dystonia. Neuropathol Appl Neurobiol 38:520-534.

Penfield W, Rasmussen T (1950). The cerebral cortex of man: a clinical study of localization of function. New York: Macmillan.

Perlmutter JS, Mink JW (2004). Dysfunction of dopaminergic pathways in dystonia. Adv Neurol 94:163-170.

Peterson BW (2004). Current approaches and future directions to understanding control of head movement. Prog Brain Res 143:369-381.

Peterson BW, Richmond FJ (1988). Control of head movement. New York: Oxford University Press.

Petit L, Beauchamp MS (2003). Neural basis of visually guided head movements studied with fMRI. J Neurophysiol 89:2516-2527.

Picard N, Strick PL (2001). Imaging the premotor areas. Curr Opin Neurobiol 11:663-672.

Piccinin CC, Santos MC, Piovesana LG, Campos LS, Guimaraes RP, Campos BM, Torres FR, Franca MC, Amato-Filho AC, Lopes-Cendes I, Cendes F, D'Abreu A (2014a). Infratentorial gray matter atrophy and excess in primary craniocervical dystonia. Parkinsonism Relat Disord 20:198-203.

Piccinin CC, Piovesana LG, Santos MC, Guimaraes RP, De Campos BM, Rezende TJ, Campos LS, Torres FR, Amato-Filho AC, Franca MC, Jr., Lopes-Cendes I, Cendes F, D'Abreu A (2014b). Diffuse decreased gray matter in patients with idiopathic craniocervical dystonia: a voxel-based morphometry study. Front Neurol 5:283.

Pirio Richardson S (2014). Enhanced dorsal premotor-motor inhibition in cervical dystonia. Clin Neurophysiol.

Pizoli CE, Jinnah HA, Billingsley ML, Hess EJ (2002). Abnormal cerebellar signaling induces dystonia in mice. J Neurosci 22:7825-7833.

Poldrack RA, Mumford JA, Nichols TE (2011). Handbook of functional MRI data analysis, 1 Edition. New York: Cambridge University Press.

Prell T, Peschel T, Kohler B, Bokemeyer MH, Dengler R, Gunther A, Grosskreutz J (2013). Structural brain abnormalities in cervical dystonia. BMC Neurosci 14:123.

Proudlock FA, Gottlob I (2007). Physiology and pathology of eye-head coordination. Prog Retin Eye Res 26:486-515.

Prudente CN, Hess EJ, Jinnah HA (2014). Dystonia as a network disorder: What is the role of the cerebellum? Neuroscience 260C:23-35.

Prudente CN, Stilla R, Buetefisch CM, Singh S, Hess EJ, Hu X, Sathian K, Jinnah HA (2015). Neural substrates for head movements in humans: a functional magnetic resonance imaging study. J Neurosci 35:9163-9172.

Quartarone A, Hallett M (2013). Emerging concepts in the physiological basis of dystonia. Mov Disord 28:958-967.

Raethjen J, Deuschl G (2012). The oscillating central network of essential tremor. Clin Neurophysiol 123:61-64.

Raike RS, Hess EJ, Jinnah HA (2015). Dystonia and cerebellar degeneration in the leaner mouse mutant. Brain Res.

Raike RS, Pizoli CE, Weisz C, van den Maagdenberg AM, Jinnah HA, Hess EJ (2012). Limited regional cerebellar dysfunction induces focal dystonia in mice. Neurobiol Dis 49:200-210.

Raike RS, Weisz C, Hoebeek FE, Terzi MC, De Zeeuw CI, van den Maagdenberg AM, Jinnah HA, Hess EJ (2013). Stress, caffeine and ethanol trigger transient neurological dysfunction through shared mechanisms in a mouse calcium channelopathy. Neurobiol Dis 50:151-159.

Rajagopalan N, Humphrey PR, Bucknall RC (1989). Torticollis and blepharospasm in systemic lupus erythematosus. Mov Disord 4:345-348.

Ramdhani RA, Kumar V, Velickovic M, Frucht SJ, Tagliati M, Simonyan K (2014). What's special about task in dystonia? A voxel-based morphometry and diffusion weighted imaging study. Mov Disord.

Ramnani N (2006). The primate cortico-cerebellar system: anatomy and function. Nat Rev Neurosci 7:511-522.

Rasmussen T, Penfield W (1948). Movement of head and eyes from stimulation of human frontal cortex. Res Publ Assoc Res Nerv Ment Dis 27 (1 vol.):346-361.

Richmond FJ, Corneil BD, Singh K (1999). Animal models of motor systems: cautionary tales from studies of head movement. Prog Brain Res 123:411-416.

Rizzolatti G, Fogassi L, Gallese V (2002). Motor and cognitive functions of the ventral premotor cortex. Curr Opin Neurobiol 12:149-154.

Rosales RL, Dressler D (2010). On muscle spindles, dystonia and botulinum toxin. Eur J Neurol 17 Suppl 1:71-80.

Sadnicka A, Hoffland BS, Bhatia KP, van de Warrenburg BP, Edwards MJ (2012). The cerebellum in dystonia - Help or hindrance? Clin Neurophysiol 123:65-70.

Saint Hilaire MH, Burke RE, Bressman SB, Brin MF, Fahn S (1991). Delayed-onset dystonia due to perinatal or early childhood asphyxia. Neurology 41:216-222.

Sano K, Yoshioka M, Mayanagi Y, Sekino H, Yoshimasu N (1970). Stimulation and destruction of and around the interstitial nucleus of Cajal in man. Confin Neurol 32:118-125.

Sarna JR, Hawkes R (2003). Patterned Purkinje cell death in the cerebellum. Prog Neurobiol 70:473-507.

Schlerf JE, Verstynen TD, Ivry RB, Spencer RM (2010). Evidence of a novel somatopic map in the human neocerebellum during complex actions. J Neurophysiol 103:3330-3336.

Schmahmann JD, Doyon J, McDonald D, Holmes C, Lavoie K, Hurwitz AS, Kabani N, Toga A, Evans A, Petrides M (1999). Three-dimensional MRI atlas of the human cerebellum in proportional stereotaxic space. Neuroimage 10:233-260.

Scholz VH, Flaherty AW, Kraft E, Keltner JR, Kwong KK, Chen YI, Rosen BR, Jenkins BG (2000). Laterality, somatotopy and reproducibility of the basal ganglia and motor cortex during motor tasks. Brain Res 879:204-215.

Schwarz CS, Bressman SB (2009). Genetics and treatment of dystonia. Neurol Clin 27:697-718, vi.

Scott BL, Jankovic J (1996). Delayed-onset progressive movement disorders after static brain lesions. Neurology 46:68-74.

Shaikh AG, Wong AL, Zee DS, Jinnah HA (2013). Keeping your head on target. J Neurosci 33:11281-11295.

Shill HA, Adler CH, Sabbagh MN, Connor DJ, Caviness JN, Hentz JG, Beach TG (2008). Pathologic findings in prospectively ascertained essential tremor subjects. Neurol 70:1452-1455.

Shirley TL, Rao LM, Hess EJ, Jinnah HA (2008). Paroxysmal dyskinesias in mice. Mov Disord 23:259-264.

Song CH, Fan X, Exeter CJ, Hess EJ, Jinnah HA (2012). Functional analysis of dopaminergic systems in a DYT1 knock-in mouse model of dystonia. Neurobiol Dis 48:66-78.

Standaert DG (2011). Update on the pathology of dystonia. Neurobiol Dis 42:148-151.

Steeves TD, Day L, Dykeman J, Jette N, Pringsheim T (2012). The prevalence of primary dystonia: A systematic review and meta-analysis. Mov Disord.

Stoessl AJ, Martin WR, Clark C, Adam MJ, Ammann W, Beckman JH, Bergstrom M, Harrop R, Rogers JG, Ruth TJ, et al. (1986). PET studies of cerebral glucose metabolism in idiopathic torticollis. Neurol 36:653-657.

Takada M, Sugimoto T, Hattori T (1993). MPTP neurotoxicity to cerebellar Purkinje cells in mice. Neurosci Lett 150:49-52.

Talairach J, Tournoux P (1988). Co-planar stereotaxic atlas of the human brain: 3-dimensional proportional system: an approach to cerebral imaging. New York: Thieme Medical Publishers.

Tanabe LM, Kim CE, Alagem N, Dauer WT (2009). Primary dystonia: molecules and mechanisms. Nature reviews Neurology 5:598-609.

Tarlov E (1969). The postural effect of lesions of the vestibular nuclei: a note on species differences among primates. J Neurosurg 31:187-195.

Tarlov E (1970). On the problem of the pathology of spasmodic torticollis in man. J Neurol Neurosurg Psychiatry 33:457-463.

Tarsy D, Simon DK (2006). Dystonia. N Engl J Med 355:818-829.

Teo JT, van de Warrenburg BP, Schneider SA, Rothwell JC, Bhatia KP (2009). Neurophysiological evidence for cerebellar dysfunction in primary focal dystonia. J Neurol Neurosurg Psychiatry 80:80-83.

Thesen S, Heid O, Mueller E, Schad LR (2000). Prospective acquisition correction for head motion with image-based tracking for real-time fMRI. Magn Reson Med 44:457-465.

Thompson ML, Thickbroom GW, Mastaglia FL (1997). Corticomotor representation of the sternocleidomastoid muscle. Brain 120 (Pt 2):245-255.

Thomsen K, Offenhauser N, Lauritzen M (2004). Principal neuron spiking: neither necessary nor sufficient for cerebral blood flow in rat cerebellum. J Physiol 560:181-189.

Tinazzi M, Rosso T, Fiaschi A (2003). Role of the somatosensory system in primary dystonia. Mov Disord 18:605-622.

Tolosa E, Montserrat L, Bayes A (1988). Blink reflex studies in focal dystonias: enhanced excitability of brainstem interneurons in cranial dystonia and spasmodic torticollis. Mov Disord 3:61-69.

Ugawa Y, Uesaka Y, Terao Y, Hanajima R, Kanazawa I (1995). Magnetic stimulation over the cerebellum in humans. Ann Neurol 37:703-713.

van den Heuvel MP, Hulshoff Pol HE (2010). Exploring the brain network: a review on resting-state fMRI functional connectivity. Eur Neuropsychopharmacol 20:519-534.

van der Meer JN, Tijssen MA, Bour LJ, van Rootselaar AF, Nederveen AJ (2010). Robust EMG-fMRI artifact reduction for motion (FARM). Clin Neurophysiol 121:766-776.

van Duinen H, Renken R, Maurits NM, Zijdewind I (2008). Relation between muscle and brain activity during isometric contractions of the first dorsal interosseus muscle. Hum Brain Mapp 29:281-299.

van Gaalen J, Pennings RJ, Beynon AJ, Munchau A, Bloem BR, van de Warrenburg BP (2012). Cervical dystonia after ear surgery. Parkinsonism Relat Disord 18:669-671.

van Rootselaar AF, Maurits NM, Renken R, Koelman JH, Hoogduin JM, Leenders KL, Tijssen MA (2008). Simultaneous EMG-functional MRI recordings can directly relate hyperkinetic movements to brain activity. Hum Brain Mapp 29:1430-1441.

Vasavada AN, Li S, Delp SL (1998). Influence of muscle morphometry and moment arms on the moment-generating capacity of human neck muscles. Spine (Phila Pa 1976) 23:412-422.

Vasin N, Medzhidov MR, Shabalov VA (1985). [Stereotaxic destruction of the interstitial nucleus of Cajal on spastic torticollis]. Zh Vopr Neirokhir Im N N Burdenko:3-7.

Vemula SR, Xiao J, Zhao Y, Bastian RW, Perlmutter JS, Racette BA, Paniello RC, Wszolek ZK, Uitti RJ, Van Gerpen JA, Hedera P, Truong DD, Blitzer A, Rudzinska M, Momcilovic D, Jinnah HA, Frei K, Pfeiffer RF, LeDoux MS (2014). A rare sequence variant in intron 1 of THAP1 is associated with primary dystonia. Molecular genetics & genomic medicine 2:261-272.

Vidailhet M, Jutras MF, Grabli D, Roze E (2013). Deep brain stimulation for dystonia. J Neurol Neurosurg Psychiatry 84:1029-1042.

Walker FO, Walker JM, Matsumoto RR, Bowen WD (1990). Torticollis, midbrain, and sigma receptors. Mov Disord 5:265.

Walsh RA, Whelan R, O'Dwyer J, O'Riordan S, Hutchinson S, O'Laoide R, Malone K, Reilly R, Hutchinson M (2009). Striatal morphology correlates with sensory abnormalities in unaffected relatives of cervical dystonia patients. J Neurol 256:1307-1313.

Wenning GK, Tison F, Elliott L, Quinn NP, Daniel SE (1996). Olivopontocerebellar pathology in multiple system atrophy. Mov Disord 11:157-162.

Werle RW, Takeda SY, Zonta MB, Guimaraes AT, Teive HA (2014). The physical, social and emotional aspects are the most affected in the quality of life of the patients with cervical dystonia. Arq Neuropsiquiatr 72:405-410.

White T, O'Leary D, Magnotta V, Arndt S, Flaum M, Andreasen NC (2001). Anatomic and functional variability: the effects of filter size in group fMRI data analysis. Neuroimage 13:577-588.

Wichmann T (2008). Commentary: Dopaminergic dysfunction in DYT1 dystonia. Exp Neurol 212:242-246.

Willoughby EW, Anderson NE (1984). Lower cranial nerve motor function in unilateral vascular lesions of the cerebral hemisphere. Br Med J (Clin Res Ed) 289:791-794.

Xiao J, Ledoux MS (2005). Caytaxin deficiency causes generalized dystonia in rats. Brain Res Mol Brain Res 141:181-192.

Xiao J, Uitti RJ, Zhao Y, Vemula SR, Perlmutter JS, Wszolek ZK, Maraganore DM, Auburger GDM, Leube BDM, Lehnhoff K, Ledoux MS (2012). Mutations in CIZ1 cause adult onset primary cervical dystonia. Ann Neurol 71:458-469.

Xiao J, Bastian RW, Perlmutter JS, Racette BA, Tabbal SD, Karimi M, Paniello RC, Blitzer A, Batish SD, Wszolek ZK, Uitti RJ, Hedera P, Simon DK, Tarsy D, Truong DD, Frei KP, Pfeiffer RF, Gong S, Zhao Y, LeDoux MS (2009). High-throughput mutational analysis of TOR1A in primary dystonia. BMC Med Genet 10:24.

Xiao J et al. (2010). Novel THAP1 sequence variants in primary dystonia. Neurology 74:229-238.

Yamada H, Fujimoto K, Yoshida M (1995). Neuronal mechanism underlying dystonia induced by bicuculline injection into the putamen of the cat. Brain Res 677:333-336.

Yang Q, Hashizume Y, Yoshida M, Wang Y, Goto Y, Mitsuma N, Ishikawa K, Mizusawa H (2000). Morphological Purkinje cell changes in spinocerebellar ataxia type 6. Acta Neuropathol 100:371-376.

Yousry TA, Schmid UD, Alkadhi H, Schmidt D, Peraud A, Buettner A, Winkler P (1997). Localization of the motor hand area to a knob on the precentral gyrus. A new landmark. Brain 120 (Pt 1):141-157.

Yuen P, Baxter DW (1963). The morphology of Marinesco bodies (paranucleolar corpuscles) in the melanin-pigmented nuclei of the brain-stem. J Neurol Neurosurg Psychiatry 26:178-183.

Zadro I, Brinar VV, Barun B, Ozretic D, Habek M (2008). Cervical dystonia due to cerebellar stroke. Mov Disord 23:919-920.

Zhang C, Zhu Q, Hua T (2010). Aging of cerebellar Purkinje cells. Cell Tissue Res 341:341-347.

Zhang L, Yokoi F, Jin YH, DeAndrade MP, Hashimoto K, Standaert DG, Li Y (2011). Altered dendritic morphology of Purkinje cells in DYT1 ΔGAG knock-in and purkinje cell-specific DYT1 conditional knockout mice. PLoS One 6:e18357.

Zhao Y, DeCuypere M, LeDoux MS (2008). Abnormal motor function and dopamine neurotransmission in DYT1 DeltaGAG transgenic mice. Exp Neurol 210:719-730.

Zoons E, Booij J, Nederveen AJ, Dijk JM, Tijssen MA (2011). Structural, functional and molecular imaging of the brain in primary focal dystonia--a review. Neuroimage 56:1011-1020.

Zweig RM, Jankel WR, Whitehouse PJ, Casanova MF, Hedreen JC, Price DL (1986). Brainstem pathology in dystonia. Neurol 36:74-75.

Zweig RM, Hedreen JC, Jankel WR, Casanova MF, Whitehouse PJ, Price DL (1988). Pathology in brainstem regions of individuals with primary dystonia. Neurol 38:702-706.